# Examination of drug-adapted cancer cell lines as pre-clinical models of acquired resistance

**2017**

**Emily Saintas**

**A thesis submitted to the University of Kent for the degree of Doctor of Philosophy**

**University of Kent**

**Faculty of Sciences**

## Declaration

No part of this thesis has been submitted in support of an application for any degree or other qualification of the University of Kent, or any other University or Institution of learning.

Emily Saintas Date 21.09.17

**Acknowledgements**

First and foremost, I would like to thank my supervisor Martin for his support and unwavering belief in what I was capable of achieving. I have truly appreciated every challenge and opportunity that has been given to me during the course of my PhD as well the guidance I have received.

I would also like to thank my wonderful family for their support, encouragement and excitement at the work I have been completing and never losing faith in me. In particular my parents for continuing the financial flow and ensuring that I didn't ever worry and to my sister, to whom I hope I continue to be a good role model and to show her how worthwhile it is to take chances, grasp opportunities and to work hard at something you believe in.

To my husband Joey, for his understanding behind my drive for wanting to complete a PhD in a field that means so much to me. For always helping me with all manner of crises that have arisen and supporting us both for so long. I am eternally grateful for the kindness and love that I have been lucky enough to receive throughout all my studying at Kent.

To the lovely friends I have made in this University and department who have provided support, training and a helping hand whenever needed. I truly cherish all the friendships I have made.

And finally, I congratulate myself, for not allowing a disease to take over my life and to change my plans, not once but three times and to keep pursuing the degree I wanted.
I dedicate the work carried out in this thesis to those who I met along the way, those who are no longer with us and for those that continue to fight with the aid of cancer research, which I hope to always be a part of.

## Table of contents

## List of Figures and tables

## List of abbreviations

ABCB1 – ATP Binding Cassette Transporter 1

ALK - Anaplastic Lymphoma Kinase

ALL - Acute Lymphoblastic Leukaemia

ATCC-SDO - American Type Culture Collection Standard Development Organisation

BER – Base Excision Repair

CABA – Cabazitaxel

CARBO – Carboplatin

CDDP – Cisplatin

CDK – Cyclin Dependent Kinase

CHO – Chinese Hamster Ovary

CKI – Cyclin Kinase Inhibitors

CLL - Chronic Lymphocytic Leukemia

CML – Chronic Myeloid Leukemia

CNV - Copy Number Variants

ctDNA – Circulating Tumour DNA

CTR1- Copper Transporter Receptor 1

DACARB – Dacarbazine

DAPI – 4',6-Diamidino-2phenylindole

DDR - DNA Damage Response

DDR2 - Discoidin Domain-containing Receptor 2

DME - Drug Metabolising Enzymes

DMF – Dimethylformamide

DMSO – Dimethyl Sulfoxide

DNA- Deoxyribonucleic Acid

DOCE – Docetaxel

EDTA – Ethylenediaminetraacetic Acid

EGFR – Epidermal Growth Factor Receptor

EPO-B – Epothilone-B

ER – Oestrogen Receptor

ERC - Endocytic Recycling Compartment

ETO – Etoposide

FBS – Foetal Bovine Serum

FISH – Fluorescence *in situ* Hybridisation

FITC – Fluorescein Isothiocyanate

GD2 - disialoganglioside

GEMCIT – Gemcitabine

GST - Glutathione-S-Transferases

HCC - Hepatocellular Carcinoma Cell Line

Hela – Henrietta Lacks

HES – Human Endometrial Epithelial Cell Line

ICGC - International Cancer Genome Consortium

ICLAC - International Cell Line Authentication Committee

IGF1R – Insulin-like Growth Factor 1 Receptor

IMDM - Iscove's Modified Dulbecco's Media

IR – Insulin Receptor

KCI – Potassium Chloride

mABs - Monoclonal Antibodies

MALDI-IMS - Matrix-Assisted Laser Desorption Ionisation -Imaging Mass Spectrometry

MALDI-TOF– Matrix-Assisted Laser Desorption Ionisation Time of Flight Mass Spectrometry

MDR – Multidrug Resistance

MDR 1 – Multidrug Resistance Protein 1

MELPH – Melphalan

MOI – Multiplicities of infection

MRP1 – Multidrug Resistance-Associated Protein 1

MRP4- Multi-Resistance associated Protein 4

MTT - 3-(4,5-dimethlythiazol-2-yl)-2,5-diphenyltetrazolium bromide

NER – Nucleotide Excision Repair

NHS – National Health System

NSCLC – Non-Small Cell Lunch Cancer

OXALI – Oxaliplatin

PBS – Phosphate Buffered Saline

PCA – Principal Component Analysis

PCL – Paclitaxel

PDGFRB - Beta-type platelet-derived growth factor receptor

PTEN - Phosphatase and Tensin homolog

RCCL – Resistant Cancer Cell Line collection

RTCA – Real Time Cell Analyser

SDS - Sodium Dodecyl Sulphate

SELDI-ToF - Surface-Enhanced Laser Desorption/Ionization Mass Spectrometry

STR – Short Tandem Repeat

T-VEC – Talimogene Laherparepvec

TCGA - The Cancer Genome Atlas

TFA – Trifluoroacetic Acid

TKI – Tyrosine Kinase Inhibitors

TOPO – Topotecan

UGT - Uridine Diphospho-Glucuronoslytransferases

UVC – Ultraviolet Light C

VCR – Vincristine

VINB – Vinblastine

VINO – Vinorelbine

## Abstract

Resistance formation to chemotherapy remains a major reason for the failure of cancer therapies. This project investigated the use of drug-adapted cancer cell lines as models of acquired resistance in cancer at different levels. Firstly, we investigated MALDI-ToF fingerprinting approaches in order to establish a reliable method for the authentication of cell lines of the same genetic origin. Indeed, the MALDI-ToF based spectra of a panel of parental neuroblastoma cell lines and their sub-lines adapted to a range of cytotoxic anti-cancer drugs resulted in promising results. However, the method needs to be further optimised to reliably authenticate all cell lines. For the understanding of the processes underlying resistance formation in cancer cell lines, it is essential to better understand the intra-cell line heterogeneity in parental cancer cell lines prior to resistance formation. The investigation of ten single cell derived clonal sub-lines of the Neuroblastoma cell line UKF-NB-3 by methods including chromosome painting and determination of drug resistance profiles revealed a noticeable level of intra-cell line heterogeneity. Next, we established a standardised drug adaptation assay that enables the comparison of the potential of a drug to induce resistance in a certain cancer cell line. Finally, we introduced and characterised a novel oxaliplatin-adapted sub line of the neuroblastoma cell line SK-N-AS. Taken together, this project resulted in improved methods for use and investigation of drug adapted cancer cell lines as models of acquired drug resistance in cancer.

# Chapter 1

# Introduction

## 1.1 Cancer statistics and background

In 2015 there were approximately 360,000 new cases of cancer in the UK alone and of these cases the most prevalent were breast, prostate, lung and bowel which accounted for 53% of diagnoses (Cancer Research UK at http://www.cancerresearchuk.org/). There were over 160,000 deaths in 2016 from cancer, despite the improvements in cancer treatments and the discovery of new therapeutics. Although the treatment of certain cancers has continued to advance and subsequently so have survival rates, others such as pancreatic continue to be problematic to diagnose and successfully treat with improved patient outcomes (Kamisawa, T., Wood, L.D., Itoi, T and Takaori, K 2016). As the emergence of cancer-drug resistance is ever more prevalent, it is therefore imperative that research into new therapeutics and discovery of new drug-targets continues alongside a more comprehensive understanding of drug resistance mechanisms (Gottesman, M.M 2002).

## 1.2 Cancer and tumorigenesis

Simply put, cancer is defined as the uncontrollable growth of cells following acquisition of mutations with the potential to undergo metastases and proliferate throughout the body. In order to develop into a tumour there are further processes a cancerous cell undergoes which are known as the hallmarks of cancer as shown in Figure 1 (Hanahan, D and Weinberg, R.A 2011). Characteristics relevant to this project are sustained proliferative signalling as the cell cycle is no longer controlled by regulators such as receptor tyrosine kinases therefore cancer cells can enhance signalling of receptors such as the epidermal growth factor receptor (EGFR) to promote growth (Okayama, H., Kohno, T., Ishii, Y., Shimada, Y., Shiraishi, K *et al* 2012). Mutations in tumour suppressors are common in many cancer types and are essential for proliferative growth in cancerous cells. Tumour suppressors include TP53, a DNA damage sensor which induces apoptosis and PTEN, a regulator of the P13K-AKT-mTOR pathway, with nuclear functions as well as interactions with TP53 via nutlin (Song, M.S., Salmena, L and Pandolfi, P.P 2012). Alongside mutations in tumour suppressors, cancer is also caused by alterations to oncogenes, which encode proteins for regulation of proliferation and growth in cells. These include transcription factors, growth factor receptors, signal transducers and apoptosis regulators (Croce, C.M 2008). Examples of mutated transcription factors include TRIM24 in prostate cancer, involved in the degradation of p53 and augmentation of the androgen receptor (AR) (Groner, A.C., Cato, L., Tribolet-Hardy, J.d., Bernasocchi, T., Janouskova, H *et al* 2016). And FOXA1, an established oncogene, found to be increased in metastatic breast cancer and is required for proliferation in tamoxifen-resistant cells (Schrijver, W., Schuurman, K., van Rossum., A., Droog, M., Jeronimo, C *et al* 2018). Growth factor

receptor mutations are well documented such as EGFR leading to deregulation in signalling and inducing proliferation in cancers such as non-small-cell lung cancer (NSCLC) (Normanno, N., Denis, M.G., Thress, K.S., Ratcliffe, M and Reck, M 2017) and ErbB-2/HER2 in breast cancer (Mitri, Z., Constantine, T and O'Regan, R., 2012). Mutations in growth factor receptors result in alterations in signal transduction pathways as well as in oncogenes encoding members of these pathways. Examples include the P13K-PKB/Akt pathway which is commonly mutated in cancer cells which has a major role in tumour development and is a viable drug target (Fresno Vara, J.A., Casado, E., de Castro, J., Cejas, P., Belda-Iniesta, C *et al* 2004). Apoptosis regulation is also affected by activation of oncogenes such as the *BCL2* gene which promotes cell survival via inhibition of pro-apoptotic proteins BAX and BAK (Delbridge, A.R.D., Grabow, S., Strasser, A and Vaux, D.L 2016).

Genomic instability and mutation are also hallmarks relevant to this study, due to our research into chromosomal changes in cancer cells and possible underlying mutations related to resistance mechanisms. A variety of therapeutics used throughout this study also impact on the hallmarks and have been chosen to analyse a variety of responses to drug targets. Taken together, it is therefore essential to understand the hallmarks of cancer. This enables further understanding of processes which may be valid drug targets or mechanisms of drug-resistance, which can then be therapeutically exploited.

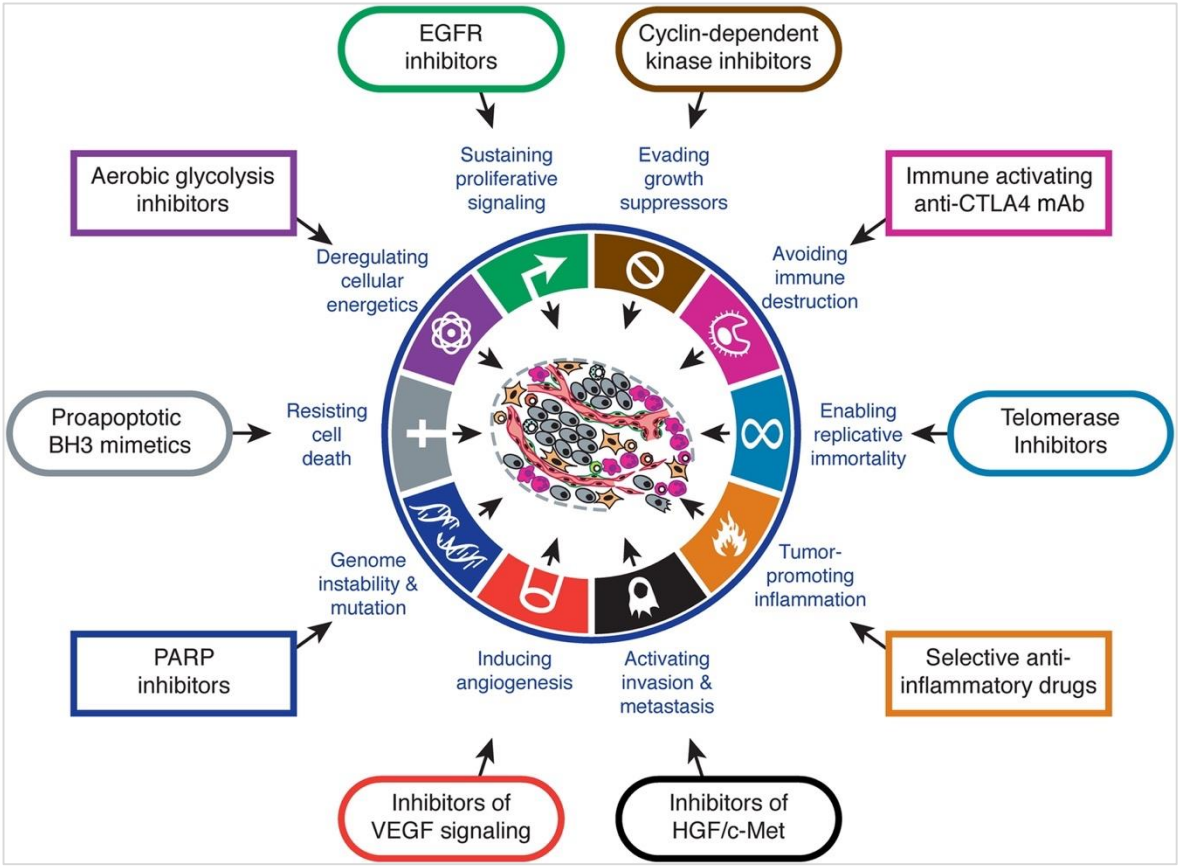


Figure 1: The Hallmarks of cancer (Hanrahan, D and Weinberg, R.A 2011) with the types of anti-cancer therapy that can be applied to each hallmark in order to overcome the oncogenic effect. For this project our main focus was around genome instability and mutation and sustaining proliferative signalling but a multitude of different therapeutics with a variety of mechanisms displayed above were tested on cell lines.

### 1.2.1 Biomarkers in cancer

Current diagnosis of cancer depends on several factors such as the type of cancer and the time of diagnosis. Solid cancers, such as neuroblastoma or breast may present with symptoms which result in detection of the disease, via routine screening or a biomarker may also determine disease presence. Biomarkers are of particular interest for three key reasons: firstly, to successfully advance targeted therapy development, it is essential to continue to investigate whether the biomarker being targeted is more effective in comparison, to pre-existing treatments. Secondly, to determine whether a patient is at risk of developing cancer and finally to establish whether a positive outcome would occur in a patient receiving the targeted treatment (Joshi, G 2016).

Research carried out by Sawyers, C.L 2008 state the difficulty faced in the discovery of biomarkers is identifying an ideal patient as a candidate who matches the marker needed to test the new line of therapeutics. In order to have a high success rate using biomarkers, there needs to be further advances in the clinic determining whether a targeted therapy will be successful.

There have however, been many successes in discovering biomarkers and treatment responses such as the treatment of breast cancer. It is established protocol to check for molecular markers such as the oestrogen receptor (ER) and subsequently treat with a corresponding therapeutic such as tamoxifen (James, C.R., Quinn, J.E., Mullan, P.B., Johnston, P.G and Harkin, D.P., 2007). As well as determining genes such as the *BRCA1* in patients, which indicates a higher susceptibility of developing the disease and therefore treatment options can be addressed (Davies, H., Glodzik, D., Morganella, S., Yates, L.R., Staaf, J *et al* 2017). However, if a patient presents with a heterogeneous tumour which is discovered at a late, aggressive stage, a single effective biomarker is almost impossible to find. This leads to intensive systemic therapy in order to eradicate the disseminated disease. Furthermore, a targeted therapeutic approach following an identified biomarker can invariably lead to resistance and treatment failure.

### 1.2.2 Treatment of cancer

Cancer is currently treated in a multitude of ways, the most common can include one or a combination of the following: surgery, chemotherapy, radiotherapy, immunotherapy and hormone therapy. Although systemic chemotherapy has had remarkable cure rates in cancers such as testicular, through the use of effective heavy platinum drugs there are still concerns of adverse effects, tumour sensitivity and relapse in patients (Khan, O and Protheroe, A 2007). This has led to the development of targeted therapies and personalised medicine with the aim to increase the therapeutic window and prevent side effects caused by previous chemotherapy treatments, but the main limitation is drug resistance. Targeted treatments have a much higher probability of a tumour developing acquired resistance (Russo, M., Misale, S., Wei, G., Siravenga, G., Crisafulli, G., *et al* 2016). There are two clear classes of resistance: intrinsic and acquired, with the former arising before treatment occurs and the tumour having pre-existing genetic and epigenetic factors

contributing to resistance to therapies. Acquired resistance is the basis of the work presented in this thesis, usually occurring following a period of the tumour initially being drug-sensitive before relapsing and resistance occurring. In some cases, regression occurs initially, but the tumour can then relapse with such an aggressive phenotype that treatment options are often exhausted (Kim, J.J and Tannock, I.F 2005). This reduction in sensitivity is imperative to uncover and a great deal of research has been carried out to discover which mechanisms occur to enable this.

In recent years there has been a concerted effort to develop new treatments which promise fewer adverse effects and greater response rates when compared to systemic therapies. This has led to the design of molecularly targeted and 'targeted therapies' antibodies or small molecules such as kinase inhibitors which specifically target cancer specific motifs. Examples of more contemporary targeted treatments include Imatinib, a tyrosine kinase inhibitor used to treat Chronic Myeloid Leukaemia (CML) has a five-year survival rate of 90% (Miranda, M.B., Lauseker, M., Kraus, M-P., Proetel, U., Hanfstein, B *et al* 2016). And vemurafenib which inhibits the MAPK pathway in 60% patients who present with the V600E *BRAF* mutation in malignant melanoma (Chapman, P.B., Hauschild, A., Robert, C., Haanen, J.B., Ascierto, P *et al*., 2011).

The development of resistance is a serious issue with targeted therapies and although both the diagnosis and treatment of some types of cancer has improved, five-year survival rates in cancers such as pancreatic and high-risk malignancies still continue to be very low and require significant research into new therapeutics to increase patient survival rates (Taieb, J., Pointet, A.L., Van Laethem, J.L., Laquente, B., Pernot, S *et al* 2017).

### 1.2.3 The cellular proteome in cancer

Characterisation of the cancer cell proteome (i.e. the entirety of the proteins expressed within a cell) are a fundamental aspect of understanding the development and progression of the disease as well as providing potential drug targets (Lawrence, R.T, Perez, E.M., Hernandez, D., Miller, C.P., Haas, K.M *et al* 2015). For example, the proteome is utilised in the classification of breast cancer types according to receptor status which clinically relates to appropriate treatment options for the patient. (Howlader, N., Altekruse, S.F., Li, C.I., Chen, V.W., Clarke, C.A *et al* 2014). More recently, large scale studies such as The Cancer Genome Atlas (TCGA) and the International Cancer Genome Consortium (ICGC) have worked on characterising tens of thousands of tumours to better understand the proteomics underlying cancer development (Xhao, W, Li, J and Mills, G.B 2017). The study of proteomics is essential in the understanding and subsequent treatment of cancer and is particularly applicable in detecting changes in resistant models. Interestingly, using this approach and analysing at the protein level rather than genetic may reflect more cellular functions and differences between subtypes (Tyanova, S., Albrechtsen, R., Kronqvist, P., Cox, J., Mann, M *et al* 2016).

Using mass spectrometry-based proteomics for researching cancers is an important analytical technique due to its sensitivity, rapidity and being highly quantitative (Lam, S.W., Jimenez, C.R., and Boven, E 2013). Matrix-assisted laser desorption/ionisation (MALDI) time-of-flight (ToF) imaging mass spectrometry has a multitude of applications in areas such as diagnostics and research. In particular, its application in investigating tumour heterogeneity by analysing components of the tumour which would include multiple sub-clones if present (Kriegsmann, J., Kriegsmann, M and Casadonte, R 2014). Swiatly, A., Horala, A., Hadjuk, J., Matysiak, J., Nowak-Markwitz, E *et al* 2017 discuss the use of MALDI-TOF-MS to identify proteomic patterns in ovarian cancer by comparing a healthy control group versus disease samples with the aim to identify potential biomarkers.

Further successes in the use of MALDI-TOF also include the application of identifying microorganisms, and the subsequent diagnosis of infectious diseases by comparison of findings with a known database (Hadjuk, J., Matysiak, J and Kokot, Z.J 2016). It is this approach we investigate in this thesis to assess the potential of MALDI-ToF in identifying drug-resistant sub-lines from the sensitive parental cell lines as a means of authentication.

### 1.3.1 Neuroblastoma

In this project neuroblastoma cell lines were used as a model system to investigate drug-resistance. This included using both sensitive parental cell lines such as UKF-NB-3 and SK-N-AS alongside a variety of drug-adapted sub-lines to clinically relevant drugs and single-cell derived clones.

Neuroblastoma is a paediatric cancer with a median diagnosis age of 17-monthsand is thought to arise from neural crest tissue and form embryonal tumours in the sympathetic nervous system (Maris, J.M 2010). With a mortality rate of over 50%, children who present with stage IV aggressive neuroblastoma have the lowest survival rates due to refractory complications or relapse (Cheung, N-K. V., and Dyer, M.A 2013). Approximately 30% of tumours arise in the adrenal medulla, 60% in the abdominal paraspinal ganglia and the remaining 10% arise from ganglia in the chest, head, neck and pelvis (Louis, C.U and Shohet, J.M 2014). As a complicated and heterogeneous disease neuroblastoma also presents in a varied manner, with disease outcomes altered in different patients. The disease can regress spontaneously in some patients, but children over the age of 1 with metastatic disease when diagnosed, have a poor prognosis (Brodeur, G.M 2003). The disease can also present with a high number of metastases and despite intensive therapy can still result in a 40% survival rate (Oldridge, D.O., Wood, A.C., Maris, J.M., 2015). Other factors taken into consideration include age at time of diagnosis, stage of disease and tumour location. In particular, patients who present with localised tumours have a higher survival rate, between 70%– 98% and this may be due to the chance of removing the tumour and if there is no metastatic disease present (Tonini, G.P 2017). The differences in disease response in patients may be due to the intra-tumoural heterogeneity in neuroblastoma and the development of acquired drug resistance leading to treatment failure.

### 1.3.2 Aetiology of Neuroblastoma

Neuroblastoma is an extremely complex disease which presents clinically in a variety of ways as well as the ability to spontaneously regress with no previous markers. There are two types of neuroblastoma, familial and sporadic, with familial only accounting for ~2% of cases with a germline mutation in the anaplastic lymphoma kinase (ALK) gene (Mosse, Y.P., Laudenslager, M., Longo, L., Cole, K.A., Wood, A., *et al* 2008). ALK is a member of the branch of the insulin receptor (IR) family of receptor tyrosine kinases (RTKs) and is expressed in cells of the central and peripheral nervous system (Azarova, A.M., Gautam, G and George, R.E 2011). ALK is involved in in the development of sympathoadrenal lineage of the neural crest and is a precursor to transduction pathways of RAS/MAPK and P13K/AKT often mutated in cancer cells (Cheung, N.K.V and Dyer, M.A 2013). Furthermore, activation of ALK it is often seen alongside an amplification of MYCN and may relate to a poor patient outcome (Zhu, S., Lee, J.S., Gui, F., Shin, J., Perez-Atayde, A.R *et al*, 2012). The most common finding in sporadic neuroblastoma is the amplification of MYCN*,* thought to promote growth of the tumour through up-regulation of gene transcription is seen in approximately 22% of neuroblastoma tumours and is correlated with poor prognosis and evidence of metastatic disease (Kaneko, M., Tsuchida, Y., Mugishima, H., Ohnuma, N., Yamamoto, K *et al* 2002). MYCN regulates cells in the developing central nervous system and is involved in growth, differentiation and survival and is expressed in the developing neural crest (Cheung, N-K.V and Dyer, M.A 2013).

An extensive classification of neuroblastoma diagnosis has been implemented to ensure patients are given the best treatment options. These include the some of the following prognostics but a total of 13 factors are used: DNA diploidy, tumour differentiation, chromosomal abnormalities and MYCN status (Diede, S.J 2014). Furthermore, patients are grouped into risk categories following diagnosis which essentially includes very low, low, intermediate and high risk (Cohn, S.L., Pearson, A.D.J., London, W.B., Monclair, T., Ambros, P.F *et al* 2009).

### 1.3.3 Treatment of Neuroblastoma

Neuroblastomas are highly heterogenic in nature making not only diagnosis difficult but the designing of effective biomarkers and new treatments a challenge. Furthermore, even with intensive chemotherapy, surgery, radiotherapy and immunotherapy there are still 60% of patients who relapse with subsequent resistant tumours (Eleveld, T., Oldridge, D.A., Bernard, V., Koster, J., Daage, C *et al* 2015). Better outcomes lie in discovering how certain features of the tumour relate to its biology and how this information can then be translated into a clinical setting. In targeted therapy, one aim has been to identify mutations within the tumour and then developing specific therapeutics, but this is coupled with the ever-present issue of acquired resistance. But as the disease is heterogeneous and presents differently, identifying a successful tumour target in neuroblastoma is much harder with a low frequency of common mutations. As stated by Cheung,

N-K. V and Dyer, M.A 2013, it is thought that a clearer understanding of the developmental biology of the disease will allow for new approaches.

Current treatment of neuroblastoma includes surgical removal of tumours in low-risk patients with no metastatic disease present and if necessary following chemotherapy treatment to reduce the size of the tumour (Swift, C.C., Eklund, M.J., Kraveka, J.M. and Alazraki, A.L 2018). However, with high-risk patients a more aggressive approach is needed with combination therapy such as chemotherapy and radiotherapy but following an initial response to chemotherapy a large majority of these patients will develop resistance to therapy and relapse (Eleveld, T., Oldridge, D.A., Bernard, V., Koster, J., Daage, C *et al* 2015). Recent studies discuss the findings of possible targets in relapsed neuroblastomas due to a high frequency of genetic aberrations and mutations. With an emphasis on understanding the current genetic landscape of a tumour and not at diagnosis to better assess treatment (Padovan-Merhar, O.M., Raman, P., Ostrovnaya, I., Kalletla, K., Rubnitz, K.R *et al* 2016). The use of drug-adapted cell lines is an invaluable tool in this research to better understand the current genomic landscape of a tumour. Chromosomal analysis has also been extensively researched to determine patterns in neuroblastoma and possible diagnostic and treatment options. Analysing chromosomal changes is another diagnostic technique and a loss of heterozygosity (LOH) at chromosome 1p and 11q is a frequent mutation seen in neuroblastoma (Attiyeh, E.F., London, W.B., Mosse, Y.P., Wang, Q., Winter, C., *et al* 2005). High risk patients with stage 4 disease often present with several CNV (copy number variants) and the tumours of these patients contain multiple chromosomal abnormalities (Tonini, G.A 2017).

Immunotherapy is another therapeutic approach but has had some difficulty due to low expression levels of antigens. However, disialoganglioside (GD2) is highly expressed on the majority of neuroblastoma cells and is a promising target for both diagnosis and treatment with the use of monoclonal antibodies (mABs) (Seeger, R.C 2011).

As amplification of MYCN represents approximately 20% of all neuroblastomas and 45% of high risk it is a valid target to use in treatment of the disease. (Barone, G., Anderson, J., Pearson, A.D.J., Petrie, K and Chesler, L 2013). A recent study analysed the efficacy of inhibitors such as vismodegib, which targets the NF-kB and mTOR pathway, alongside he chemotherapy drug topecan in non-MYCN and MYCN amplified neuroblastomas. The combination of the two drugs had the highest activity in vitro and vivo with decreased tumour growth (Chaturvedi, N.K., McGuire, T.R., Coulter, D.W., Shukla, A., McIntyre, E.M *et al* 2016).

A great deal of research has been carried out on neuroblastoma and patient outcomes have improved but further research is needed to understand the resistance mechanisms underlying relapse of the disease. This is the reason neuroblastoma cell lines were used for the research carried out in this project, including both sensitive and resistant sub-lines to a range of therapeutics. In particular, to better understand the intra-cell line heterogeneity and the clonal evolution seen in these cell lines and responses to drugs with varied mechanisms.

### 1.4 Multidrug resistance

Multidrug resistance (MDR) in cancer is an important issue that needs addressing in the effective treatment and management of cancer.

In cancers such as neuroblastoma, patients are initially responsive to chemotherapy with late stage disease but then develop acquired resistance leading to relapse and eventually treatment failure. As an example, both MRP1 and MRP4 (multi-resistance associated protein) have an increased expression and altered N-link glycosylation which leads to resistance in ovarian tumour cell lines to the platinum drug oxaliplatin (Beretta, G.L., Benedetti, V., Cossa, G., Assaraf, Y.G., Bram, E *et al* 2010). It Is therefore imperative to understand the underlying resistance mechanisms in order to overcome them in the designing of new therapeutics and possible diagnostic markers of the emergence of resistance. The most commonly known mechanisms of multidrug resistance include: decreased drug uptake, increased drug efflux, activation of detoxifying systems, activation of DNA repair mechanisms and evasion of drug induced apoptosis (Housman, G., Byler, S., Heerboth, S., Lapinska, K., Longacre, M., Snyder, N *et al* 2014).

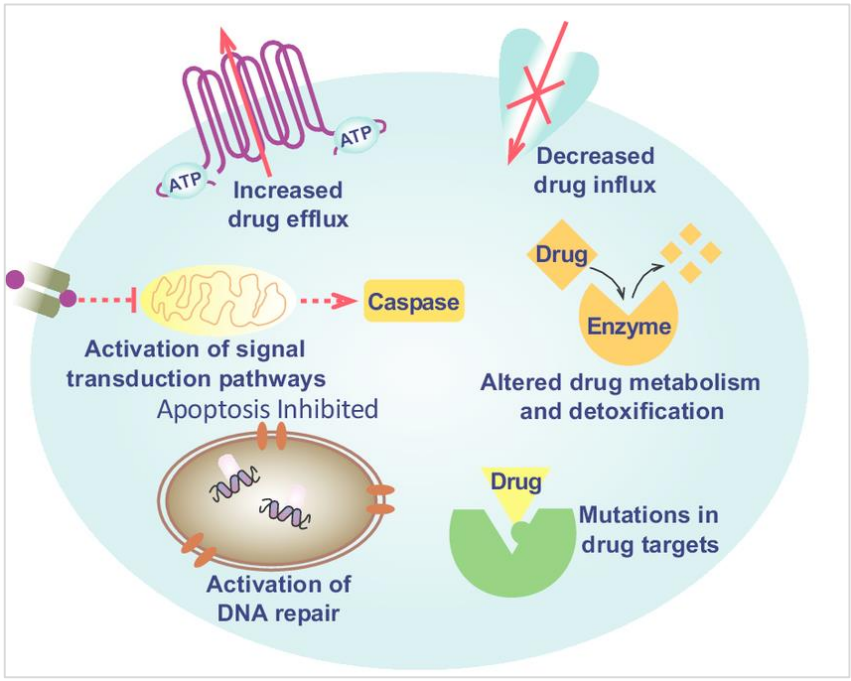


Figure 2: Multidrug resistance mechanisms in cancer cells with the seven key categories: decreased drug influx, increased drug efflux through ATP binding cassette transporters, altered drug metabolism and detoxification, mutations in drug targets, activation of transduction pathways and activation of DNA repair (Yang, X., Cheng, Y., Luo, N and Changyang, G 2014).

#### 1.4.1 ATP binding cassette transporters

The most extensively studied mechanism for multidrug resistance is the ATP binding cassette (ABC), transporters responsible for the efflux of drugs but other mechanisms such as: cell cycle arrest and checkpoint alteration, reduced uptake of drug and sequestering of drugs inside the cytoplasm in lysosomes (Szakacs, G., Paterson, J.K., Ludwig, J.A., Boothe-Genthe, C., and Gottesman, M.M 2006).

One of the members of the ABC transporter family is ABCB1, also known as multidrug resistance protein 1 (MDR1) or P-glycoprotein is commonly overexpressed and linked with resistance to chemotherapeutics in a multitude of cancers including neuroblastoma (Fletcher, J.I., Haber, M., Henderson, M.J. and Norris, M.D 2010). ABCB1 effluxes a spectrum of anti-cancer drugs with differing methods of action including, among others: vinca alkaloids, taxanes and kinase inhibitors (Katayama, K., Noguchi, K and Sugimoto, Y 2014). This reduces the toxicity to the cancerous cells allowing them to continually proliferate in the presence of lower concentrations of the drug therefore driving resistance. An elevated expression of ABCB1, therefore, is indicative of poor prognosis due to its role in resistance (Vaidyanathan, A., Sawyers, L., Gannon, A.L., Chakravarty, P., Scott, A.L 2016). Decreased uptake of a drug within a cell is another factor in MDR such as a reduced uptake of methotrexate due to decreased expression of the reduced-folate carrier (SLC19A1/ hRFCT) (Gillet, J.-P and Gottesman, M.M 2009). The SLC family includes passive and ion-coupled transporters and any mutations to these transporters could impact the amount of drug transported into a cell. Further research discusses the suppression of endocytosis in relation to drug resistance which may work in conjunction with drug efflux ultimately reducing the concentration of drug within a cell and therefore allowing continual proliferation (Pisco, A.O, Jackson, A.D and Huang, S 2014). A reduced uptake of the drug cisplatin in cancer cells can be due to changes in endocytosis by membrane protein mislocalisation such as transferrin which is linked to the endocytic recycling compartment (ERC) which is altered in resistant cells. (Liang, X-J., Mukherjee, S., Shen, D-W., and Maxfield, F.R 2006). Another major influx transporter, the copper transporter receptor 1 (CTR1) has also been shown to have a role in platinum drug resistance and reduced accumulation of the therapeutics (Kilari, D., Guancial, E and Kim, E.S 2016).

### 1.4.2 Altered drug metabolism and detoxification

Drug metabolism, the chemical alteration of a therapeutic by the body, is clearly an important process in the treatment of cancer which can be exploited by cancer cells to prevent uptake of the drug and subsequent cell death. This can also include drug metabolising enzymes (DMEs) which regulate the activation and deactivation of therapeutics and those altered in tumours include among others: glutathione-S-transferases (GSTs) and uridine diphospho-glucuronoslytransferases (UGTs) (Pathania, S., Bhatia, R., Baldi, A., Singh, R and Rawal, R.K 2018). GSTs are detoxification enzymes which in normal cells, offer protection from oxidative stress as well as inhibition of the MAPK pathway. An increase in GSTs can then lead to drug resistance for example, cisplatin and doxorubicin resistance have been linked to an increase in the production of glutathione and detoxification caused by its transferases (Mansoori, B., Mohammadi, A., Davudian, S., Shirjang, S and Baradaran, B 2017). Ovarian cancer can also present with high expression of GSTs including GSTP1, reducing the efficacy of platinum-based therapeutics and facilitating resistance. (Sawyers, L., Ferguson, M., Ihrig, B., Young, H., Chakravarty, P *et al* 2014).

### 1.4.3 Activation of DNA repair

In normal cells, DNA repair mechanisms including nucleotide excision repair (NER) and base excision repair (BER) ensure that genomic integrity of DNA is preserved, and repair damage via a complex network known as the DNA damage response (DDR) (Torgovnick, A and Schumacher, B 2015). Cells with DNA that is irreparable and extensive damage enter apoptosis, necrosis or senescence (Gillet, J-P and Gottesman, M.M 2009). However, in cancerous cells which have acquired resistance, defective DNA damage repair allows proliferation of cancerous cells and an increase in mutation without leading to cell necrosis. This increase in mutations can lead to outgrowths of phenotypes which select for resistance to chemotherapy as well as further DNA damage, leading to a combination of further MDR mechanisms. Cells treated with the DNA-damaging agent cisplatin develop resistance via decreased membrane transport, increased DNA repair and increased tolerance to DNA damage (Kelland, L 2007).

### 1.4.4 Mutations in drug targets

Alterations in drug targets is a well-documented mechanism of drug resistance as cancer treatment usually relies on the interaction between a therapeutic and an intracellular enzyme. A change in these enzymes occurs in resistant cells to render the drug target useless. Mutations in drug targets can also cause structural changes which can lead to acquired resistance as the drug may no longer be active (Kumar, T., Chaudhary, K., Gupta, S., Singh, H., Kumar, S *et al* 2013). There is a great deal of crossover with other mechanisms due to the alterations in drug targets, but examples include EGFR which is targeted by erlotinib and gefitinib, but resistance occurs, and this is due to additional mutations to EGFR which cannot be overcome (Regales, L., Gong, Y., Shen, R., de Stanchina, E., Vivanco, I *et al* 2009).

### 1.4.5 Activation of signal transduction pathways

Resistance can also be caused by alterations in signalling pathways which control upstream or downstream processes. This can lead to an up-regulation in gene expression or produce proteins with favourable mutations such as proliferation and apoptosis evasion (Sever, R and Brugge, J.S. 2015). Signal transduction pathway mutations can cause and/or effect previous mechanisms discussed as resistant cells are able to utilise multiple mechanisms. Mutations in these pathways can have effects on RTKs, GTPases, lipid kinases as well as transcription factors and cyclins. Therefore, the activation of these pathways in resistant cells is a method of continual cell growth as well as the other hallmarks of cancer. The continuous unregulated growth of cancerous cells leads to further mutations and increased heterogeneity leading to difficulties in subsequent treatment of (Sever, R and Brugge, J.S. 2015).

### 1.5 Clonal evolution

The concept of clonal evolution was first proposed by Peter Nowell in the late 1970s, he conceptualised the theory that tumours start from a single progenitor cell having undergone a series of mutations. Only one mutation was necessary to instigate the selection process and present an advantageous genotype which would lead to the outgrowth of the tumour (Nowell, P.C 1976). Nowell also described the notion of personalised therapies, with each patients' disease presenting individually as well as the difficulties arising with resistant sub-clones. Further research tells us that cancer is indeed an evolutionary process which Greaves, M and Maley, C.C 2012 describe as an expansion of clones and a diversification of genetics resulting in the selection of certain clones. These three processes together increase the chances of advantageous mutations promoting pro-oncogenic effects such as proliferation and resistance to certain therapeutics. Figure 3 illustrates the different sub-clones which exist within a tumour and how some of these clones can lead to further outgrowths of multi-clonal populations. This is due to the Darwinian evolution of cancer cells and the selection of the fittest clones, with those able to withstand and proliferate in the presence of drug continually growing within the tumour (De Sousa E Melo F., Vermeulen, L., Fessler, E and Medema, J.P 2013). Due to uncontrolled rapidly growing cells within a tumour, the rate of copy error is much higher giving rise to a variety of mutations (Burrell, R.A., McGranahan, N., Bartek, J and Swanton, C 2013) and further selection.

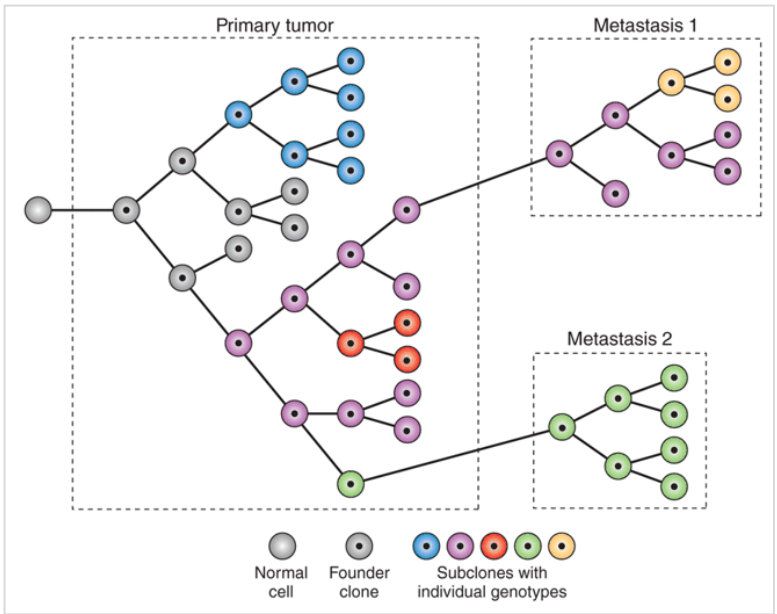


Figure 3: The process of clonal evolution in a primary tumour with a multitude of different sub-clones derived from a single normal cell. The founder clone drives the growth of further sub-clones within the with two leading to metastatic growths. Further clonal evolution is observed in metastasis 1 (Caldas, C 2012).

The addition of therapeutics is a selective pressure and can drive clonal selection and the heterogeneity of a tumour (Greaves, M and Maley, C.C 2012). With the use of therapeutics

potentially enhancing the genetic drift it is vital therefore, to comprehend the impact this has on the tumour environment. When a patient is diagnosed it is vital that the correct treatment is administered to ensure that the entire tumour is successfully eradicated which is indicative through the use of systemic treatment rather than a targeted approach (Marjanovic, N.D., Weinberg, R.A and Chaffer, C.L 2013). Interestingly, further analysis using whole exome sequencing of cancer cells revealed that intra-tumour heterogeneity and therefore clonal evolution was found at both the primary and metastases sites as illustrated in Figure 3 (Caldas, C 2012). Clonal evolution and heterogeneity are both essential in the research surrounding drug resistance and part of this thesis investigated the similarities and differences seen between a sensitive parental cell line and 10 single-cell derived clones. This allowed us to look in depth into the clones in the presence of certain drugs, their growth patterns and chromosomal changes. Alongside single-cell derived clones we also use drug-adapted sub-lines to compare and this could determine underlying evolutionary processes that could lead to drug resistance. Ultimately the aim, is to discover novel tumour markers, new drug targets and diagnostic markers for resistant cancers.

### 1.6 Tumour heterogeneity

A deeper understanding of the heterogeneity involved in tumours is paramount to uncovering the key to successfully treating drug resistance. Cancer is a dynamic process and the genomic landscape within a tumour is continuously evolving due to the tumour microenvironment and response to external therapeutic pressures. Genetic changes (as well as transcriptomic, epigenetic and phenotypic) gives rise to heterogeneity in the tumour with cancerous cells presenting different sensitivity responses to anti-cancer drugs (Dagogo-Jack, I and Shaw, A.T., 2017).

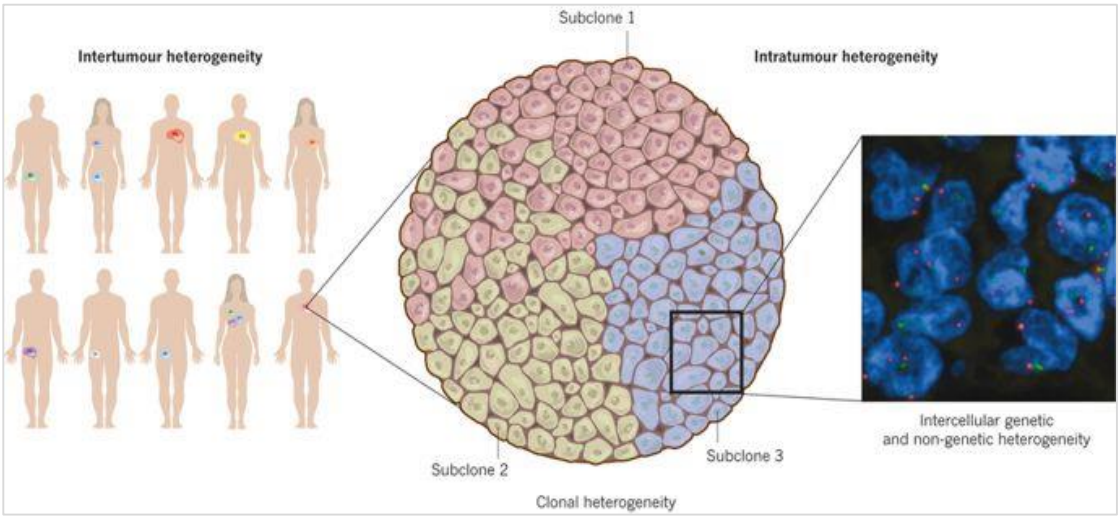


Figure 4: Inter-tumour heterogeneity illustrated as patients with the same tumour type presenting differently as well as different genetic changes within tumours in the patient. And intra-tumour heterogeneity with a tumour presenting with more than one sub-clone which can give rise to altered gene expression highlighted using FISH with chromosome 2 in red, chromosome 18 in green and DNA in blue (Burrell, R.A., McGranahan, N., Bartek, J and Swanton, C 2013).

There are two types of heterogeneity as illustrated in figure 4. Inter-tumour heterogeneity occurs as different genetic changes in different tumours from a single patient as well as between patients with the same tumour type and intra-tumour heterogeneity where there is a presence of more than one clone of cancer cells within the tumour (Yancovitz, M., Litterman, A., Yoon, J., Ng, E., Shapiro, R.L *et al* 2012). The focus of the research in this project was on intratumoural heterogeneity.

### 1.6.1 Intra-tumour heterogeneity

It is well documented that patients presenting with the same cancer type can have completely different responses to treatment due to the varied genetic landscape bought about by heterogeneous tumours. This is known as intra-tumour heterogeneity and in addition, cancer diseases are characterised by tremendous intra-tumour heterogeneity (De Sousa E Melo F., Vermeulen, L., Fessler, E and Medema, J.P 2013). Evolutionary processes in the genetically unstable cancer cells largely drive this process and there are three major factors which includes: mutation, selection and drift (Sottoriva, A., Barnes, C.P. and Graham, T.A., 2017). Cancer cells are subject to many selective pressures including effects exerted by the tumour microenvironment and anti-cancer therapies. Even in the absence of a selective pressure, cancer cells are subject to a genetic drift due to their mutator phenotype. This increases the intra-tumour heterogeneity and in turn the likelihood that cells within the cancer population can survive or adapt to changes in the microenvironment (for example during metastasis formation) and to anti-cancer therapies. The key mutation is the driver mutation which is believed to give rise to the disease, initially followed by passenger mutations which give fundamental information on the development of the cancer population over time. Finally, the drift is described as the likelihood that all cells within the population have the potential to produce further cells that will continue to survive. (Sottoriva, A., Barnes, C.P. and Graham, T.A., 2017), (Burrell, R.A., McGranahan, N., Bartek, J and Swanton, C 2013). The tumour microenvironment adds more complexity to the issue as it influences phenotypes of cancerous and non-cancerous cells and changes the intra-tumour heterogeneity further (Rybinksi, B and Yun, K 2016). Following chemotherapy, this can lead to a regression of the tumour, a reduction in tumour size, or relapse followed by the emergence of further outgrowths of advantageous clones, as described previously in clonal evolution. It is this varied response which makes treating heterogeneous tumours so difficult and therefore hard to predict what the patient outcome will be. There is a great deal of variation seen in tumours that derive from the same cell type which leads to chromosomal aberrations, patient outcome and importantly drug sensitivity (Burrell, R.A., McGranahan, N., Bartek, J and Swanton, C 2013). Multiple studies have now shown that the higher the level of intra-tumour heterogeneity the less likely the patient is to respond favourably to therapeutics, particularly those which are targeted (O'Connor, J.P.B., Rose, C.J., Waterton, J.C., Carano, R.A.D., Parker, G.J.M *et al* 2014). Advances in techniques such as single-cell sequencing has allowed a more comprehensive approach into determining expression profiles of

heterogenous cancer populations (Ngan, E.S-W 2015). If only a small section of the tumour is removed, the analysis may not capture the full extent of the intra-tumoural heterogeneity. The treatment regimen is then based on this analysis which may pave the way for selection pressure on the tumour and subsequent resistance (Marusyk, A.V and Polyak, K 2013).

We are able to study the intra-tumour heterogeneity in the cell lines we used for this project and observe the differences seen in populations derived from the same cell type using a cohort of 10 single-cell derived clone cell lines. Using fluorescence *in situ* hybridisation (FISH) as a method we observed changes in chromosomal aberrations between cell lines i.e. genomic instability as well as drug sensitivity assays and growth kinetics. As therapeutic pressures can drive evolutionary processes within the tumour, the use of drug-resistant sub-lines and observing these differences, in this project was paramount to observing these changes.

### 1.7 Genome instability in Cancer

Due to the high levels of genetic instability in cancerous cells there are a high number of chromosomal aberrations due to the rapidly dividing cells inducing many mutations. It is a characteristic of most cancer cells and is one of the hallmarks of cancer. Genomic stability is essential for normal cell growth including prevention of DNA replication errors and tumour cells have mutations which enable the bypassing of these checkpoints. There are thought to be three main mechanisms of genomic instability: increased frequency of base pair mutation due to the loss of function in DNA repair genes BER and NER, decreased mismatch repair impacting on microsatellites within the tumour and chromosomal instability (Yao, Y and Dai, W 2014). An understanding of chromosome abnormalities in cancer is crucial to tracking diagnosis and disease progression and the work in this thesis focused on chromosomal changes between cell lines. These aberrations can then be analysed in cohorts of patients to determine if there are any continuous patterns, which indicate areas such as prognosis, resistance mechanisms and drug sensitivity. One such example is FISH analysis of neuroblastoma documented by (Bogen, D., Brunner, C., Walder, D., Ziegler, A., Abbasi, R *et al* 2016) where the research carried out indicated an aberration of the 11q deletion. The intra-tumour heterogeneity of tumours can be researched by the use of FISH to discover specific biomarkers for resistance, diagnosis and treatment Studies carried out in neuroblastoma suggest that the damage that the chromosomes undergo in particular, within the tumour microenvironment is indicative of a key role in the growth of the tumour. A common mutation on chromosome 1p was discovered with links to poor prognosis and alongside this a tumour suppressor gene KIF1Bβ was located in this region of the chromosome and knockout of KIF1Bβ led to a major increase in proliferation and tumour growth (Tonini, G.P, 2017). There has been extensive research into reoccurring characteristic chromosomal aberrations seen in cancers to utilise in treatment. One example is the anaplastic lymphoma kinase (ALK) gene located on chromosome 2 and is altered in cancers including non-small-cell lung cancer (NSCLC) and

neuroblastoma, crizotinib was developed to target this mutation (Holla, V.R., Elamin, Y.Y., Bailey, A.M., Johnson, A.M., Litzenburger, B.C *et al* 2017). However, the issue lies following the discovery of a specific target in drug resistance and indeed with crizotinib cancer cells can develop alternative ALK pathways such as EGFR and INGR (Doebele, R.C., Pilling, A.B., Aisner, D.L., Kutateladze, T.G, Le, A.T *et al* 2012).

Although many types of cancer continue to have successes and improvements in outcome, it is the heterogeneous nature of cancer that contributes to low success rates, higher mortality and a difficulty in searching for valid drug targets (Allison, K.H. and Sledge, G.W. 2014). To conclude, certain cancers, such as high-risk neuroblastoma, are intrinsically difficult to treat owing to the intra-tumour heterogenicity due to genomic instability bought about by various cellular changes.

### 1.8 Use of cell lines in research

Cancer cell lines have been a leading model for the investigation of cancer cell biology and for the identification of anti-cancer drug targets and anti-cancer drugs (Sharma, S.V., Haber, D.A and Settleman, J 2010, Iorio, F., Knijnenburg, T.A., Vis, D.J., Bignell, G.R., Menden, M.P *et al.*, 2016). It is important to use cell lines as a model as it is not possible to monitor tumour progress throughout treatment. As the majority of tumours are analysed fully following removal from a patient, studying the progression of a tumour and the cell populations could indicate changes which may lead to the emergence of certain clones, which are resistant to chemotherapeutics and can result in treatment failure. Cancer cell lines also play a major role in the investigation of acquired drug resistance. Since it has been shown that the resistance mechanisms underlying acquired resistance can substantially differ from those underlying intrinsic resistance (Hata, A.N., Niederst, M.J., Archibald, H.L., Gomez-Caraballo, M., *et al* 2016, Carter, L., Rothwell, D.G., Mesquita, B., Smowton, C., Leong, H.S *et al.,* 2017), pre-clinical model systems of acquired drug resistance are needed to fill this gap. Pre-clinical models enable:

1) the detailed systems level monitoring of processes in cancer cell populations in response to therapy over time which is limited in the clinical setting due to intra-tumour heterogeneity (Zardavas, D., Irrthum, A., Swanton, C and Piccart, M 2015; Esposito, A., Criscitiello, C., Locatelli, M., Milano, M., Curigliano, G 2016).

2) The study of a large number of different cancer treatments (which is clinically limited by patient numbers and patients' right to the best available therapy).

3) Extensive functional studies including the comparative testing of different therapy regimens in a given cancer population (clinically, every individual patient can only be treated once). In particular, 'exceptional responders' i.e. the small number of patients with a specific form of cancer that can benefit from a treatment that is usually not used for this indication (Zardavas, D., Irrthum, A., Swanton, C and Piccart, M 2015; Mehra N, Lorente, D and de Bono, J.S.,2015), are very difficult to identify.

Cancer cell lines enable the generation of a large number of individual models needed to cover the complexity of the resistance formation process. Major resistance mechanisms have been discovered in drug-adapted cell lines, e.g. the ATP binding cassette (ABC) transporters ABCB1 (Juliano, R.L and Ling, V., 1976) and ABCB1 (Cole, S.P., Bhardwaj, G., Gerlach, J.H., Mackie, K.E., Grant, C.E *et al.,* 1992). Moreover, drug-adapted cancer cell lines have been successfully used by different research groups to identify and investigate clinically relevant acquired resistance mechanisms to anti-cancer drugs which are targeted (Engelman, J.A., Zejnullahu, K., Mitsudomi, T., Song, Y., Hyland, C *et al* 2007; Nazarian, R., Shi, H., Wang, Q., Kong, X., Koya, R.C *et al* 2010; Michaelis, M., Rothweiler, F., Barth, S., Cinatl, J., van Rikxoort, M *et al* 2011; Poulikakos, P.L., Persaud, Y., Janakiraman, M., Kong, X., Ng, C *et al* 2011; Michaelis, M., Rothweiler, F., Agha, B., Barth, S., Voges, Y *et al* 2012; Joseph, J.D., Lu, N., Qian, J., Sensintaffar, J., Shao, G *et al* 2013; Korpal, M., Korn, J.M., Gao, X., Rakiec, D.P., Ruddy, D.A *et al* 2013; Crystal, A.S., Shaw, A.T., Sequist, L.V., Friboulet, L., Niederst, M.J., *et al* 2014; Hata, A.N., Niederst, M.J., Archibald, H.L., Gomez-Carabello, M., Siddiqui, F.M *et al* 2016; Jung, J., Lee, J.S., Dickson, M.A., Schwartz, G.K., Le Cesne, A *et al* 2016) and cytotoxic (Domingo-Domenech, J., Vidal, S.J., Rodriguez-Bravo, V., Castillo-Martin, M., Quinn, S.A *et al* 2012; Zahreddine, H.A., Culjkovic-Kraljacic, B., Assouline, S., Gendron, P., Romeo, A.A *et al*., 2014; Gollner, S., Oellerich, T., Agrawal-Singh, S., Schenk, T., Klein, H.U *et al* 2017; Schneider, C., Oellerich, T*.,* Baldauf, H.M., Schwartz, S.M., Thomas, D., *et al* 2017). In addition, a screen in a panel of drug-adapted urothelial cancer cell lines identified the vinca alkaloids: vinblastine and vinflunine, the approved second line therapeutic for metastatic urothelial cancer, as the most effective compounds (Vallo, S., Michaelis, M., Rothweiler, F., Bartsch, G., Gust, K.M *et al* 2015).

There are of course limitations to the use of cancer cell lines, which include the inability to mimic the exact tumour microenvironment as well as changes that can occur in culturing (Wilding, J.L and Bodmer W.F 2014). However, in order to study cancer effectively, with cells that need to be readily and easily available, a model system is ideal to observe mechanisms such as resistance and cell growth patterns which could in turn enable us to discover potential biomarkers and drug targets. Therefore, drug adapted cell lines which allow for a broad application, are an important aspect of understanding mechanisms of resistance in cancer cells as to constantly remove biopsies from a patient over time to monitor tumour development is not feasible. In the work carried out for this thesis and to study the development of resistance, culturing and analysing neuroblastoma and adapting the cell lines to different clinically relevant chemotherapy drugs was vital to obtain the research presented.

### 1.8.1 Authentication of cell lines in research

Cell line misidentification remains an important issue in cell line-based research and undermines research efforts. This problem has been acknowledged since the 1950s with reports indicating HeLa

cells to be one of the main cell line contaminants as they are known to out-grow other cells due to their rapid and robust growth (Masters, J.R.W., 2010).

The effects of misidentification are widespread due to the fact that the cell line being researched, and later in results published, may not be the cell line it was originally deemed to be. One such example, the cell line KU7 (a urothelial carcinoma cell line) was in fact contaminated with HeLa following 30 years of research with the cell line (Jager, W., Horiguchi, Y., Shah, J., Hayashi, T., Awrey, S., Gust, K.M *et al*., 2013). This highlights a concern with using cell lines as a model for further research, carried out by other labs and if it is found to be either cross-contaminated or indeed a different cell line, a substantial amount of money and time has been wasted. Furthermore, retractions may also occur due to irreproducibility with cell lines, examples include Clement, V., Marino, D., Cudalbu, C., Hamou, M.F., Mlynarik, V *et al* 2010 and their research group retracting an article due to cell line contamination. A further example, with over 1000 articles published, is MDA-MB-435, a triple negative breast cancer cell line, described as a melanoma cell line M14 (Freedman, L.P., Gibson, M.C., Ethier, S.P., Soule, H.R., Neve, R.M., *et al* 2015). Consequently, there is clearly a need for authentication of cell lines, the current gold standard is short tandem repeat (STR) profiling in order to verify cell line origin and the generation of databases such as the US National Centre for Biotechnology Information, to compile STR data (Masters, J.R., Thomson, J.A., Daly-Burns, B., Reid, Y.A., Dirks, W.G *et al.,* 2001).

Originally used as a forensic method, STR profiling analyses the length of loci in short DNA sequences with a varying number of repeats allowing a comparison between cell lines (Somaschini, A., Amboldi, N., Nuzzo, A., Scacheri, E., Ukmar, G *et al.,* 2013). This issue also led to the assembly of American Type Culture Collection-Standard Development Organisation (ATCC-SDO), with the aim of ensuring proper practice and cell line standards in aid to reduce the issues surrounding misidentification (Masters, J.R. 2012). However, there is still an unwillingness to report findings which implies that there is still a great deal of cell lines being used which are not of the genetic origin they are believed to be.

Whilst STR profiling enables the differentiation between cell lines of different origin, it does not discriminate between cell lines of the same genetic origin. Since this project deals with isogenic cell lines i.e. single-cell derived clonal and drug adapted sub-lines, we investigated the development of a method to authenticate the cell lines. MALDI-ToF is clinically used in the diagnosis of bacterial pathogens and diseases (Seng, P., Drancourt, M., Gouriet, F., La Scola, B., Fournier, P.E *et al* 2009). Research using MALDI-ToF for bacterial identification has shown great success demonstrating that by using this method, 95.4% of 1660 bacteria samples collected were correctly identified using MALDI-ToF rather than the usual Gram staining and other testing methods (Seng, P., Drancourt, M., Gouriet, F., La Scola, B., Fournier, P.E *et al* 2009). With these promising findings and based on a protocol that had been developed to characterise Chinese Hamster Ovary (CHO) cell lines for industrial biotechnology purposes (Povey, J.F., O'Malley, C.J., Root, T., Martin, E.B., Montague, G.A

*et al*, 2014), we investigated the prospects of the method for authenticating drug-adapted cancer cell lines. If proven to differentiate in the future, we hope to compose a database of mass spec fingerprints for each cell line and allow for rapid identification and conformation that the correct cell line has been used for each set of data.

### 1.9 Project aims

This project investigates different aspects of the use of cancer cell lines for research:

1) Authentication of cell lines of the same genetic origin:

Since this project uses cell lines of the same generic origin (single cell derived clones and drug-adapted sub-lines), we examined to which extent a MALDI-ToF based method (Povey, J.F., O'Malley, C.J., Root, T., Martin, E.B., Montague, G.A *et al*, 2014) and analysis of the proteome is suited to discriminate between these cell lines.

2) Investigation of intra-cell line heterogeneity in the Neuroblastoma cell line UKF-NB-3:

Although intra-cell line heterogeneity has been acknowledged (Goodspeed, A., Heiser, L.M., Gray, J.W and Costello, J.C 2016), it has not been subject to systematic investigations. Hence, we investigated the UK-F-NB-3 cell line, sub-lines which have been adapted to a wide range of anti-cancer drugs (Vogues, Y., Michaelis, M., Rothweiler, F., Schaller, T., Schneider, C., *et al.,* 2016; Loschmann, N., Michaelis, M., Rothweiler, F., Voges, Y., Balonova, B *et al*., 2016; Michaelis, M., Agha, B., Rothweiler, F., Loschmann, N., Voges, L *et al.,* 2015; Loschmann, N., Michaelis, M., Rothweiler, F., Zehner, R., Cinatl, J., *et al* 2013) and its intra-cell line heterogeneity. Single cell-derived clonal UK-F-NB-3 sub lines were characterised for chromosomal aberrations by: multi-colour FISH, for drug sensitivity and their growth kinetics.

3) Establishment of a standardised drug adaptation protocol to compare the potential of drugs with the same drug targets to induce resistance in a given cancer cell line population:

Although it is known that different anti-cancer drugs differ in their potential to induce resistance in a given cancer cell population, assays to document and quantify these effects are missing. To fill this gap, here we established a standardised adaptation protocol and compared the potential of four different stabilizing agents with closely related mechanisms of action: cabazitaxel, docetaxel, epothilone-B and paclitaxel (Dumontet, C. and Jordan, M.A., 2010; Kavallaris, M., 2010).

4) Introduction of a novel SK-N-AS sub-line with acquired resistance to oxaliplatin:

Among models of acquired drug resistance to platinum drugs, oxaliplatin-adapted models are particularly lacking. Hence, we here introduce a novel oxaliplatin-adapted sub line of the non-MYCN-amplified Neuroblastoma cell line SK-N-AS.

# Chapter 2

# Materials and methods

## 2.1 Cell lines and tissue culture

### 2.1.1 Tissue culture and continuous passage of cell lines

Cell lines were maintained in Iscove's Modified Dulbecco's Media (IMDM) (Invitrogen, UK) supplemented with 10% (v/v) Foetal Bovine Serum (FBS) (Sigma–Aldrich, Dorset, UK) and 100 IU/mL penicillin and 100 µg / mL streptomycin (Invitrogen, UK) at 37°C and 5% $CO_2$. Cells were passaged at 70-80% confluency every 5-7 days in a laminar flow cabinet. Cells were washed using sterile Phosphate Buffered Saline (PBS) prepared from pre-formulated tablets (Oxoid Limited, UK) according to manufacturer's instructions. Cells were then detached from the flask using 0.05% (w/v) trypsin - 0.02% EDTA (w/v) solution (Invitrogen, UK) prior to re-suspension in fresh IMDM supplemented with FBS and antibiotics. Drug-adapted cells were, unless stated otherwise, maintained in the presence of the adaptation concentration of the respective drug to sustain the selection pressure. Passage of cell lines was carried out by multiple lab members including Lara Sanders, Lyto Yiangou, Georgia Walden, Victor Aderemi, Hannah Onafuye and Joanna Bird.

### 2.1.2 Cell lines used in this study and their characteristics

| Cell line | MYCN-amplified | Drug concentration | ALK status |
|---|---|---|---|
| UKF-NB-3 | Yes | N/A | ALK mutation |
| UKF-NB-3 single cell-derived Clone 1 | Yes | N/A | ALK mutation |
| UKF-NB-3 single cell-derived Clone 2 | Yes | N/A | ALK mutation |
| UKF-NB- 3 single cell-derived Clone 3 | Yes | N/A | ALK mutation |
| UKF-NB-3 single cell-derived Clone 4 | Yes | N/A | ALK mutation |
| UKF-NB-3 single cell-derived Clone 7 | Yes | N/A | ALK mutation |
| UKF-NB-3 single cell-derived Clone 24 | Yes | N/A | ALK mutation |
| UKF-NB-3 single cell-derived Clone 56 | Yes | N/A | ALK mutation |

| | | | |
|---|---|---|---|
| UKF-NB-3 single cell-derived Clone 64 | Yes | N/A | ALK mutation |
| UKF-NB-3 single cell-derived Clone 80 | Yes | N/A | ALK mutation |
| UKF-NB-3 single cell-derived Clone 93 | Yes | N/A | ALK mutation |
| UKF-NB-3r Oxaliplatin$^{2000}$ | Yes | 2000 ng/ml | ALK mutation |
| UKF-NB-3r Cisplatin$^{1000}$ | Yes | 1000 ng/ml | ALK mutation |
| UKF-NB-3r Carboplatin$^{2000}$ | Yes | 2000 ng/ml | ALK mutation |
| IMR-5 | Yes | N/A | |
| IMR-5r Oxaliplatin$^{4000}$ | Yes | 4000 ng/ml | |
| IMR-5r Vincristine$^{10}$ | Yes | 10 ng/ml | |
| IMR-5r Docetaxel$^{20}$ | Yes | 20 ng/ml | |
| IMR-5r Vinorelbine$^{20}$ | Yes | 20 ng/ml | |
| IMR-5r Dacarbazine$^{40}$ | Yes | 40 ng/ml | |
| IMR-5r Paclitaxel$^{20}$ | Yes | 20 ng/ml | |
| IMR-5r Cisplatin$^{1000}$ | Yes | 1000 ng/ml | |
| IMR-5r Vinblastine$^{20}$ | Yes | 20 ng/ml | |
| IMR-5r Gemcitabine | Yes | 20 ng/ml | |
| IMR-32 | Yes | N/A | WT expressed |
| IMR-32r Oxaliplatin$^{800}$ | Yes | 800 ng/ml | WT expressed |
| IMR-32r Carboplatin$^{1000}$ | Yes | 100 µg/ml | WT expressed |
| IMR-32r Topotecan$^{7.5}$ | Yes | 7.5 ng/ml | WT expressed |
| IMR-32r Melphalan$^{500}$ | Yes | 500 ng/ml | WT expressed |
| IMR-32r Etoposide$^{100}$ | Yes | 100 ng/ml | WT expressed |
| IMR-32r Gemcitabine$^{25}$ | Yes | 25 ng/ml | WT expressed |
| SK-N-AS | No | N/A | |
| SK-N-ASr Oxaliplatin$^{4000}$ | No | 4000 ng/ml | |

UKF-NB-3 was established from a bone marrow metastasis of a patient suffering from a *MYCN*-amplified stage IV neuroblastoma (Kotchetkov, D.R., Driever, P.H., Cinatl, J., Michaelis, M., Karaskova, J *et al* 2005). IMR-32 another *MYCN* amplified cell line, established from an abdominal metastasis, was obtained from DSM (Braunschweig, Germany,). IMR-5, a clonal sub-line of IMR-32, was obtained from Dr Angelika Eggert (University Hospital Essen, Germany). The non *MYCN*-amplified SK-N-AS cell line was obtained from ATCC (Manassas, VA, US).

All resistant sub-lines were established by continuous exposure to stepwise increasing drug concentrations as previously described (Michaelis, M, Rothweiler, F, Barth, S., Cinatl, J., van Rikxoort, M *et al* 2011) and derived from the Resistant Cancer Cell Line (RCCL) collection (www.kent.ac.uk/stms/cmp/RCCL/RCCLabout .html). As a control for later experiments described in chapter 6, the SK-N-AS$^{r}$OXALI$^{4000}$ sub-line, SK-N-AS$^{r}$OXALI$^{-4000}$, was cultivated for at least 10 passages in the absence of oxaliplatin.

### 2.1.3 Drugs

All drugs used in this study were purchased from (Cambridge Biosciences, Cambridge, UK) and dissolved in DMSO (Sigma, Dorset, UK). Cisplatin was obtained from (Sigma, Dorset, UK) and dissolved in 0.9% NaCl solution. Carboplatin was purchased from (SUN Pharmaceutical Industries, Leeds, UK) and dissolved in 5% glucose solution (Sigma, Dorset, UK) Oxaliplatin solution in 5% glucose was obtained from TEVA UK (Castleford, UK) and stored at -20 $^{0}$C.

| | |
|---|---|
| Docetaxel | Oxaliplatin |
| Paclitaxel | Carboplatin |
| Epothilone-B | Cisplatin |
| Melphalan | Cabazitaxel |
| Dacarbazine | Losmapimod |
| Vincristine | 2-methoxyestradiol |
| Vinblastine | Gemcitabine |
| Gemcitabine | Doxorubicin |
| Doxorubicin | Vinorelbine |
| Vinorelbine | Topotecan |
| Topotecan | Etoposide |
| Etoposide | Crizotinib |
| NVP-TAE-684 | |

**Table 1**: All therapeutics used in all results chapters of this thesis with a range of mechanisms discussed in the introduction

## 2.2. Development and assessment of resistance

### 2.2.1 Cell viability MTT Assay

To test the cell viability in the presence of different drugs, the 3-(4,5-dimethlythiazol-2-yl)-2,5-diphenyltetrazolium bromide (MTT) assay was used. This colorimetric assay is based on the colour change of yellow MTT being reduced to an insoluble purple formazan by mitochondrial

dehydrogenases in viable cells only. Following the plate reading at the end of the experiment, the higher the absorbance value, the higher the concentration of formazan which therefore indicates a higher number of viable cells present. The MTT protocol was adapted from (Mosmann, T, 1983) as previously described (Michaelis, M., Matousek, J., Vogel, J.U., Slavik, T., Langer, K *et al* 2000). MTT (Serva Electrophoresis, Cambridge, UK) solution (2mg/mL) was prepared by dissolving MTT in PBS and sterile filtration through a 0.2 µM filter and was stored at 4 $^{0}$C and protected from light.

### 2.2.2 MTT Experiment set up

Cells were grown as described in 2.1.1, until they were 70- 80% confluent and seeded into a 96 well plate (Greiner Bio-One CellStar, Greiner LTD, UK) with 5000 cells per well. Cells were counted using a haemocytometer, after diluting 20 µL re-suspended cells with 20 µL PBS and 40 µL trypan blue (Sigma-Aldrich, Dorset, UK).

An 8-point serial dilution was prepared separately in a deep well drug block (VWR, Leicestershire, UK) with drugs of interest added to supplemented IMDM. The dilutions were then added to corresponding wells in the 96 well plate with two drugs tested in triplicate on each plate against the cell line. None of the outer wells were used due to evaporation but media was added to limit this effect on the main wells. Figure 5 explains the three steps in setting up the experiment, table 2A illustrates the pipetting scheme for the MTT assay. Two controls were also included in each plate, with column 11 containing only 100 µl per well of supplemented IMDM for background and column 2 containing 50 µl of media and 50 µl of cells. Table 2B illustrates the addition of 50 µl of cells in each of the wells including column 2. The scheme for table 2C highlights the addition of the 8-point serial drug dilution series which was carried out for two different drugs and in triplicate. Drug dilutions were carried out at 2x the final concentration to account for dilution from IMDM media added previously to wells. The cells were then incubated for 120 hours at 37 $^{0}$C and 5% $CO_2$. 25 µL 0.2 % (w/v) MTT solution was added to each well and incubated for a further 4 hours. 20% Sodium Dodecyl Sulphate (SDS) (Fisher Scientific, Loughborough, UK) in 1:1 MilliQ water: Dimethylformamide (DMF) (Fisher Scientific, Loughborough, UK) adjusted to pH 4.7 was added to each well and incubated overnight to solubilise formazan. MTT plates were read at 600 nm using a BMG Labtech Fluostar Omega plate reader (Aylesbury, UK)

### 2.2.3 Cell viability MTT assay data analysis

Using the OD readings following the plates being read at 600nm, the relative viability values were calculated using the following equation:

Value in the well – Average mean of only IMDM wells / Average mean of IMDM and cells wells – Average mean of only IMDM wells. These data were then used to calculate $IC_{50}$ values using the Calcusyn software.

Table 2A: Addition of supplemented IMDM to column 2 and 11 as controls

| | 1 | 2 | 3 | 4 | 5 | 6 | 7 | 8 | 9 | 10 | 11 | 12 |
|---|---|---|---|---|---|---|---|---|---|---|---|---|
| A | | | | | | | | | | | | |
| B | | 50 | | | | | | | | | 100 | |
| C | | 50 | | | | | | | | | 100 | |
| D | | 50 | | | | | | | | | 100 | |
| E | | 50 | | | | | | | | | 100 | |
| F | | 50 | | | | | | | | | 100 | |
| G | | 50 | | | | | | | | | 100 | |
| H | | | | | | | | | | | | |

Table 2B: Addition of 50µL of cells to each of the wells highlighted

| | 1 | 2 | 3 | 4 | 5 | 6 | 7 | 8 | 9 | 10 | 11 | 12 |
|---|---|---|---|---|---|---|---|---|---|---|---|---|
| A | | | | | | | | | | | | |
| B | | 50 | 50 | 50 | 50 | 50 | 50 | 50 | 50 | 50 | | |
| C | | 50 | 50 | 50 | 50 | 50 | 50 | 50 | 50 | 50 | | |
| D | | 50 | 50 | 50 | 50 | 50 | 50 | 50 | 50 | 50 | | |
| E | | 50 | 50 | 50 | 50 | 50 | 50 | 50 | 50 | 50 | | |
| F | | 50 | 50 | 50 | 50 | 50 | 50 | 50 | 50 | 50 | | |
| G | | 50 | 50 | 50 | 50 | 50 | 50 | 50 | 50 | 50 | | |
| H | | | | | | | | | | | | |

Table 2C: Addition of the 8-point serial drug dilution carried out for two different drugs

| | 1 | 2 | 3 | 4 | 5 | 6 | 7 | 8 | 9 | 10 | 11 | 12 |
|---|---|---|---|---|---|---|---|---|---|---|---|---|
| A | | | | | | | | | | | | |
| B | | | 1 | 2 | 3 | 4 | 5 | 6 | 7 | 8 | | |
| C | | | 1 | 2 | 3 | 4 | 5 | 6 | 7 | 8 | | |
| D | | | 1 | 2 | 3 | 4 | 5 | 6 | 7 | 8 | | |
| E | | | 1 | 2 | 3 | 4 | 5 | 6 | 7 | 8 | | |
| F | | | 1 | 2 | 3 | 4 | 5 | 6 | 7 | 8 | | |
| G | | | 1 | 2 | 3 | 4 | 5 | 6 | 7 | 8 | | |
| H | | | | | | | | | | | | |

Figure 5: Pipetting scheme for MTT assay with table 2A illustrating addition of media, 2B addition of cells and 2C addition of 8-point serial dilution.

### 2.3 Drug adaptation protocol

Cell lines were passaged every seven days as described in 2.1.1, one week with the $IC_{50}$ concentration of the investigated drugs (docetaxel, paclitaxel, epothilone-B and cabazitaxel) was added and one week without the addition of the drug. Initially, 500,000 cells/ 25cm$^2$ were used in the weeks with drug and 50,000 cells/ 25cm$^2$ in the weeks without drug. When the cells started to adapt to the investigated drugs, the cell numbers had to be adjusted also to 10,000 cells/ 25cm$^2$ in the weeks with drug (please refer to the results section for details).

### 2.4 Proteomic analyses and bioinformatics

This was a collaborative project with another lab group within the department where I dealt with the cell line harvesting and preparation before Jane Povey from the Smales Lab treated the samples on the MALDI-ToF.

### 2.4.1 Collection of cell pellets for intact cell MALDI-TOF mass spectroscopy analysis

Cell lines were grown to 80% confluent and passaged as described in 2.1.1 for a minimum of 3 weeks with the required concentration of drug before harvesting samples of 6.25 x $10^4$ cells. This sample was then centrifuged at 900 g (Eppendorf, Stevenage, UK) for 5 minutes, supernatant was removed, and cells were washed with 200 µL PBS and centrifuged as before. The supernatant was removed, and cells were washed with 200 µL 0.35 M sucrose (Sigma, Dorset, UK) and centrifuged. The supernatant was removed, and cell pellets were stored at -80 $^o$C.

### 2.4.2 Preparation of cell pellets for intact cell MALDI-ToF analysis

Cell pellets were then tested using MALDI-ToF Mass Spectroscopy Analysis and the data analysed as described by (Povey, J.F., O'Malley, C.J., Root, T., Martin, E.B., Montague, G.A *et al*, 2014).
Cell pellets were thawed to room temperature after removal from -80$^0$C then resuspended in 50 µL of matrix solution. The matrix solution consisted of 20 mg / mL saturated sinapinic acid added to a matrix buffer of 40% acetonitrile, 0.06% TFA and placed in a sonicating water bath for 15 minutes before centrifugation. The resuspended cell sample was then incubated for 3 hours at 4 $^0$C before 1 µL was spotted onto a 384 MTP ground steel MALDI-ToF plate (Bruker) before air-drying and then placed into the MALDI-ToF instrument (Bruker Ultraflex). The spectra of the pellets were collected using settings described in Povey, J.F., O'Malley, C.J., Root, T., Martin, E.B., Montague, G.A *et al*, 2014 and calibration within the machine. Following acquisition of data this was then analysed using MATLAB.

### 2.4.3 Generation of PCA (Principal Component Analysis) data

Following the acquisition of the spectra collected from the MALDI-ToF ms instrument (Bruker Ultraflex) machine, principal component analysis was used to analyse the whole cell samples. PCA is well established technique of multivariate analysis (Jolliffe, I.T, 2002) and known as a form of multidimensional scaling.

Principal Component 1, which has the largest possible variance was used in generation of the data alongside principal component 2 and 3 as other variables. Using these principal components, or variables, we identified which cell lines grouped together to indicate differences and similarities where they overlapped. Please see further information in the results in chapter 3.

## 2.5 Fluorescence *in situ* Hybridisation (FISH) including full genome painting and analysis

### 2.5.1 Preparation of fresh KCl buffer and fixing reagent

A fresh stock solution of 750mM KCl (Sigma–Aldrich, Dorset, UK) was made immediately before use and a working concentration of 75mM was made with milliQ water and warmed to 37 $^0$C in a water-bath before use. Fresh fixing reagent (75% methanol and 25% acetic acid) both (Sigma-Aldrich, Dorset, UK) was also made immediately before use in a fume cupboard.

### 2.5.2 Fluorescence in-situ hybridisation (FISH) preparation of cell lines

Cells were cultivated as described in 2.1.1 until 70-80 % confluent in 25cm$^2$ cell culture flasks, which corresponds to approximately 5 x 10$^6$ cells/ 25cm$^2$. 100 ng/mL (w/v) of demecolcine (Sigma-Aldrich, Dorset, UK) solution was added to the flask and then put back into the incubator at 37 $^0$C and 5% $CO_2$ for 40 minutes with the aim to arrest the maximum number of cells in metaphase. After 40 minutes all medium was removed, cells were subsequently washed carefully with sterile PBS before being detached using 0.05% (w/v) trypsin-0.02% (w/v) EDTA solution. Cells were then re-suspended in IMDM supplemented with FBS and antibiotics and centrifuged at 300 g for 5 minutes.

The waste media was removed and the cell pellet remaining in the falcon tube was re-suspended drop wise with 6 mL of warmed 75 mM KCl and then placed into a water bath at 37$^0$C for 12 minutes. After 12 minutes 8 mL of fresh fixing reagent was carefully added at an angle to form two clear distinctive layers. The falcon tube was then inverted several times to mix the two solutions and then centrifuged at 300 g for 5 minutes. All supernatant was removed, and 6 mL of fresh fixing reagent was added to the pellet to re-suspend and then once again centrifuged at 300 g for 5 minutes. The washing process was repeated a further 6 times until finally suspending the pellet in 6 mL of fixing reagent.

### 2.5.3 Preparation of microscope slides for analysis of mitotic phases

10 µL of the 6 mL suspension (containing the cells and fixing reagent) was then dropped onto a SUPERFROST™ slide (ThermoFisher Scientific, UK), followed by the addition of 10 µL of fresh fixing solution. This was left to air dry fully before a cover slip with a thin line of VECTASHIELD® Mounting Medium with DAPI solution (VECTOR Laboratories, Peterborough, UK) was placed firmly over the slide and all air bubbles removed.

This initial test slide was used to determine the mitotic index of the sample which in this context is the number of cells arrested in metaphase identified within a sample. The mitotic index needs to be over 10 to order to progress to the next stage of chromosome painting to ensure there are enough separate metaphases to observe. Once confirmed using the test slide the Cytocell Chromoprobe Multiprobe® OctoChrome™ (Cytocell, Cambridge, UK) kit was used. Table 3 indicates the scope of the experiment as 11 full genomes were analysed from the UK-F NB-3 cell line including the parental and the 10 single cell derived clones from the parentals.

Furthermore, each device from Cytocell allows the user to identify 3 chromosomes in each of the 8 squares by using whole chromosome painting probes for three different chromosomes in three different colour fluorophores; red, green and blue highlighted enabling analysis of an entire genome on one device. All single cell derived UK-F NB-3 clones were analysed in addition to the original UKF-NB-3 parental cell line from where they originated.

| Cell line tested | |
|---|---|
| UKF-NB-3 | UKF-NB-3 single cell-derived Clone 24 |
| UKF-NB-3 single cell-derived Clone 1 | UKF-NB-3 single cell-derived Clone 56 |
| UKF-NB-3 single cell-derived Clone 2 | UKF-NB-3 single cell-derived Clone 64 |
| UKF-NB- 3 single cell-derived Clone 3 | UKF-NB-3 single cell-derived Clone 80 |
| UKF-NB-3 single cell-derived Clone 4 | UKF-NB-3 single cell-derived Clone 93 |
| UKF-NB-3 single cell-derived Clone 7 | |

Table 3: All cell lines tested in the Fluorescence in Situ Hybridisation protocol to investigate intra-cell line heterogeneity by observing chromosome pattern and abnormalities.

Following the manufacturer's instructions, 10 µL of the 6 mL solution was added to each of the squares and allowed to air-dry before following the manufacturers guidelines and hybridising the samples with the device. Following hybridisation, a minimum of 10 images per square were captured using SmartCapture3 and Incremental Capture programs on an Olympus, HAMAMATSU, ORCA – ER microscope.

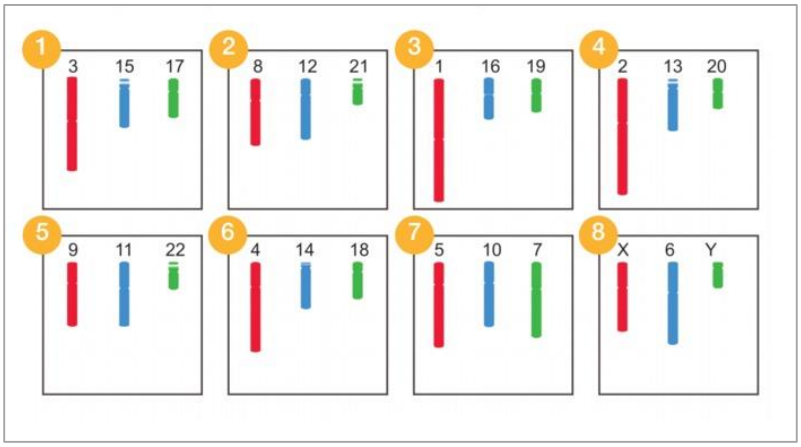


Figure 6: Schematic diagram of the Cytocell Chromoprobe Multiprobe® OctoChrome™ which allows the user to identify three chromosomes per square using fluorescent probes which detect the whole chromosomes and therefore all 24 chromosomes on one slide.

## 2.6 UKF- NB-3 Clone doubling times and growth kinetics using Roche xCELLigence Real Time Cell Analyser (RTCA)

UKF-NB-3 Clone growth curves and doubling times were determined using the RTCA system (ACEA Biosciences, Inc.) following the manufacturer's instructions.

# Chapter 3

# Cell line authentication by Intact cell MALDI-ToF mass spectrometry analysis

## 3.1 Introduction

Since the use of cell lines in research and now with thousands of labs performing tissue culture, cell line misidentification has been identified as a major issue for over 45 years (Editorial, 2009). The first established cell line was the HeLa cell line in 1951, from a cervical tumour biopsy taken from patient Henrietta Lacks that were found to grow successfully in a lab and in 2013 were cited in over 75,000 papers (Callaway, E., 2013).

It has been discovered that HeLa is one of the most common cell line contaminants in several different examples across multiple disciplines and can therefore render results impossible to reproduce in the reported cell line. Kniss and Summerfield 2014, report that the human endometrial epithelial cell line (HES), which was developed in their laboratory in 1989, was in fact contaminated with HeLa. The hepatocellular carcinoma HCC cell line has more than 100 cell lines derived from it including BEL7402 and SMMC7721 which alongside BEL704 and QGY7701 were identified as HeLa reported by another research group, (Rebouissou, S., Zucman-Ross, J., Moreau, R., Qui, Z and Hui, L 2017). Further reports of 'false cell lines' from (Drexler, H.G., Dirks, W.G., MacLeod, R.A and Uphoff, C.C., 2017) examined 848 leukemia, myeloma and lymphoma cell lines from 1990 – 2014 and concluded that cell lines derived from secondary sources maintained a high cross contamination percentage of 14-18% resulting in a risk of 1:6 of working with a false cell line. To summarise, according to the International Cell Line Authentication Committee (ICLAC) roughly 400 cell lines are misidentified (Capes-Davis, A., Theodosopoulos, A.G., Drexler, H.G., Kohara, A., MacLeod, R.A., *et al* 2010).

All of this taken together paints a very worrying picture and how widespread the issue is with the potential use of incorrectly identified cell lines. What this has led to is a need to develop methods to authenticate cell lines effectively, which, from all examples given is clearly essential. Almost all HeLa contaminations were discovered using STR analysis, which is the method of choice for detecting cell line aberrations, this process works by using primers and amplifying specific loci in cell line (Masters, J.A., Thomson, J.A., Daly-Burns, B., Reid, Y.A., Dirks, W.G., *et al* 2001). This is an inexpensive, fairly rapid addition to any research lab ensuring the identity of the cell lines used and has high levels of success. STR can therefore be used to identify cell lines from different genetic origins but there is still a prevalence of contaminated cell lines due to labs not rigorously testing their cell lines.

Another method used in the identification of intact bacteria is MALDI-ToF mass spectrometry, which has shown great success and clinical relevance. The identification of bacteria has been so effective due to the library of known fingerprints taken from intact bacteria, so that the bacterial cells can then be compared against this database (Wunschel, S., Jarman, K.H., Peterson, C.E.,

Valentine, N.B and Wahl, K.L *et al* 2005). The MALDI-ToF method is rapid, inexpensive and easily implemented into clinical practice with (Seng, P., Drancourt, M, Gouriet, F., La Scola, B., Fournier, P.E., *et al* 2009) reporting that it can be used as a first line technique with no prior treatments such as Gram staining. This basis of identification using MALDI-ToF for bacteria with the use of a database with a unique fingerprint has also been applied to the characterisation of mammalian cells. Zhang, X., Scalf, M., Berggren, T.W., Westphall, M.S. and Smith, L.M 2006 stated that with MALDI-ToF they were able to distinguish between three different mammalian cell lines with reproducible and unique mass spectrometry fingerprints. As well as (Rubakhin, S.S and Sweedler, J.V 2007) reporting that MALDI-ToF characterized cell to cell signaling peptides and generated mass spectral fingerprint for single cells. Povey, J.F., O'Malley, C.J., Root, T., Martin, E.B., Montague, G.A *et al*, 2014 used the intact whole cell MALDI-ToF method with the Chinese hamster ovary (CHO) cell line to predict phenotypes in mammalian cell culture.

It is this same intact whole cell method that is used in our approach to differentiate between parental and drug resistant sub-lines. Drug-adapted cell lines are essential for studying mechanisms of acquired drug resistance such as the ATP-binding cassette (ABC) transporters ABCB1 (Szakacs, G., Paterson, J.K., Ludwig, J.A, Booth-Genthe, C., and Gottesman, M.M 2006) shown to be over-expressed in cell lines resistant to multiple therapeutics.

In order to identify drug resistant sub-lines, STR cannot distinguish between the sensitive parental cell line and the subsequent derived drug resistant sub-lines, as they are isogenic. Therefore, we applied the intact whole cell MALDI-ToF approach to differentiate between isogenic cell lines and eventually create a mass spectrometry fingerprint for each drug-adapted cell line as previously described. Principal component analysis was used in this project due to the differentiation it allows groups to form dependent on similarities or differences the cell lines highlighted. The data shown in this chapter is the work of several lab members including Victor Aderemi who contributed in the acquisition of samples and cell culturing.

## 3.2 Initial analysis of the neuroblastoma cell lines UKF-NB-3 and its resistant sub lines UKF-NB-3$^{r}$CDDP$^{1000}$, UKF-NB3 $^{r}$OXALI$^{2000}$ and UKF-NB-3$^{r}$CARBO$^{2000}$

Initially, the neuroblastoma cell line UKF-NB-3 (Kotchetkov, R., Driever, P.H., Cinatl, J., Michaelis, M., Karasova, J., *et al* 2005) was compared to its cisplatin-adapted sub-line UKF-NB-3$^{r}$CDDP$^{1000}$ (Michaelis, M., Agha, B., Rothweiler, F., Löschmann, N., Voges, Y., *et al* 2015) to see if it was in principle, possible to differentiate parental cell lines and their drug adapted sub-lines using an established Intact cell MALDI-ToF mass spectrometry fingerprinting method (Povey, J.F., O'Malley, C.J., Root, T., Martin, E.B., Montague, G.A., *et al* 2014). In Figure 7A using principal component analysis 1 (PCA1) and principal component analysis 2 (PCA2) it was possible to see the two cell lines separate and group with other samples from the same cell line. This clear differentiation indicated

primarily, that the method was able to distinguish between the drug-adapted UKF-NB-3$^{r}$CDDP$^{1000}$ cell line and the UKF-NB-3 parental cell line. Following analysis using PC1 and PC2 we used a further analysis of PC2 and PC3 to see if we could differentiate the cell lines any further. Figure 7B shows the results with the cell lines with two samples (one from each cell line) presenting as outliers but with the majority of samples clustered fairly close together and formed clear distinct groups.

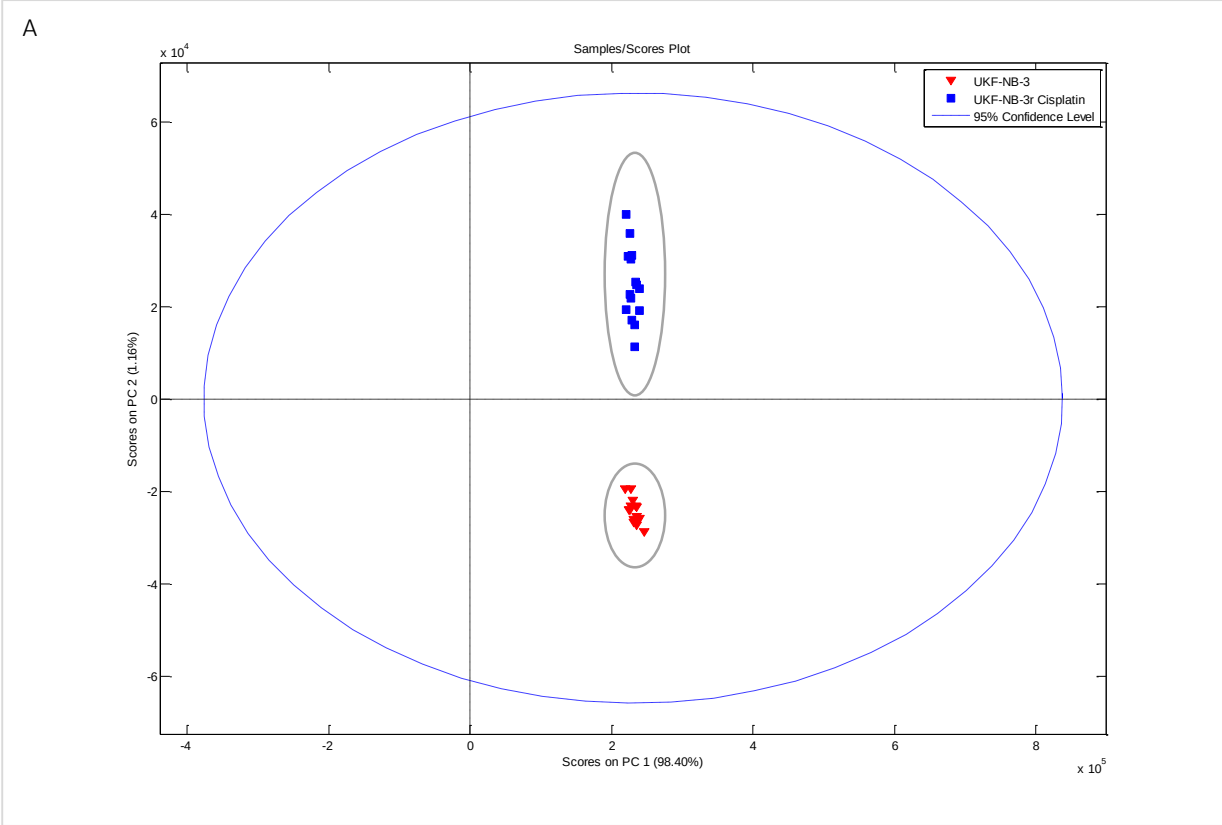


Figure 7A: Principal component analysis using PC1 and PC2 to demonstrate clear separation of UKF-NB-3 parental cell line (red) and UKF-NB-3$^{r}$CDDP$^{1000}$ (blue). As UKF-NB-3$^{r}$CDDP$^{1000}$ is derived from UKF-NB-3 this was a promising initial analysis indicating that the Intact cell method could work as a means to differentiate between cell lines. Each data point in the figure represents an individual analysis of the investigated cell line.

Following this initial promise and encouraging results using the mass spectroscopy approach, we analysed more cell lines by this method. This time a different resistant sub-line, UKF-NB3 $^{r}$OXALI$^{2000}$ resistant to oxaliplatin an alternative platinum drug, was compared with the parental cell line UKF-NB-3. Interestingly, in comparison, analysing by PCA1 and PCA2 did show some separation as shown in Figure 7C with two distinct groups seen. However, there was some overlap between the two cell lines which is highlighted with some of the UKF-NB-3 samples sitting within the UKF-NB-3$^{r}$OXALI$^{2000}$ group. When PCA2 and PCA3 was applied as shown in figure 7D this overlap was shown with UKF-NB-3$^{r}$OXALI$^{2000}$ clustering as a group but UKF-NB-3 was much more spread out instead of grouping as we have seen previously in Figure 7A and 7B. The final UKF-NB-3 resistant line investigated was UKF-NB-3$^{r}$CARBO$^{2000}$ (resistant to carboplatin) against the UKF-NB-3 parental. As shown in Figure 7E the cell lines did not form two distinct groups when PCA2 and PCA3 analysis was applied.

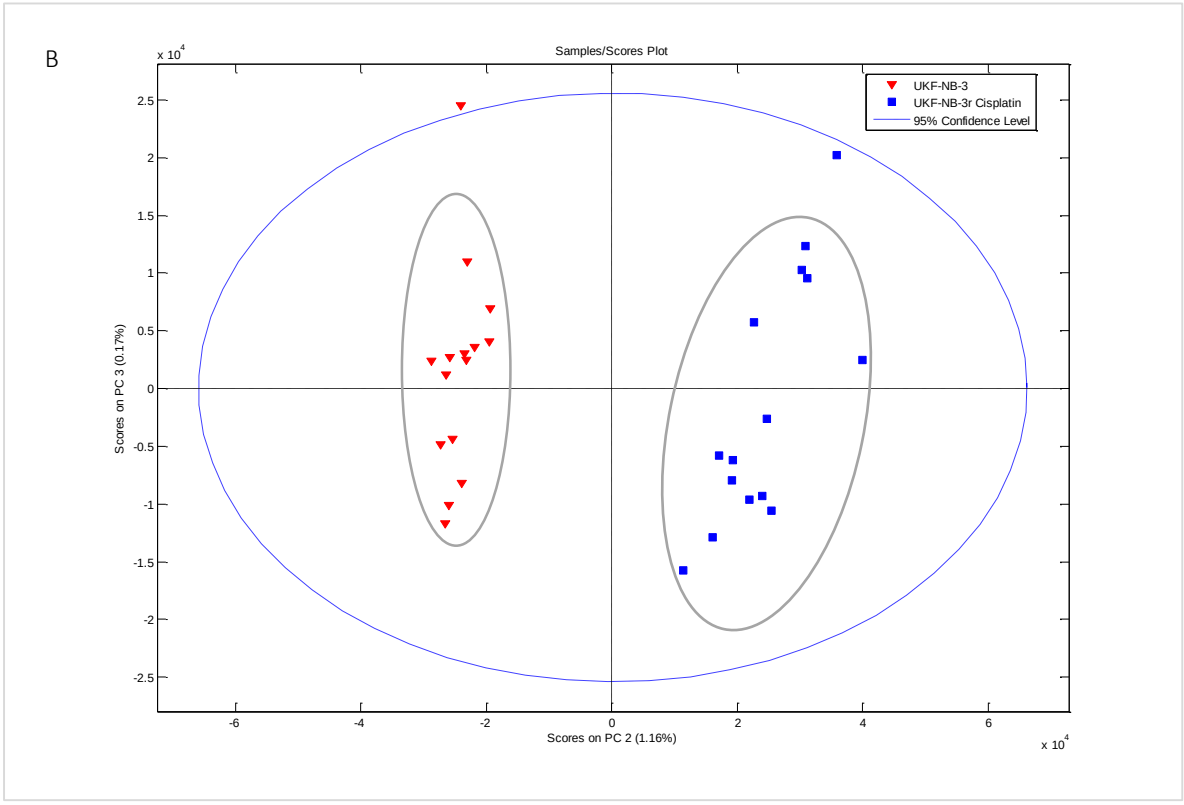


Figure 7B: Principal component analysis of UKF-NB-3 (red) and UKF-NB-3$^{r}$CDDP$^{1000}$ (blue) using PC2 and PC3 to further differentiate the cell lines and a stronger separation is seen. There is one UKF-NB-3 outlier as most other samples have grouped together, UKF-NB-3$^{r}$CDDP$^{1000}$ has more separation between the samples but still consistent grouping together with no samples crossing into the UKF-NB-3 area.

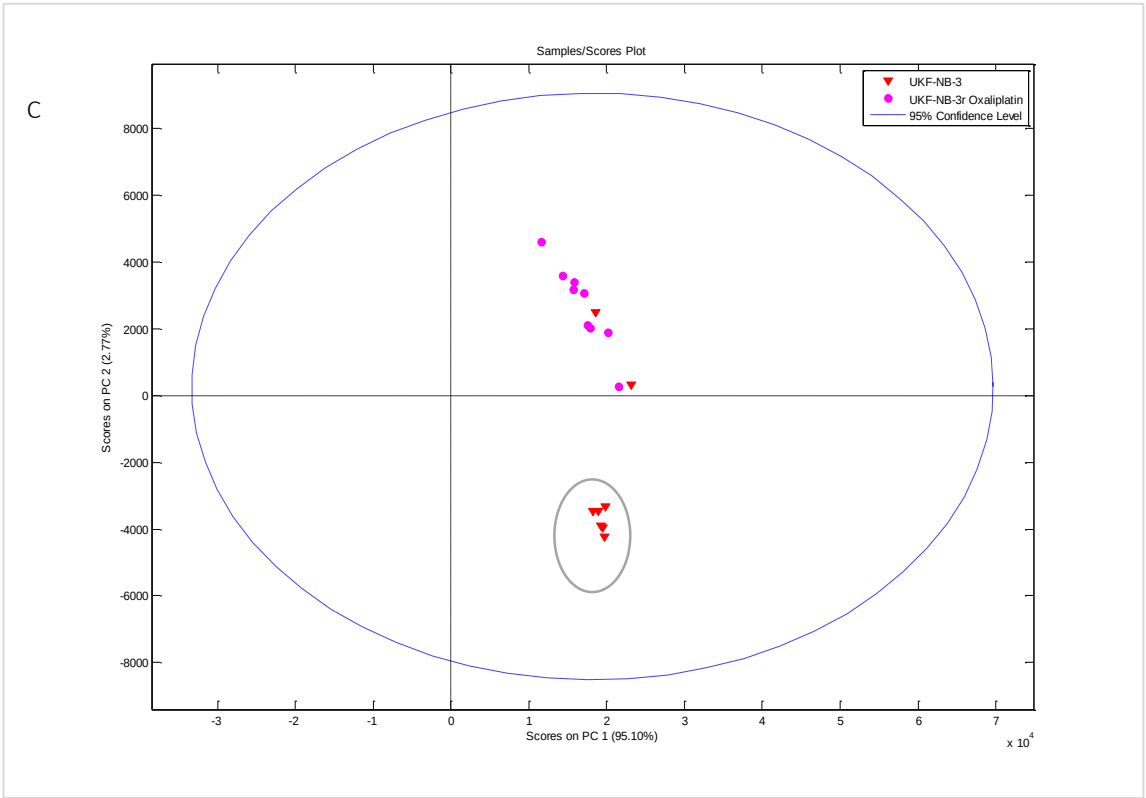


Figure 7C: Principal component analysis of UKF-NB-3 (red) and UKF-NB-3$^{r}$OXALI$^{2000}$ (pink) using PC1 and PC2 to differentiate the cell lines. Interestingly, with these two cell lines there is more overlap of UKF-NB-3 samples within the clustered group of UKF-NB-3$^{r}$OXALI$^{2000}$ as highlighted.

The samples of each cell line overlap with one another and although some of the samples do group the majority are scattered throughout. This was the only occurrence of PCA2 and PCA3 not differentiating the cell lines and this result was not seen in the other resistant sub-lines UKF-NB3 $^{r}$OXALI$^{2000}$ and UKF-NB-3$^{r}$CDDP$^{1000}$ when compared to the UKF-NB-3 parental.

Finally, the parental line UKF-NB-3 was analysed with two resistant sub-lines UKF-NB-3, UKF-NB-3$^{r}$CDDP$^{1000}$ and UKF-NB3 $^{r}$OXALI$^{2000}$ using PCA2 and PCA3 as shown in Figure 7F. The method does show three groups of the cell line samples in particular the UKF-NB3 $^{r}$OXALI$^{2000}$ which has no outliers. Both UKF-NB-3 and UKF-NB-3$^{r}$CDDP$^{1000}$ had several outliers and some samples grouped together, however we still believe the method shows promise and we decided to use different Neuroblastoma cell lines to investigate further.

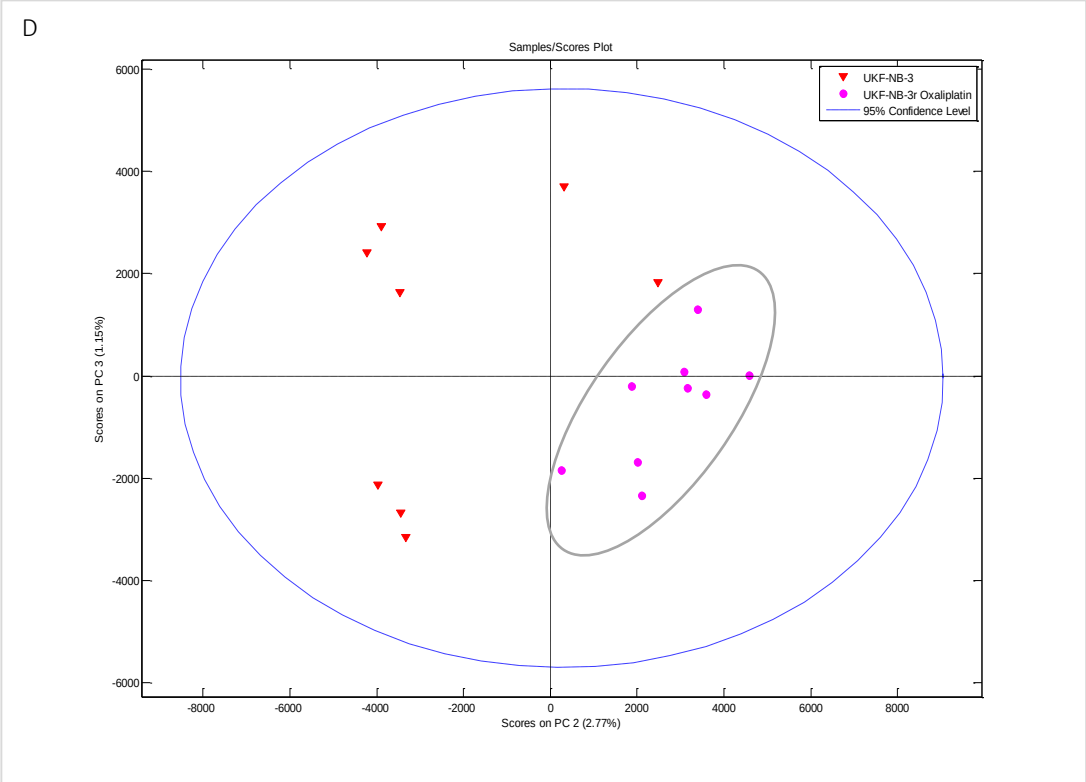


Figure 7D: Principal component analysis of UKF-NB-3 (red) and UKF-NB-3$^{r}$OXALI$^{2000}$ (pink) using PCA2 and PCA3 analysis. The UKF-NB-3 line was much more widespread in this analysis than in previous data and formed smaller clusters rather than one clear distinct group. However, these are still separate from the UKF-NB-3$^{r}$OXALI$^{2000}$ which have formed a clear differentiated group with no outliers.

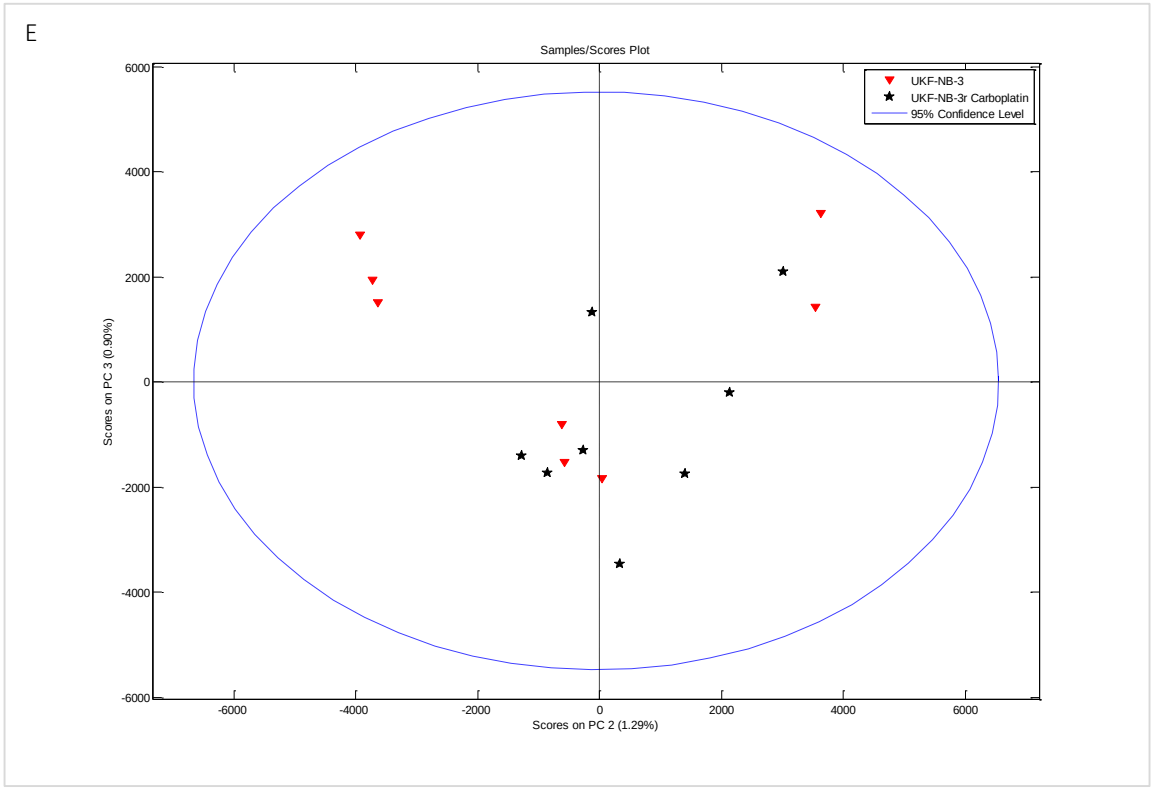


Figure 7E: Principal component analysis of UKF-NB-3 (red) and UKF-NB-3$^{r}$CARBO$^{2000}$ (black) with PCA 2 and PCA3 which previously had separated cell lines effectively. This was a different result by comparison as the two cell lines do not form two distinct groups and the samples group with each other.

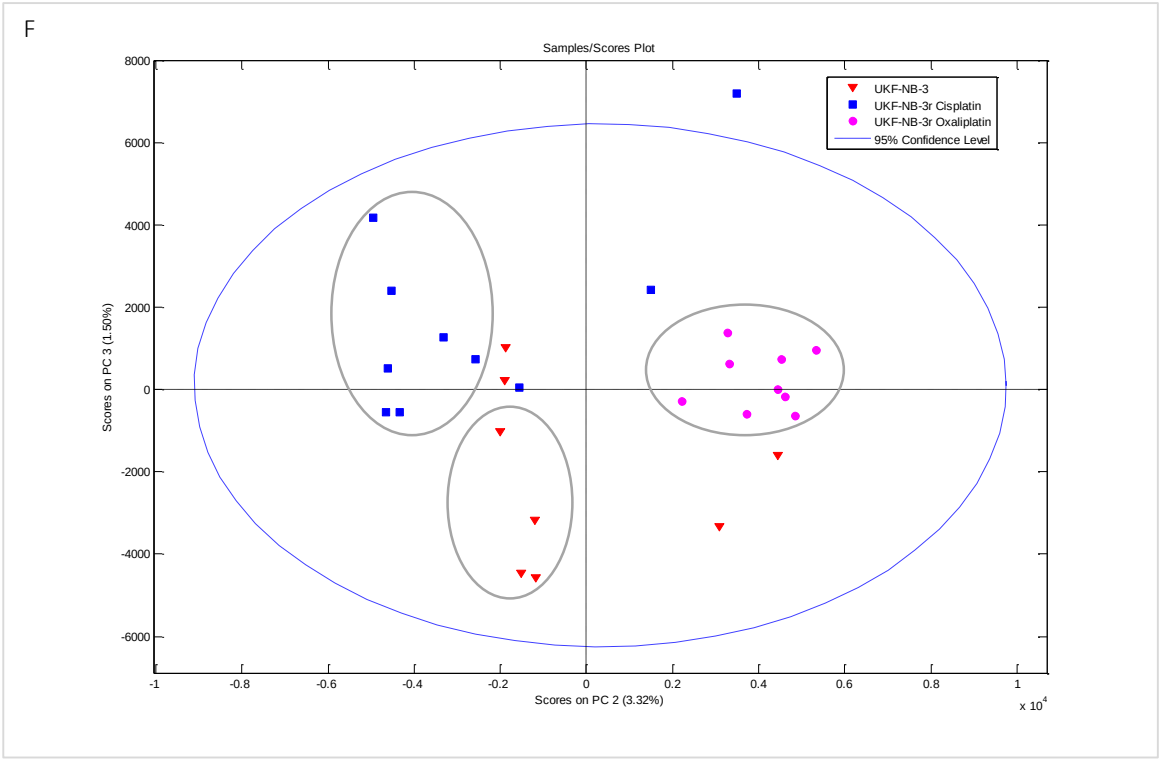


Figure 7F: Principal component analysis of three UKF-NB-3 cell lines with some clear separation into distinct groups using PCA2 and PCA3. UKF-NB-3 (red), UKF-NB-3$^{r}$CDDP$^{1000}$ and UKF-NB-3$^{r}$OXALI$^{2000}$ (pink) appear to group with UKF-NB-3$^{r}$OXALI$^{2000}$ forming the most separate and clear differentiation. UKF-NB-3$^{r}$CDDP$^{1000}$ has several outliers along with a clear group of samples which group together. UKF-NB-3 also has some samples which group but several which sit outside of the cluster and closer to UKF-NB-3$^{r}$OXALI$^{2000}$.

### 3.3 Further analysis of Neuroblastoma cell lines IMR-32 and multiple resistant sub-lines and IMR-5 a clonal sub-line of IMR-32 and multiple resistant sub-lines

Following the initial findings with UKF-NB-3, we decided to look into using another Neuroblastoma cell line, IMR-5 and a selection of derived drug-adapted cell lines including IMR-5$^{r}$CDDP$^{1000}$ (adapted to cisplatin), IMR-5$^{r}$DOCE$^{20}$ (adapted to docetaxel), IMR-5$^{r}$VCR$^{10}$ (adapted to vincristine), IMR-5$^{r}$VINB$^{20}$ (adapted to vinblastine), IMR-5$^{r}$VINOR$^{20}$ (adapted to vinorelbine), IMR-5$^{r}$OXALI$^{4000}$ (adapted to oxaliplatin), IMR-5$^{r}$DACARB$^{40}$ (adapted to dacarbazine), IMR-5$^{r}$GEMCI$^{20}$ (adapted to gemcitabine) and IMR-5$^{r}$PCL$^{20}$ (adapted to paclitaxel). As shown in Figure 8A using PCA 1 and PCA 3 some of the cell lines including IMR-5$^{r}$CDDP$^{1000}$ and IMR-5$^{r}$VCR$^{10}$ do show separation from other cell lines with IMR-5 parental grouping away from almost all other resistant sub-lines except for IMR-5$^{r}$GEMCI$^{20}$ which it overlaps with.

Further analysis of the IMR-5 cell line as shown in figure 8B confirmed that the PCA2 and PCA3 analysis is superior to the PCA1 vs. PCA3 in separating the cell lines. IMR-5 parental did form a group away from all other resistant sub-lines aside from IMR-5$^{r}$GEMCI$^{20}$ which displayed an overlap with IMR-5 seen also in Figure 8A. Interestingly, the three sub-lines with similar mechanisms of action, IMR-5$^{r}$VCR$^{10}$, IMR-5$^{r}$VINB$^{20}$ and IMR-5$^{r}$VINOR$^{20}$ did form distinct clusters with some overlap and some outliers but were also separate from IMR-5. IMR-5$^{r}$CDDP$^{1000}$ indicated with the red circle icon and highlighted in Figure 8B formed a clear group aside from all other resistant sub-lines and from the parental line. IMR-5$^{r}$DOCE$^{20}$, IMR-5$^{r}$OXALI$^{4000}$, IMR-5$^{r}$DACARB$^{40}$ and IMR-5$^{r}$PCL$^{20}$ still displayed characteristic distributions although less distinctive, grouped closer together and overlapped when compared with the other cell lines.

Next was the comparison of the Neuroblastoma cell line, IMR-32 parental with six resistant sub-lines which included: IMR-32$^{r}$OXALI$^{800}$ (adapted to oxaliplatin), IMR-32$^{r}$GEMCIT$^{25}$ (adapted to gemcitabine), IMR-32$^{r}$CARBO$^{1000}$ (adapted to carboplatin), IMR-32$^{r}$ETO$^{100}$ (adapted to etoposide), IMR-32$^{r}$TOPO$^{7.5}$ (adapted to topotecan) and IMR-32$^{r}$MEL$^{500}$(adapted to melphalan). Initial analysis as before with PCA1 and PCA3 as shown in Figure 8C indicated that this may not be the best principal component analysis method to differentiate the cell lines. IMR-32$^{r}$GEMCIT$^{25}$ appears to form two distinct groups with some as outliers and there is some crossover with IMR-32 which also forms two groups (purple). All remaining resistant sub-lines show a high degree of crossover with one another although some groups are still visible.

Further investigation using the superior PCA2 and PCA3 analysis (figure 8D), differentiation of the cell lines was much clearer. IMR-32 and IMR-32$^{r}$GEMCIT$^{25}$ as before, formed two distinct groups with some overlap from IMR-32$^{r}$OXALI$^{800}$ with IMR-32. Both IMR-32$^{r}$CARBO$^{1000}$ and IMR-32$^{r}$TOPO$^{7.5}$ were completely separated from all the other sub-lines and from the parental IMR-5 and are highlighted in Figure 8D. IMR-32$^{r}$ETO$^{100}$, IMR-32$^{r}$MEL$^{500}$ and IMR-32$^{r}$OXALI$^{800}$ formed distinctive clusters but were not completely separated and did overlap slightly with one another.

A

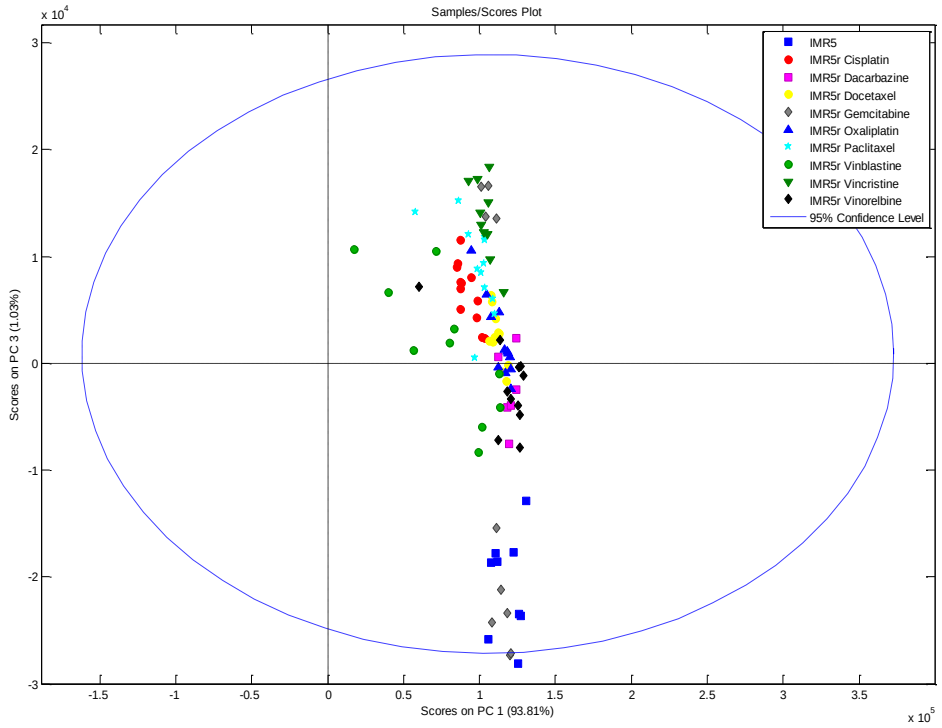


Figure 8A: Principal component analysis of IMR-5, IMR-5$^{r}$CDDP$^{1000}$, IMR-5$^{r}$DACARB$^{40}$, IMR-5$^{r}$DOCE$^{20}$, IMR-5$^{r}$GEMCI$^{20}$, IMR-5$^{r}$OXALI$^{4000}$, IMR-5$^{r}$PCL$^{20}$, IMR-5$^{r}$VINB$^{20}$, IMR-5$^{r}$VCR$^{10}$ and IMR-5$^{r}$VINOR$^{20}$ using PCA1 and PCA3. This analysis was inferior to previous PCA used and is shown by all the cell lines overlapping with one another. However, some cell lines such as IMR-5$^{r}$CDDP$^{1000}$ (red) does form a distinct group, as do IMR-5$^{r}$VCR$^{10}$ (green triangles) and IMR-5$^{r}$VINB$^{20}$ (green circles).

B

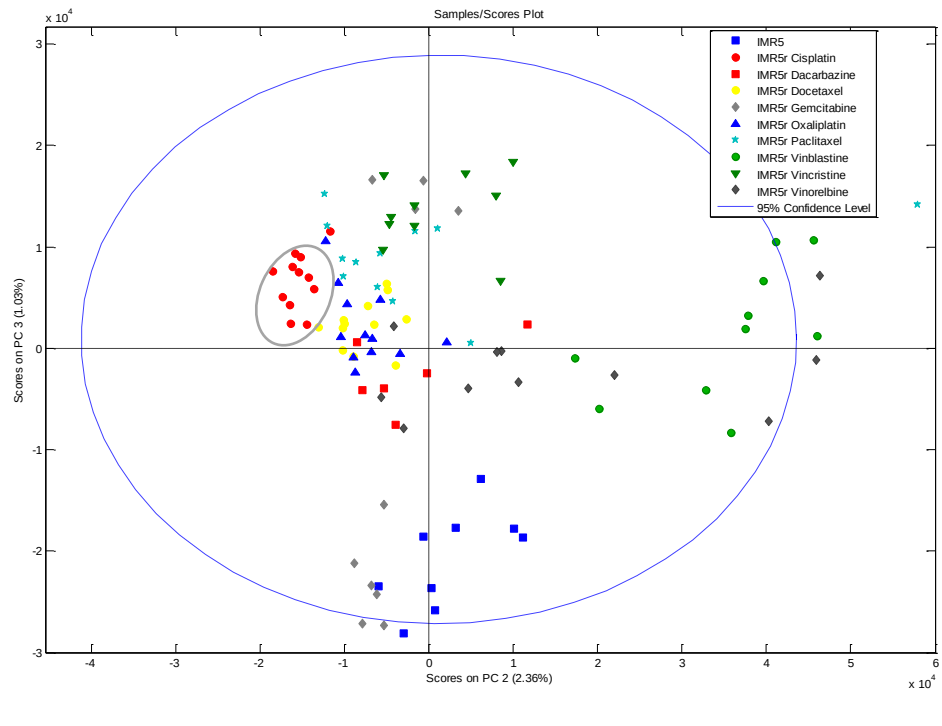


Figure 8B: Principal component analysis of IMR-5, IMR-5$^{r}$CDDP$^{1000}$, IMR-5$^{r}$DACARB$^{40}$, IMR-5$^{r}$DOCE$^{20}$, IMR-5$^{r}$GEMCI$^{20}$, IMR-5$^{r}$OXALI$^{4000}$, IMR-5$^{r}$PCL$^{20}$, IMR-5$^{r}$VINB$^{20}$, IMR-5$^{r}$VCR$^{10}$ and IMR-5$^{r}$VINOR$^{20}$ using PCA2 and PCA3. IMR-5 (blue squares) formed a distinct group despite an overlap with IMR5$^{r}$GEMCI$^{20}$. All other resistant lines formed groups separate to the parental with IMR-5$^{r}$CDDP$^{1000}$ (red circles) forming the most distinct group when compared to other resistant lines.

C

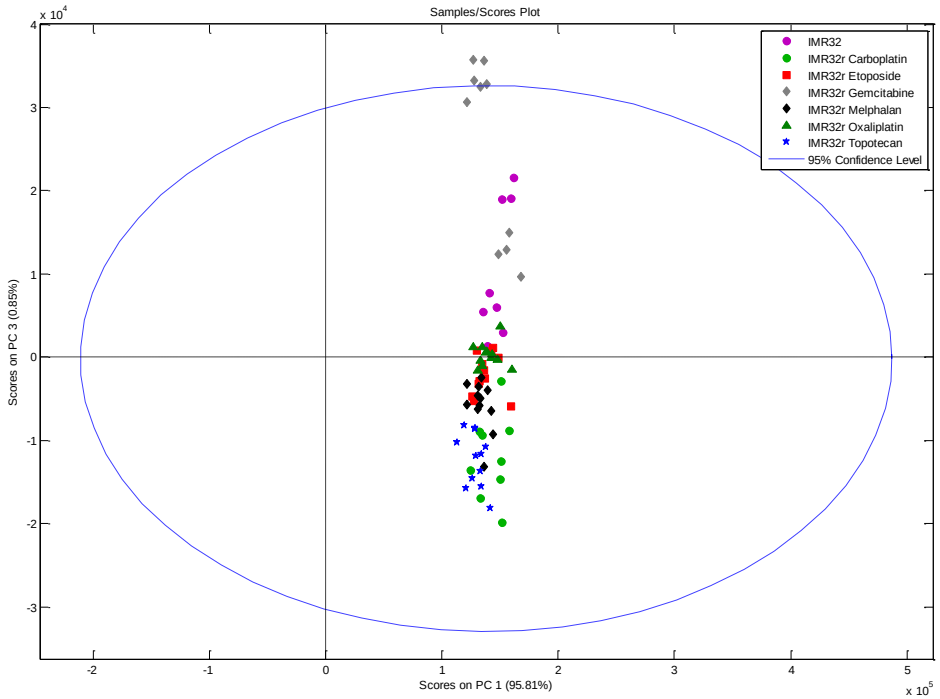


Figure 8C: Principal component analysis of IMR-32 parental with six resistant sub-lines including: IMR-32$^{r}$OXALI$^{800}$, IMR-32$^{r}$GEMCIT$^{25}$, IMR-32$^{r}$CARBO$^{1000}$, IMR-32$^{r}$ETO$^{100}$, IMR-32$^{r}$TOPO$^{7.5}$ and IMR-32$^{r}$MEL$^{500}$ using PCA1 and PCA3. As shown previously this analysis is inferior to the PCA2 and PCA3 as it does not adequately differentiate the cell and resistant sub-lines. However, it is possible to see the IMR-32 parental (purple circles) separate from the other sub-lines but there is overlap with IMR-32$^{r}$OXALI$^{800}$ and IMR-32$^{r}$GEMCIT$^{25}$.

D

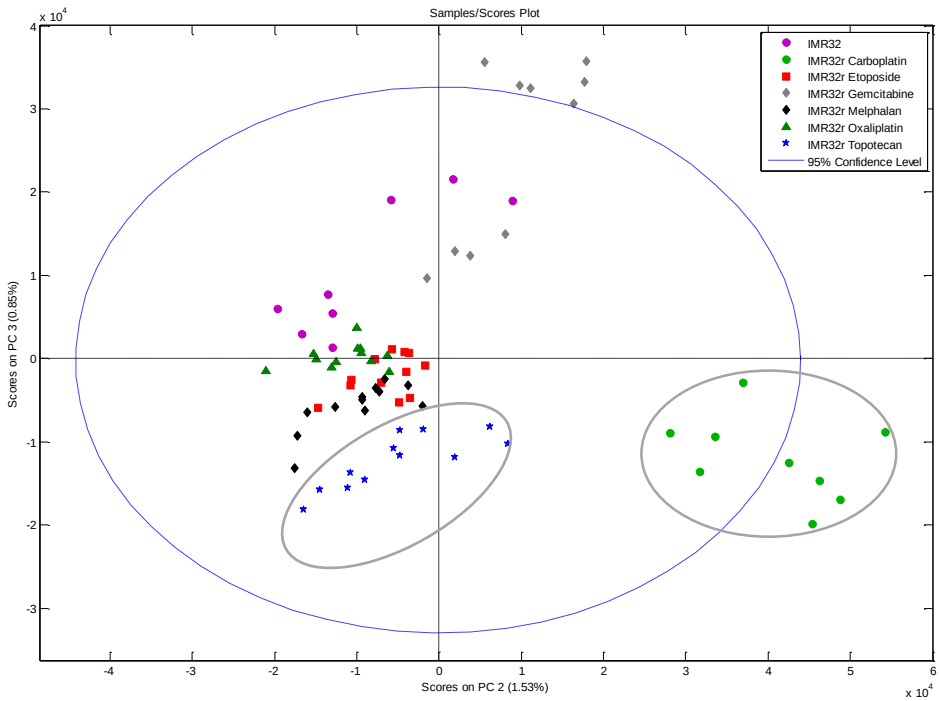


Figure 8D: Principal component analysis of IMR-32 parental with six resistant sub-lines including: IMR-32$^{r}$OXALI$^{800}$, IMR-32$^{r}$GEMCIT$^{25}$, IMR-32$^{r}$CARBO$^{1000}$, IMR-32$^{r}$ETO$^{100}$, IMR-32$^{r}$TOPO$^{7.5}$ and IMR-32$^{r}$MEL$^{500}$ using PCA2 and PCA3. As demonstrated in previous results the PCA2 and PCA3 analysis is superior and can differentiate the cell lines more effectively. Here we see IMR-32$^{r}$CARBO$^{1000}$ (green circles) and IMR-32$^{r}$TOPO$^{7.5}$ (blue stars) easily distinguishable from the other cell lines.

Finally, we compared the parental cell lines UKF-NB-3, IMR-5 and IMR-32 to investigate whether it may, in principle, be possible to authenticate cell parental cell lines by the Intact cell MALDI-ToF mass spectroscopy approach. Figure 9 shows this analysis using PCA2 and PCA3 which separated all three cell lines, which is particularly impressive given that IMR-5 is a clonal sub-line of IMR-32 (Oberthuer, A., Skowron, M., Spitz, R., Kahlert, Y., Westermann, F., *et al* 2005).

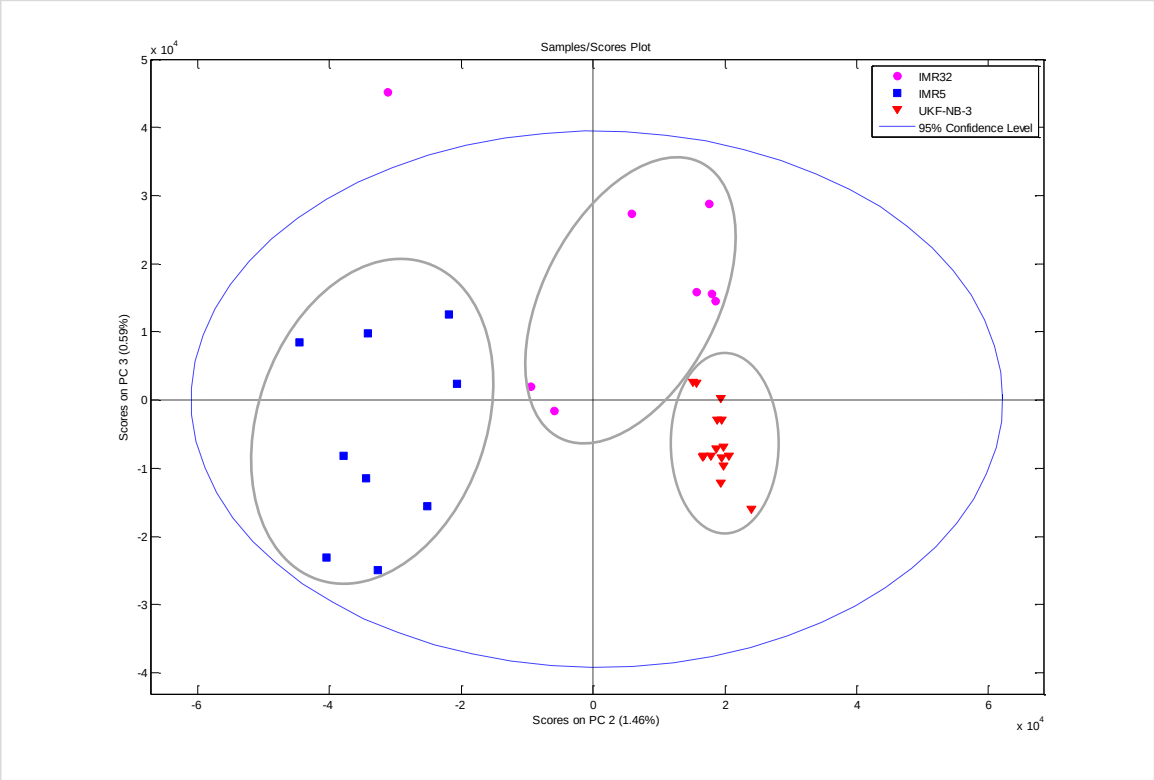


Figure 9: The Intact-cell MALDI-ToF mass spectroscopy method is able to distinguish Neuroblastoma parental cell lines from one another. Principal component analysis of IMR-32, IMR-5 (a clonal sub-line of IMR-32) and UKF-NB-3 using PCA2 and PCA3. All three cell lines formed clear distinct groups from one another including IMR-5 which is a clonal sub-line of IMR-32 indicating the method is effective even to separate parental cell lines.

### 3.4 Discussion

Principal component analysis is a well-established technique to analyse MALDI generated data and the results in this chapter does show that the Intact whole cell MALDI-ToF mass spectrometry method does work in principle to separate parental and resistant sub-lines, but the method needs further refinement.

There was clear separation within the UKF-NB-3 cell line, with UKF-NB-3 and UKF-NB-3$^{r}$CDDP$^{1000}$ as well as with UKF-NB-3$^{r}$OXALI$^{2000}$. Further evidence of the method differentiating sub-lines effectively are seen with IMR-32 and the resistant sub-lines which showed clearer separation in PCA2 and PCA3 analysis which was across all results. IMR-5 also showed promise with the method separating out drug-resistant sub-lines from IMR-5 parental.

Finally, the method clearly separated all three different neuroblastoma parental cell lines, UKF-NB-3, IMR-5 and IMR-32. It is therefore possible to separate parental cell lines of the same genetic

origin and cell lines that have been adapted to closely related drugs e.g. UKF-NB3$^{r}$CDDP$^{1000}$ UKF-NB-3$^{r}$OXALI$^{2000}$ and IMR-5$^{r}$VCR$^{10}$ IMR-5$^{r}$VINB$^{20}$.

However, it is worth stating that MALDI Imaging Mass spectrometry (MALDI-IMS) is a powerful technique, which can be used to analyse data that other methods are incapable of doing. Interestingly, it was used in the identification of cancer characteristics such as biomarkers through the identification of certain proteins and so further development of this method has real promise to show that MALDI-IMS will differentiate isogenic cell lines (Shone, C., Hofler, H and Walch, A., 2013). The field of MALDI-ToF has continued to be developed with the emergence of 3-D MALDI imaging, which can give a more detailed picture of interactions within samples which would continue to develop the authentication and differentiation of the cell lines presented in this chapter (Seeley, E and Caprioli, R., 2012).

To develop this method further there are extensions to the principal component analysis such as multiple factor analysis (MFA), which can be used after PCA (Abdi, H., Williams, L.J and Valentin, D.,2013). Developments of MALDI-ToF methods exist such as surface-enhanced laser desorption/ionization mass spectrometry (SELDI-ToF), which changes the preparation of samples and may give a more sensitive result with the differences in the parental and resistant sub-lines (Rodrigo, M.A.M., Zitka, O., Krizkova, S., Moulick, A., Adam, V., *et al* 2014).

Finally, it may be more practical to use the intact whole cell MALDI-ToF method alongside STR and drug sensitivity data to develop a combined authentication analysis technique. This would ensure a unique mass spec fingerprint for each cell line and give authenticity to the development of a database of all cell lines as a reference.

To conclude, the authentication of cell lines is essential to prevent the further widespread negative impact of misidentified cell lines. Currently, STR is the method of choice but is unable to differentiate the drug-adapted sub-lines from parental cell lines used to study acquired drug resistance. What we have described and demonstrated is the intact whole cell MALDI-ToF mass spectroscopy method is effective at differentiating between isogenic sensitive and drug-adapted resistant sub-lines. With further work it will continue to show progress as a method to authenticate, document and create a mass spectrometry database of resistant sub-lines.

# Chapter 4

# Development of a drug adaptation protocol

## 4.1 Introduction

This project has been an ongoing experiment within the group, which encompasses many lab members efforts and has spanned nearly three years of data collection which is still ongoing. The project first began with Deborah Kajewole and Lyto Yiangou and was continued by myself and Hannah Onafuye.

Based on previous observations that indicated it is much easier to adapt cancer cells to docetaxel and paclitaxel, than to cabazitaxel and epothilone-B (Martin Michaelis, personal communication) a standardised protocol was developed. The UKF-NB-3 cell line was split into 20 different cell lines with five per drug investigated as shown in Figure 10. $IC_{50}$ concentrations were determined by MTT assay following 120h incubation of the four drugs and this was replicated three times to give the final values. Docetaxel $IC_{50}$ value was 0.37 nM, epothilone-B 1 nM, paclitaxel 50 nM and finally cabazitaxel 1 nM.

The aim of the protocol was to compare directly the potential of the investigated drugs to induce resistance in the selected cell line model in this case UKF-NB-3. 2.5 x $10^6$ cells per 25cm $^2$ flask were treated with the $IC_{50}$ concentration of the investigated drugs every second week. In the other week, 2.5 x $10^5$ cells per 25cm$^2$ flask were cultivated in the absence of drug. In some cell lines, as they began to adapt to the treatment, it was necessary to reduce the cell numbers to 2.5 x $10^5$ cells also in the absence of drug as they were becoming overgrown and stressed. This is indicated in the respective figures and at the end of every week the cell numbers were recorded.

## 4.2 Cell number and $IC_{50}$ values for epothilone-B 1 nM concentration in UKF-NB-3 cells

Epothilone-B was set up as per the protocol described above with five separate cell lines, UKF-NB-3r epo-B 1, UKF-NB-3r epo-B 2, UKF-NB-3r epo-B 3, UKF-NB-3r epo-B 4 and UKF-NB-3r epo-B 5. The $IC_{50}$ concentration of epothilone-B was 1 nM. The cells were passaged at 2.5 x $10^5$ cells/ 25 cm$^2$ flask in the presence of drug, and at 2.5 x $10^4$ cells in the absence of drug. In week 19, the cell number had also to be reduced to 2.5 x $10^4$ cells in the presence of drug this is due to the cells displaying signs of stress due to high confluence at the end of the week.

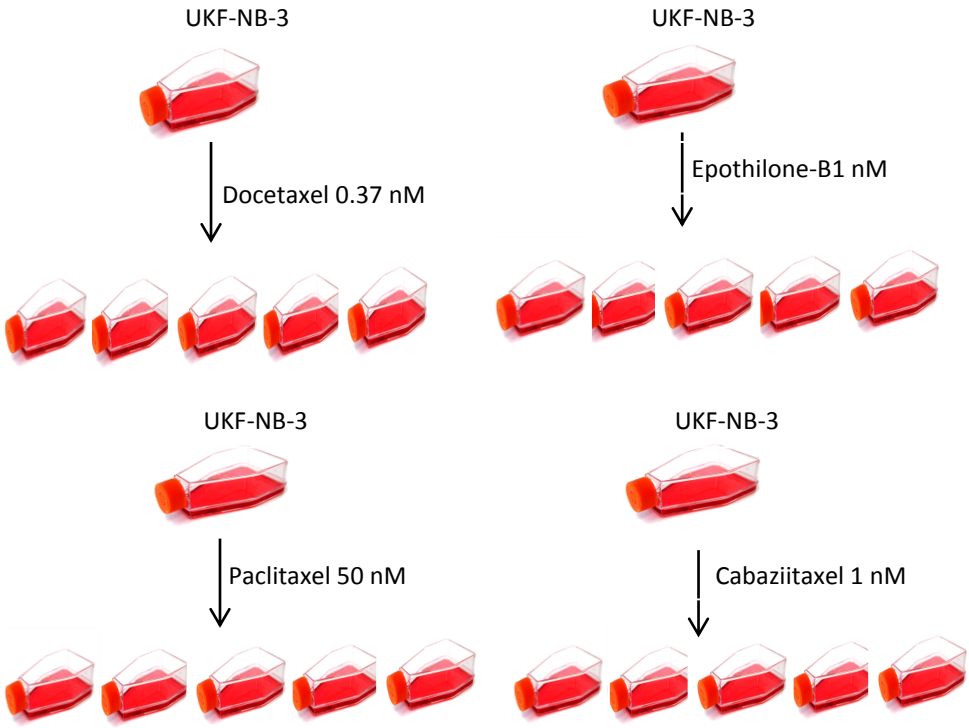


Figure 10: Schematic diagram of the drug adaptation protocol using four investigated drugs including $IC_{50}$ concentrations of docetaxel, epothilone-B, paclitaxel and cabazitaxel. MTT assays were carried out on the parental UKF-NB-3 line to determine the $IC_{50}$ concentration for each drug. Once established, UKF-NB-3 was passaged into five new flasks and these were then grown in the $IC_{50}$ concentration bi-weekly.

The UKF-NB-3r epo-B sub-lines displayed similar growth patterns but also a substantial level of heterogeneity as shown in Figure 11**.** In the first few weeks, the cell lines were characterized by higher cell numbers in the weeks in which they were treated with drug. This is most probably due to the 10-fold higher cell number that was used at the outset of the protocol. This pattern changes after week 19, in which the cell number was reduced to $2.5 \times 10^4$ cells/ $25cm^2$ flask in the presence of drug. Reduced cell numbers between week 10 and week 17 characterized all sub-lines. Despite these similarities, there are also noticeable differences, for example, a drop-in cell number was observed in UKF-NB-3r Epo-B 1 in week 4. The differences become more pronounced during the later stages of the project, for example UKF-NB-3r Epo-B 2 has a noticeable decrease in cell number in week 26 which is not seen in other sub-lines. UKF-NB-3r Epo-B 5 could not be further passaged according to the standardised adaptation protocol due to lack of viable clonogenic cells in week 17. Finally, the remaining four: UKF-NB-3r Epo-B 1, UKF-NB-3r Epo-B 2, UKF-NB-3r Epo-B 3 and UKF-NB-3r Epo-B 4 could not be further cultivated in week 47 due to a lack of viable cells.

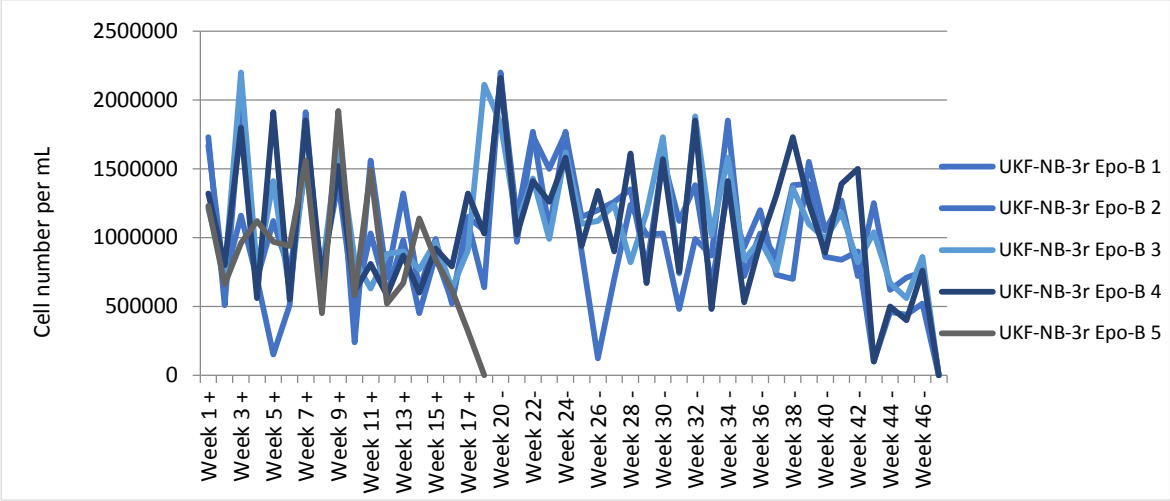


Figure 11: Cell numbers of all UKF-NB-3r epo-B 1-5 sub lines grown in $IC_{50}$ concentration of 1 nM/mL recorded in the presence and absence of drug every week. A substantial amount of heterogeneity is seen throughout the five cell lines. Please note there is no number recorded for weeks 18-20. In week 19, the cell number was reduced to 2.5 x $10^4$ cells/ 25$cm^2$ flask in the presence of drug as the cells had started to become overly confluent. UKF-NB-3r epo-B 5 could no longer be passaged after week 17 and all remaining cell lines failed in week 47 in the presence of the drug.

Alongside the cell numbers recorded weekly, we also investigated the fold change of the individual sub-lines by analysing the cell number at the beginning and the end of every passage as shown in Figure 12 and per individual cell line in Figure 13. Despite noticeable differences in detail, the basic trend is very similar in all cell lines up to week 17, when UKF-NB-3r Epo-B 5 was lost. At the beginning, cell growth is very limited in the weeks of drug treatment and seems to recover in the weeks without drug. In the surviving four cell lines, the cell number had to be reduced to 2.5 x $10^4$ cells/ $cm^2$ also in the presence of drug since the cells became too confluent. From week 19 onwards, the differences between cell growth in the weeks with and without drug were less pronounced. However, the four remaining cell lines could not be further cultivated in week 47.

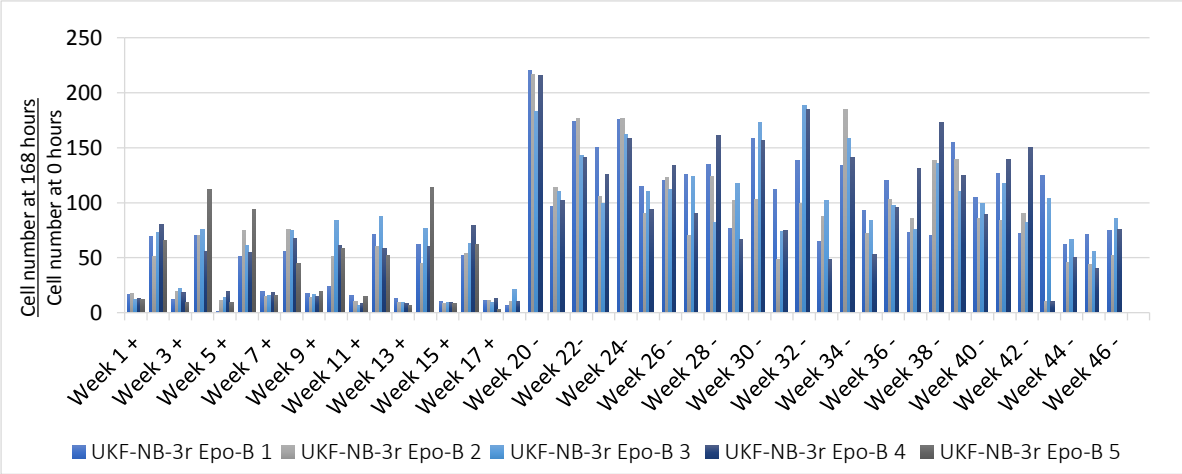


Figure 12: Fold change in cell number for all five of the UKF-NB-3r Epo-B sub-lines from weeks 1 to 47 (with the exception of UKF-NB-3 epo-B 5 following week 17). This was calculated using the cell number at the beginning and the end of every passage and following week 19 2.5 x $10^4$ cells were passaged in the presence and absence of drug. The differences are less pronounced but there are still changes within the different sub-lines.

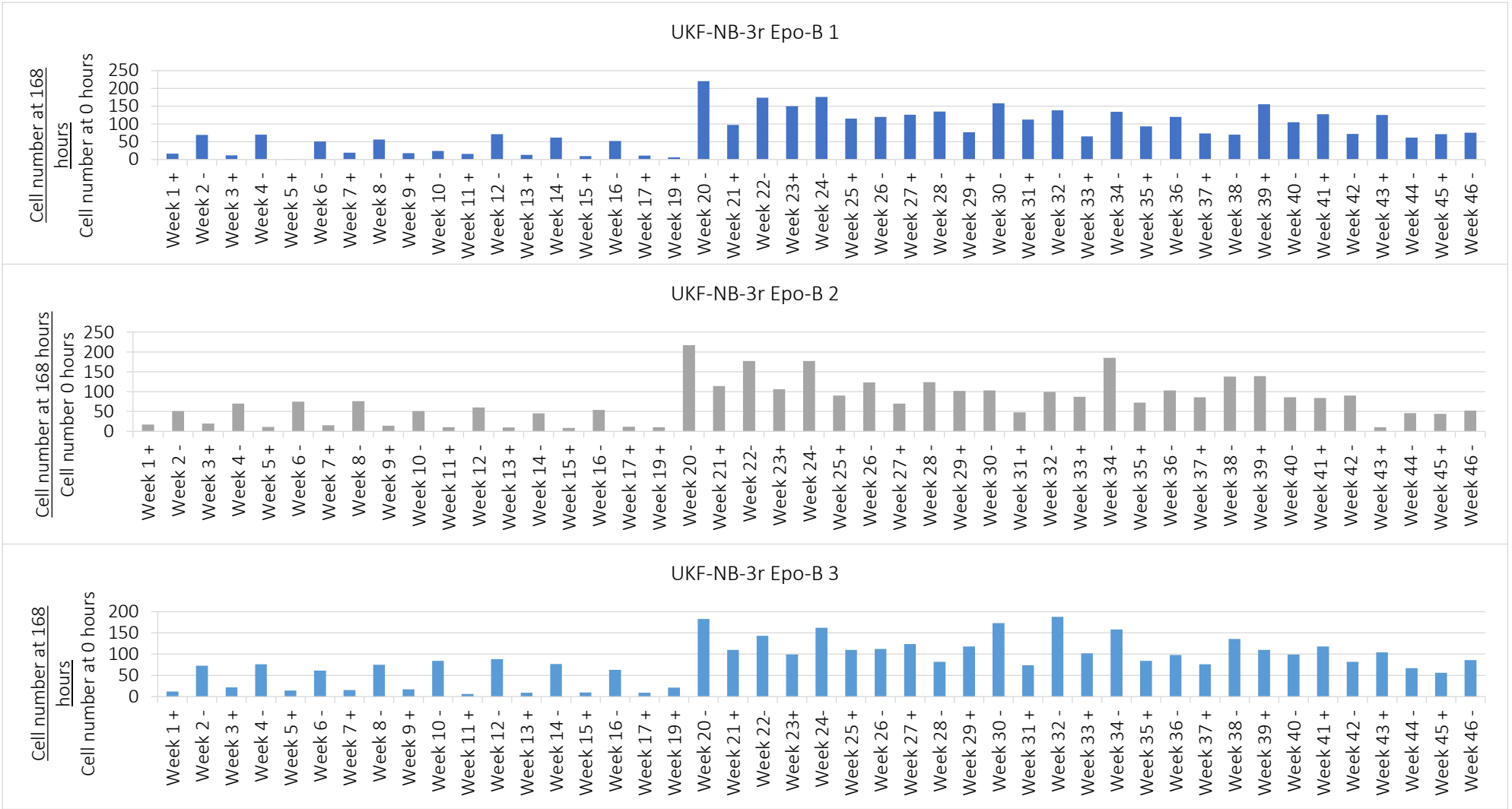
UKF-NB-3r Epo-B 1
Cell number at 168 hours / Cell number at 0 hours
250
200
150
100
50
0
Week 1 +
Week 2 -
Week 3 +
Week 4 -
Week 5 +
Week 6 -
Week 7 +
Week 8 -
Week 9 +
Week 10 -
Week 11 +
Week 12 -
Week 13 +
Week 14 -
Week 15 +
Week 16 -
Week 17 +
Week 19 +
Week 20 -
Week 21 +
Week 22-
Week 23+
Week 24-
Week 25 +
Week 26 -
Week 27 +
Week 28 -
Week 29 +
Week 30 -
Week 31 +
Week 32 -
Week 33 +
Week 34 -
Week 35 +
Week 36 -
Week 37 +
Week 38 -
Week 39 +
Week 40 -
Week 41 +
Week 42 -
Week 43 +
Week 44 -
Week 45 +
Week 46 -
UKF-NB-3r Epo-B 2
Cell number at 168 hours / Cell number 0 hours
250
200
150
100
50
0
Week 1 +
Week 2 -
Week 3 +
Week 4 -
Week 5 +
Week 6 -
Week 7 +
Week 8 -
Week 9 +
Week 10 -
Week 11 +
Week 12 -
Week 13 +
Week 14 -
Week 15 +
Week 16 -
Week 17 +
Week 19 +
Week 20 -
Week 21 +
Week 22-
Week 23+
Week 24-
Week 25 +
Week 26 -
Week 27 +
Week 28 -
Week 29 +
Week 30 -
Week 31 +
Week 32 -
Week 33 +
Week 34 -
Week 35 +
Week 36 -
Week 37 +
Week 38 -
Week 39 +
Week 40 -
Week 41 +
Week 42 -
Week 43 +
Week 44 -
Week 45 +
Week 46 -
UKF-NB-3r Epo-B 3
Cell number at 168 hours / Cell number at 0 hours
200
150
100
50
0
Week 1 +
Week 2 -
Week 3 +
Week 4 -
Week 5 +
Week 6 -
Week 7 +
Week 8 -
Week 9 +
Week 10 -
Week 11 +
Week 12 -
Week 13 +
Week 14 -
Week 15 +
Week 16 -
Week 17 +
Week 19 +
Week 20 -
Week 21 +
Week 22-
Week 23+
Week 24-
Week 25 +
Week 26 -
Week 27 +
Week 28 -
Week 29 +
Week 30 -
Week 31 +
Week 32 -
Week 33 +
Week 34 -
Week 35 +
Week 36 -
Week 37 +
Week 38 -
Week 39 +
Week 40 -
Week 41 +
Week 42 -
Week 43 +
Week 44 -
Week 45 +
Week 46 -

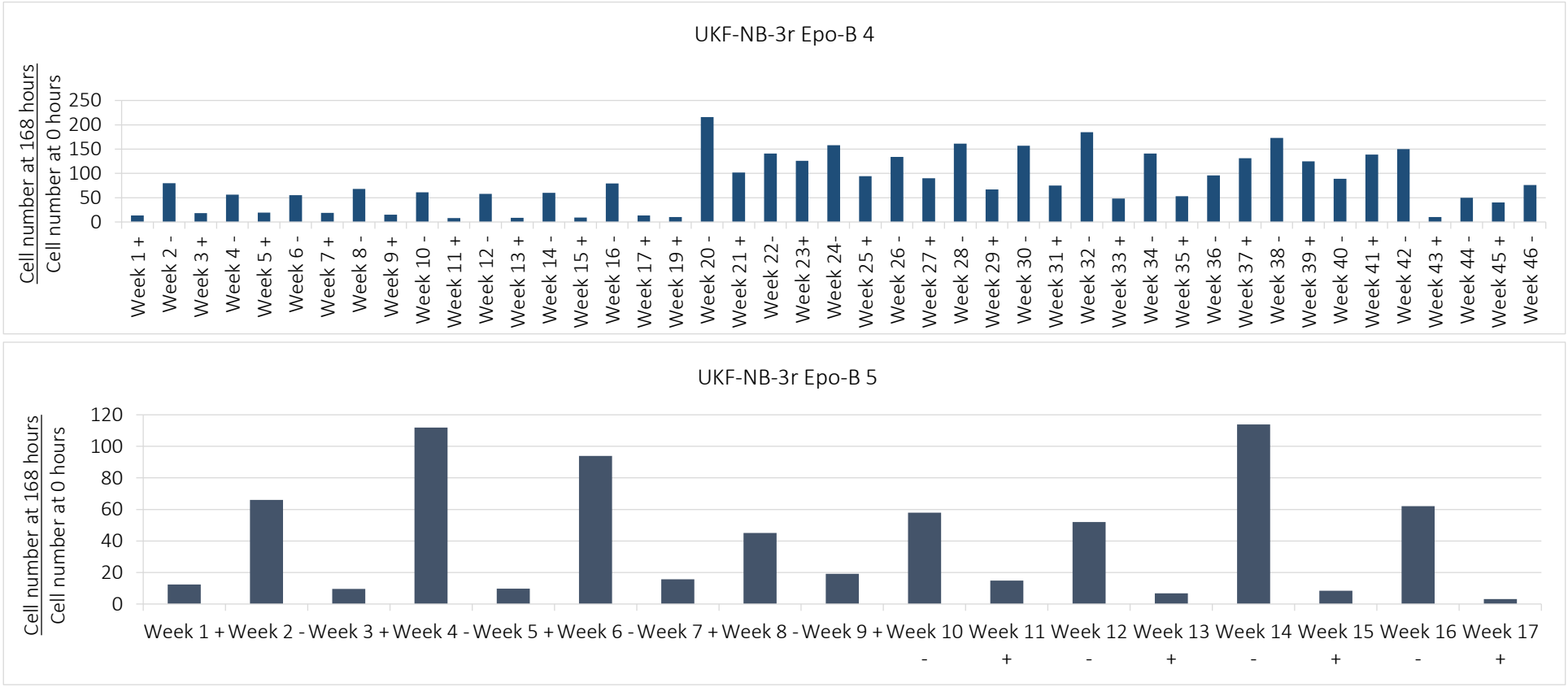


Figure 13: Individual fold change in cell number of all UKF-NB-3r Epo-B sub lines 1 – 5 over 47 weeks with UKF-NB-3r epo-B 5 unable to passage after week 17. All sub-lines exhibit similar fold change patterns for the first 19 weeks of the protocol with the fold change higher in the absence of drug. Following the change in protocol in week 19 reducing the cell number to 2.5 x $10^4$ / $cm^2$ all remaining sub-lines exhibited a difference in fold change. Towards the end of the weeks i.e. 43 onwards all cell lines appeared to have a reduced fold change in the absence and presence of drug and eventually were no longer viable enough to continue.

Alongside recording cell number, a single MTT assay was carried out every 4 weeks when possible on all cell lines as the project progressed to determine epothilone-B $IC_{50}$ concentration in the cell lines. It was only possible to carry out one single MTT as the cells were taken from a single flask with often not enough cells to perform the assay, we also had to ensure that there were enough cells to passage. Alongside the UKF-NB-3r epo-B lines MTT assays were also carried out on the sensitive UKF-NB-3 line to compare the sub-lines resistance. A 2-fold increase was defined as threshold for the definition of a sub-line as resistant. None of the sub-lines consistently displayed a >2-fold increase in the epothilone-B $IC_{50}$ concentrations during the time the sub-lines could be cultivated according to the standardised protocol. As shown in Figure 14 none of the five UKF-NB-3 sub-lines adapted to growth in the presence of epothilone-B using our standardised adaptation protocol.

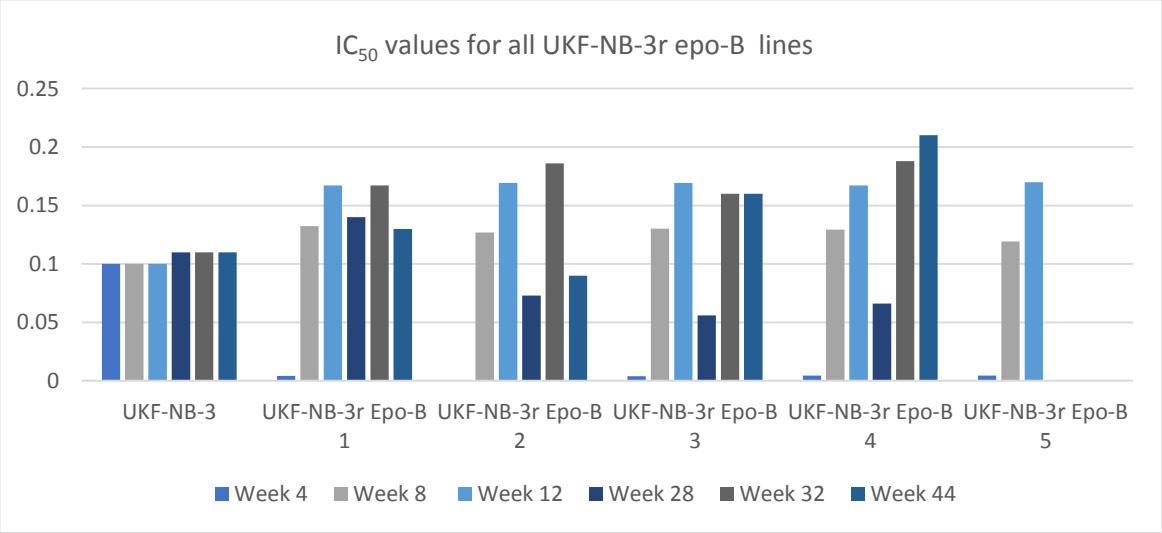


Figure 14: $IC_{50}$ values determined using 120-day MTT assays for all sub-lines UKF-NB-3r 1-5. Due to weeks with low cell number no MTT was carried out in order to continue the protocol. None of the five UKF-NB-3r epo-B cell lines showed a consistent > 2-fold increase and therefore were not resistant. Please note as only one MTT was carried out every four weeks and therefore no error bars are shown for these results.

### 4.3 Cell number and $IC_{50}$ values for cabazitaxel 0.25 nM concentration in UKF-NB-3 cells

Five sub-lines of UKF-NB-3 with the $IC_{50}$ concentration of 0.25nM/ mL cabazitaxel were set up as per the standardised protocol with cells passaged at 2.5 x $10^5$ cells/ 25 $cm^2$ flask in the presence of drug and 2.5 x $10^4$ cells in the absence of drug. In week 13, as seen with epothilone-B in week 19, the cell number of UKF-NB-3r Caba also had to be reduced to 2.5 x $10^4$ cells in the presence of drug, as the cells were becoming stressed and beginning to lose viability.

The sub-lines grew comparably for the first 13 weeks as shown in Figure 15 with all cell lines presenting the same growth pattern as seen in the UKF-NB-3r Epo-B sub-lines with higher cell numbers in the presence of the drug due to the passage of 2.5 x $10^5$ cells/ 25 $cm^2$ per flask. UKF-NB-3r Caba 4 did show a slight variation within these weeks with a decline in cell number for three weeks consecutively before displaying the same growth pattern as the other sub-lines.

Following the alteration in week 13 the growth pattern of the sub-lines changes. All sub-lines have varying decreases in cell number between weeks 14 – 17 before adopting a similar pattern again in weeks 18 -21 with the cell number increasing gradually. After week 23 passaging sub-lines UKF-NB-3r Caba 1, 3,4 and 5 was no longer possible. UKF-NB-3r Caba 2 also had a decrease in the same week but recovered with a high cell number in week 24 and continued to grow until in week 37 it to lost viability.

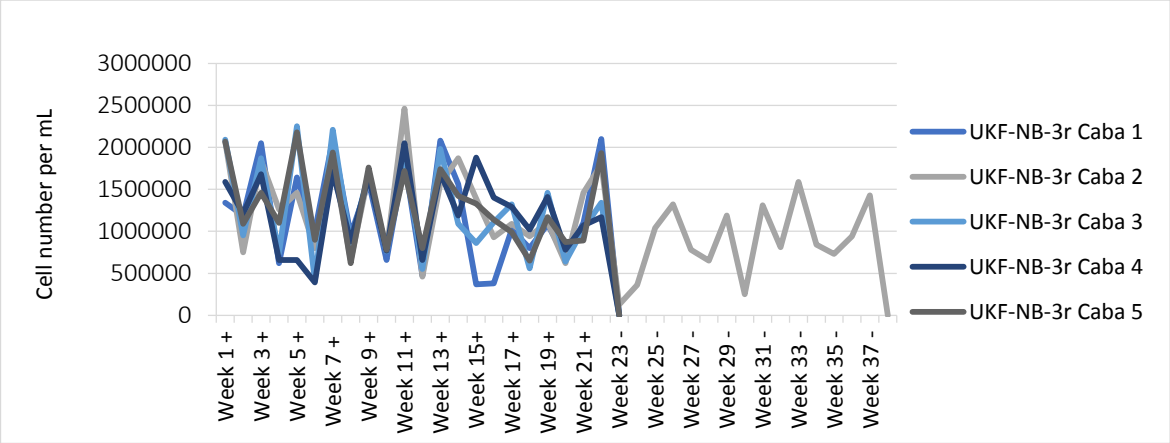


Figure 15: Cell number per mL recorded for each week for UKF-NB-3r Caba sub-lines in the presence and absence of the $IC_{50}$ concentration of 0.25 nM/mL cabazitaxel. Following the reduction in cell number in week 13 UKF-NB-3r Caba 1,3,4 and 5 failed in week 23 with UKF-NB-3r Caba 2 unable to be passaged after week 37.

The sub-line cell numbers were then analysed individually using the fold changes at the beginning and end of each week with all sublines show in Figure 16 and individually in Figure 17. The trend seen within the sub-lines is the same as the UKF-NB-3r Epo-B sub-lines with the weeks in drug displaying a reduced fold number and without drug recovering with a higher fold number. In week 13 the cell number was reduced to compensate the over-confluence of the cells in the presence of the drug and differences are seen within the sub-lines but overall the growth changes with and without drug are not as evident as before week 13.

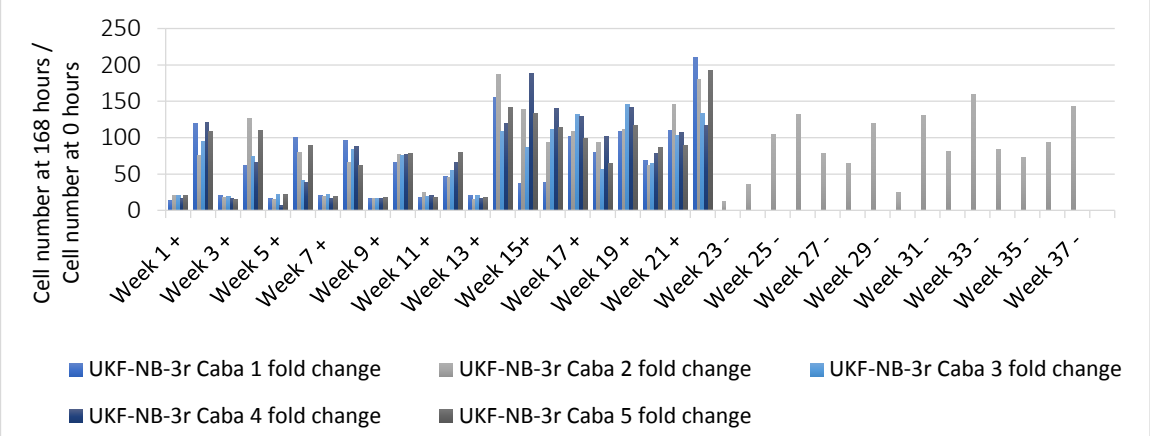


Figure 16: Fold change in cell number of UKF-NB-3r Caba sub-lines over 37 weeks with all sub-lines failing in week 23 except UKF-NB-3r Caba 2. The trend follows with sub-lines displaying reduced fold number in the weeks with the drug added and increased fold change without drug.

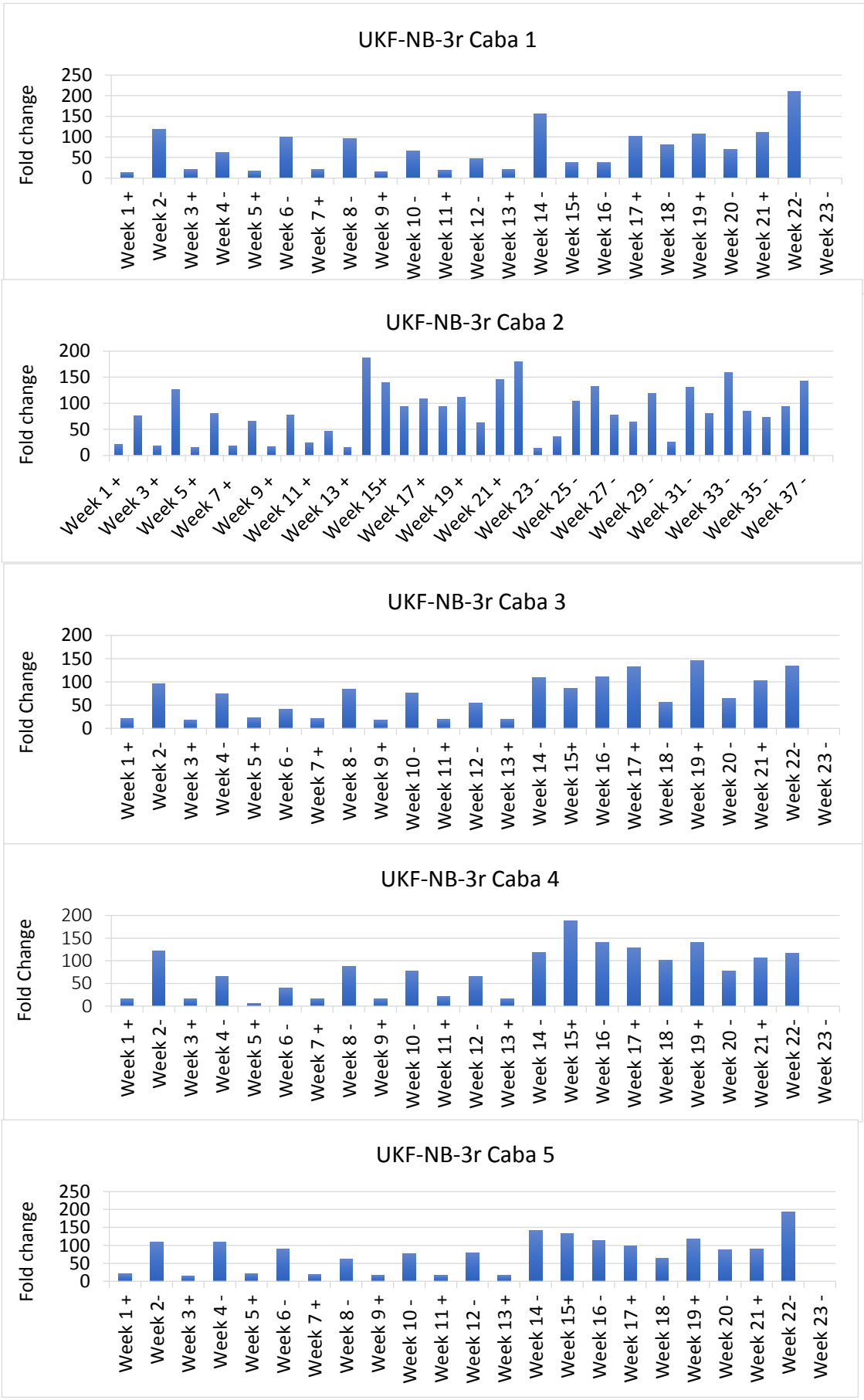


Figure 17: Individual fold change for all UKF-NB-3r Caba sub lines for 37 weeks with sub lines 1, 3, 4 and 5 failing in week 23. Sub-lines all exhibit a similar pattern up to week 13 when all sub-lines were passaged with 2.5 x $10^4$ cells in the presence of drug. All lines which failed in week 23 have a similar fold pattern. UKF-NB-3r Caba 2 has an increase in fold change until failure in week 38.

UKF-NB-3r Caba sub-lines $IC_{50}$ values were determined using an MTT assays every 4 weeks and when a 2-fold increase was observed in comparison with the UKF-NB-3 sensitive parental cell line the sub-line was deemed to resistant. Figure 9 highlights the

Figure 18 highlights that none of the cell lines, as with UKF-NB-3r Epo-B, consistently displayed a 2-fold or higher increase in $IC_{50}$. A very small increase was observed in UKF-NB-3r Caba 2, which was also the sub-line that continued the longest but never reached a 2-fold increase. Therefore, as with the UKF-NB-3r Epo-B sub-lines, none of the UKF-NB-3r Caba sub-lines adapted to the $IC_{50}$ concentration in which they were cultivated

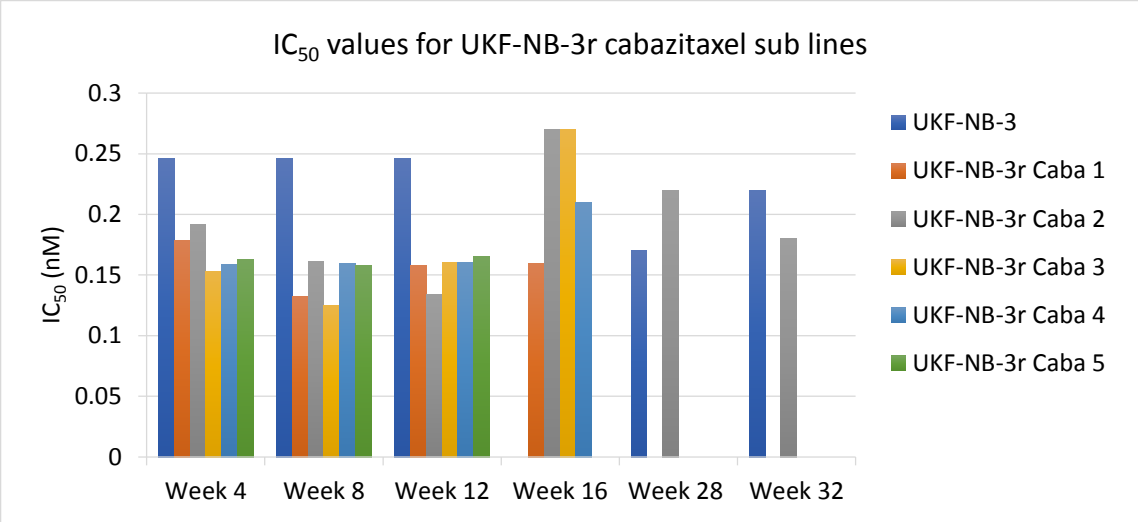


Figure 18: $IC_{50}$ values for all UKF-NB-3r Caba cell lines following a monthly MTT assay. The cell lines were run alongside the UKF-NB-3 parental cell line to compare sensitivity and a consistent >2-fold increase was the threshold for resistance formation. None of the cell lines exceeded this figure consecutively and were as sensitive if not less than UKF-NB-3.

### 4.4 Cell number, $IC_{50}$ values and drug-sensitivity profiles for 0.37 nM docetaxel concentration in UKF-NB-3 cells

Five separate UKF-NB-3 cell lines were set up as per the protocol outlined previously with an $IC_{50}$ concentration of docetaxel at 0.37 nM /mL. As with previous cell lines the cells were overly confluent in the presence of drug and this was reduced to 2.5 x $10^4$ cells/ 25$cm^2$ in week 19.

Cell number was recorded at the end of every week as shown in Figure 19. UKF-NB-3r Doce 3 decreased in cell viability very quickly and it was not possible to continue to passage the sub-line after week 3. The cell numbers were higher in the presence of drug and after the cell number change in week 19 UKF-NB-3r Doce 5 dropped in viability preventing further passage until after week 25. UKF-NB-3r Doce 2 had consecutive weeks with low cell numbers in the presence and absence of drug and eventually could no longer be passaged after week 96. Both UKF-NB-3r Doce 1 and 4 appear to level out after week 76 and continue to grow consistently in the presence and absence of drug. The fold changes observed for all five in the sub-lines are seen in Figure 20**,** and individual fold changes in Figure 21 with the expected trend of a lower fold change in the presence

of drug and a higher fold change when grown without drug as seen in the other investigated cell lines. Following week 19 the fold pattern changes within all the cell lines, with sub-lines 3 and 5 there was very low viability resulting in a reduced cell number and therefore low fold changes. All remaining sub-lines have less variation in the fold changes with consecutive weeks of sustained fold patterns. UKF-NB-3r Doce 4 has the most level of the fold changes from week 88 onwards.

$IC_{50}$ values were generated every four weeks for the sub-lines by 120h MTT assay if possible and are presented in Figure 22 as with all the other drugs investigated, an $IC_{50}$ value of > 2-fold was deemed resistant. UKF-NB-3r Doce 3 never grew to the minimum of 4 weeks before an MTT could be performed and the cell line failed in week 3. UKF-NB-3r Doce 5 never reached a >2-fold increase in comparison to the sensitive UKF-NB-3 parental and was therefore not resistant to docetaxel. UKF-NB-3r Doce 1 and 2 sub-lines after approximately a year, began to indicate a >2-fold increase, however after a period of several weeks UKF-NB-3r Doce 2 began decrease in fold change compared to the parental and following a low $IC_{50}$ value the cell line also ceased growing. UKF-NB-3r Doce 4 has always shown the highest likelihood of acquiring resistance after around 60 weeks of the protocol the sub-line indicated >5-fold resistance. UKF-NB-3r Doce 1 also began to show higher fold increases but these were much less consistent than UKF-NB-3r Doce 4.

Following these findings sub-lines UKF-NB-3r Doce 1 and 4 were further characterised using an 8-drug panel to test various target mechanisms. This panel included: docetaxel, paclitaxel, crizotinib, cisplatin, epothilone-B, topotecan, vincristine and cabazitaxel. Figure 23 and 24 show the results of the MTT assays for each of the investigated drugs on the sub-lines after a week in the presence and absence of drug and compared to the parental line UKF-NB-3 to highlight possible cross resistance. With docetaxel, all sub-line conditions were higher in $IC_{50}$ value than the UKF-NB-3 parental and UKF-NB-3r Doce 4 after a week in drug when compared with UKF-NB-3r Doce 1 had a much higher $IC_{50}$ value. This was also seen in topotecan, but the parental line had a comparable $IC_{50}$ value to the other sub-lines. An interesting finding was with paclitaxel where the two sub-lines after a week out of drug had a much higher $Ic_{50}$ than the parental and the weeks after being in the drug. Both crizotinib and vincristine resulted in $IC_{50}$ values in the UKF-NB-3r Doce 4 sub line being more resistant than the other two lines. After weeks in no drug there was higher resistance to crizotinib and the opposite in vincristine. Epothilone-B had similar results when sub-lines had been in and out of drug and UKF-NB-3r Doce 1 was higher than both UKF-NB-3r Doce 4 and UKF-NB-3. Finally, out of all the sub-lines tested UKF-NB3-r Doce 1 grown in the absence of docetaxel had the highest sensitivity to cisplatin whilst the same sub-line after a week grown in the presence of docetaxel was more resistant.

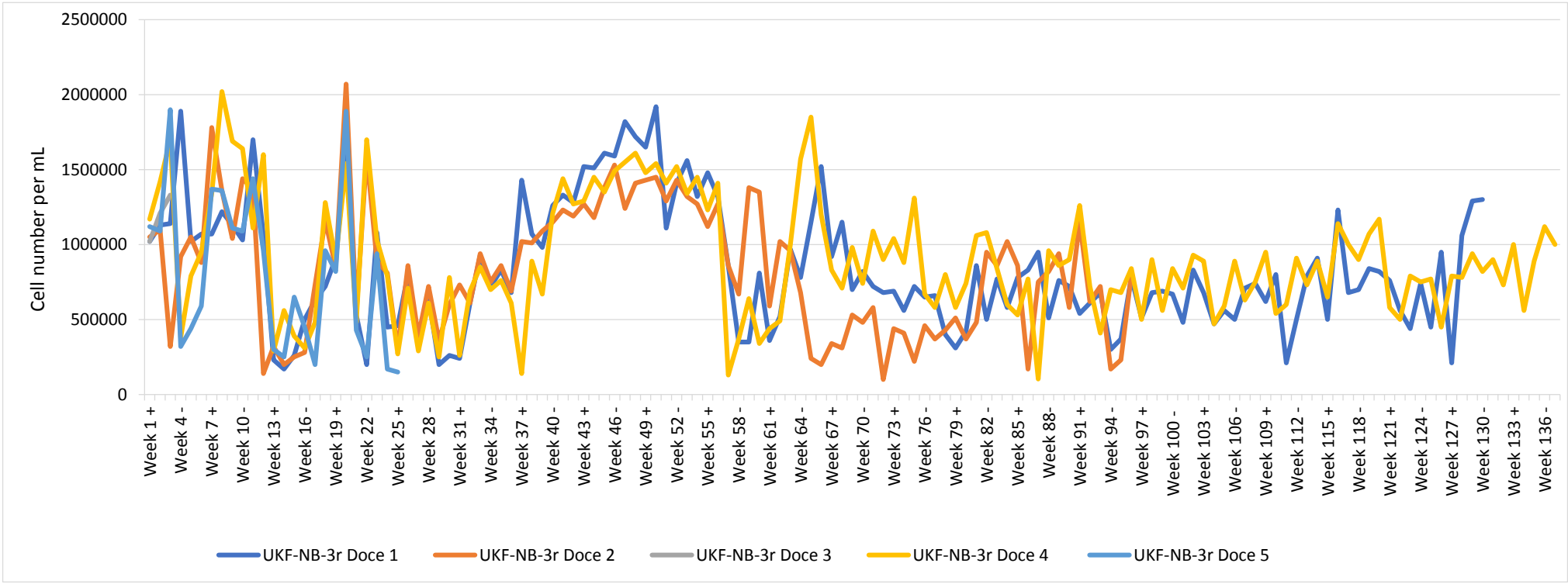


Figure 19: Cell number recorded per week both in the presence and absence of docetaxel for sub lines UKF-NB-3r Doce 1 – 5. In week 19 the cell number was reduced to 2.5 x $10^4$ cells/ 25$cm^2$ flask in the presence of drug due to over confluence and the cells becoming stressed. The cell lines have varying numbers throughout the weeks but both UKF-NB-3r Doce 1 and UKF-NB-3 Doce 4 look very similar from weeks 94 – onwards. UKF-NB-3r Doce 3 failed in week 3, UKF-NB-3r Doce 5 failed in week 35 and UKF-NB-3 Doce 2 in week 96.

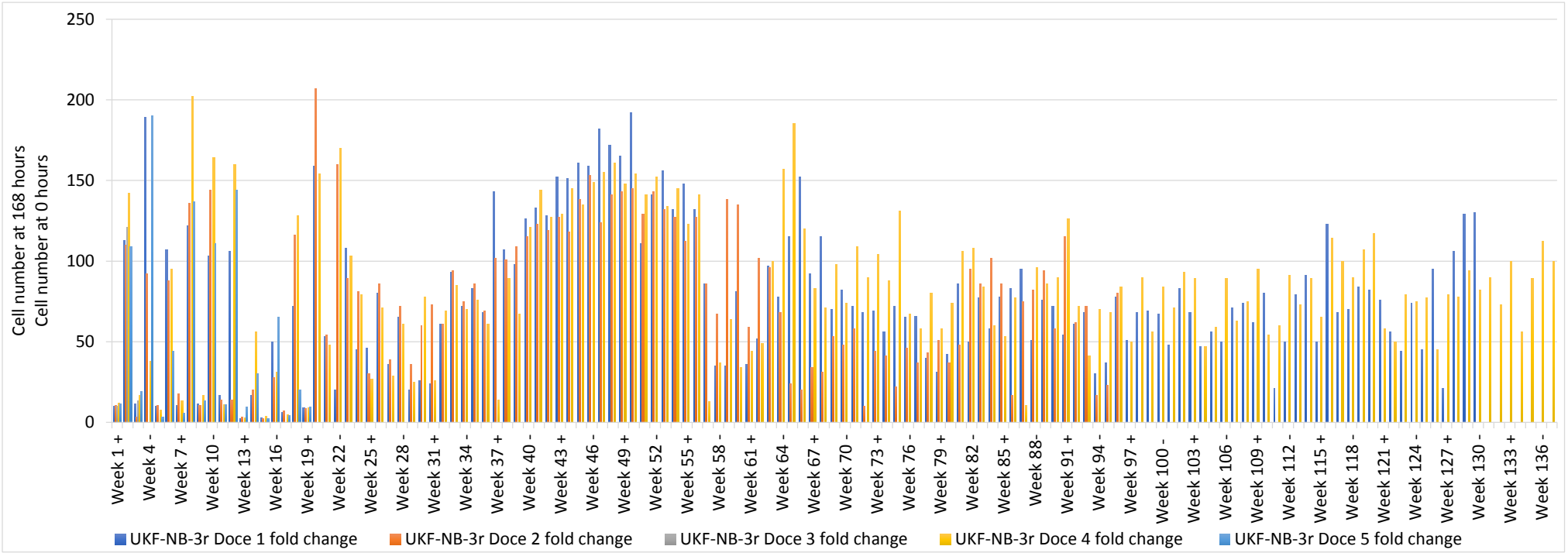


Figure 20: Fold change in cell number for all five UKF-NB-3r Doce sub lines over 137 weeks. Initially cell lines had lower fold changes in the presence of drug and higher in the absence of docetaxel. This is most likely due to the 10-fold difference in passaging. Following week 19 due to over confluence of cell lines the cell number was reduced in the weeks when docetaxel was added. However, cell lines still show a similar pattern over some weeks but only UKF-NB-3r Doce 1 and 4 continue after week 96.

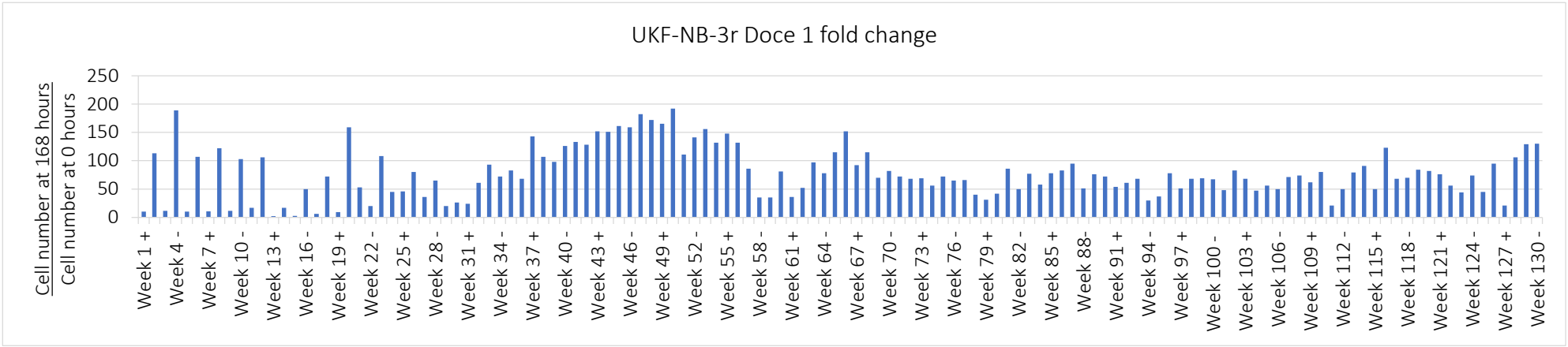
UKF-NB-3r Doce 1 fold change
Cell number at 168 hours / Cell number at 0 hours
250
200
150
100
50
0
Week 1 +
Week 4 -
Week 7 +
Week 10 -
Week 13 +
Week 16 -
Week 19 +
Week 22 -
Week 25 +
Week 28 -
Week 31 +
Week 34 -
Week 37 +
Week 40 -
Week 43 +
Week 46 -
Week 49 +
Week 52 -
Week 55 +
Week 58 -
Week 61 +
Week 64 -
Week 67 +
Week 70 -
Week 73 +
Week 76 -
Week 79 +
Week 82 -
Week 85 +
Week 88-
Week 91 +
Week 94 -
Week 97 +
Week 100 -
Week 103 +
Week 106 -
Week 109 +
Week 112 -
Week 115 +
Week 118 -
Week 121 +
Week 124 -
Week 127 +
Week 130 -

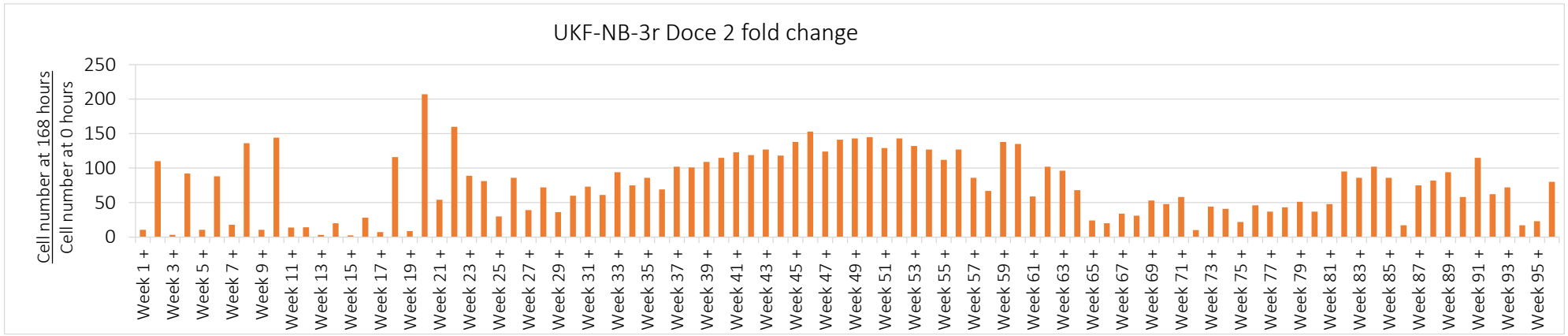
UKF-NB-3r Doce 2 fold change
Cell number at 168 hours / Cell number at 0 hours
250
200
150
100
50
0
Week 1 +
Week 3 +
Week 5 +
Week 7 +
Week 9 +
Week 11 +
Week 13 +
Week 15 +
Week 17 +
Week 19 +
Week 21 +
Week 23 +
Week 25 +
Week 27 +
Week 29 +
Week 31 +
Week 33 +
Week 35 +
Week 37 +
Week 39 +
Week 41 +
Week 43 +
Week 45 +
Week 47 +
Week 49 +
Week 51 +
Week 53 +
Week 55 +
Week 57 +
Week 59 +
Week 61 +
Week 63 +
Week 65 +
Week 67 +
Week 69 +
Week 71 +
Week 73 +
Week 75 +
Week 77 +
Week 79 +
Week 81 +
Week 83 +
Week 85 +
Week 87 +
Week 89 +
Week 91 +
Week 93 +
Week 95 +

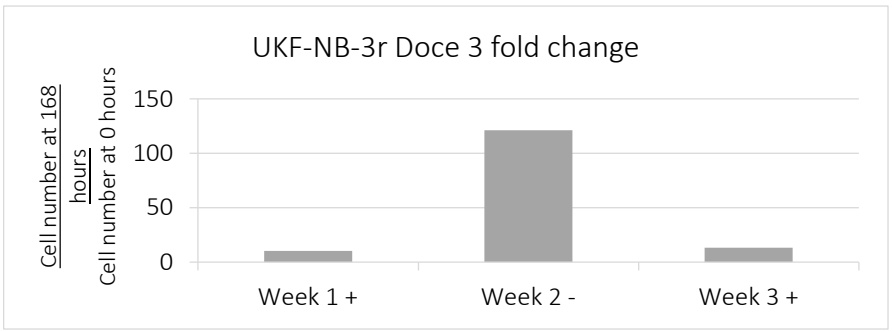
UKF-NB-3r Doce 3 fold change
Cell number at 168 hours / Cell number at 0 hours
150
100
50
0
Week 1 +
Week 2 -
Week 3 +

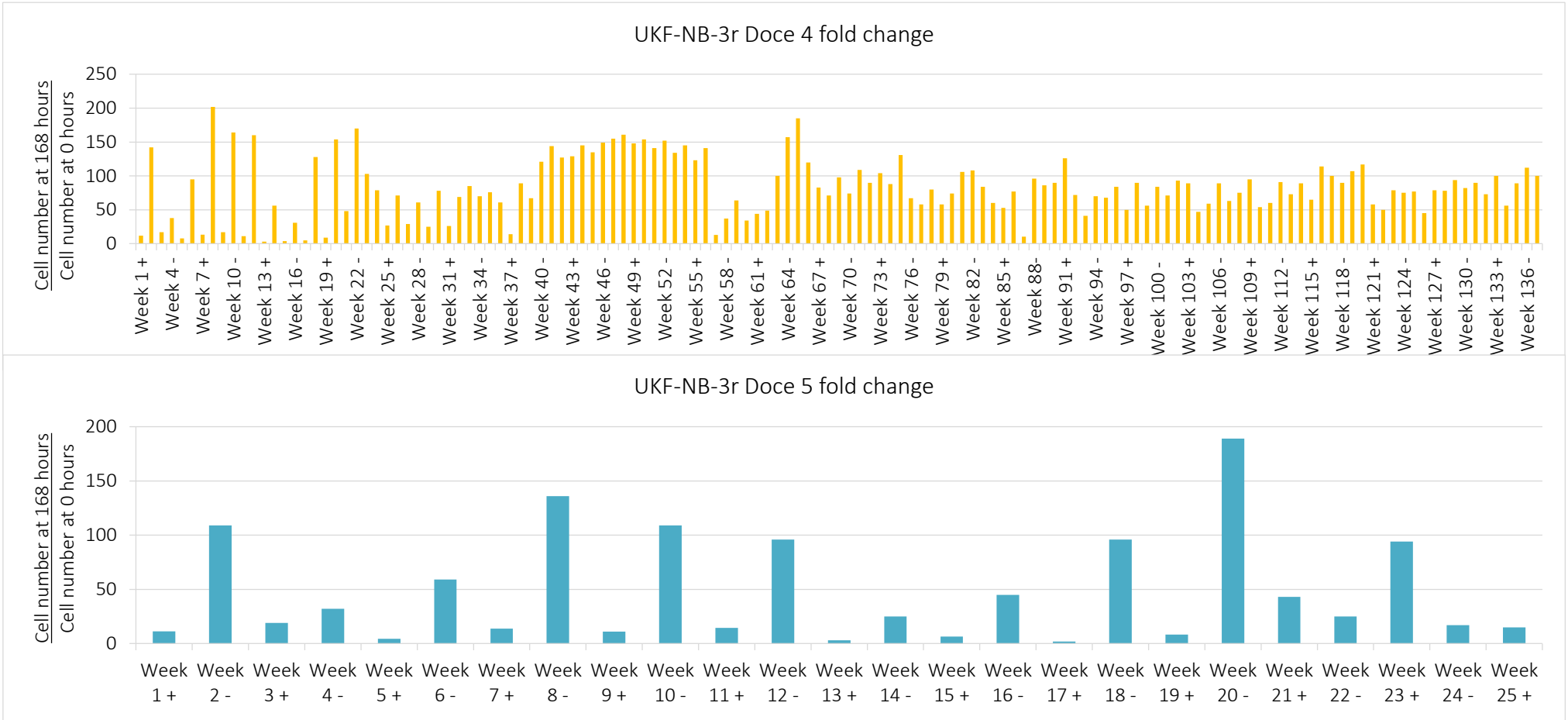


Figure 21: Individual fold changes for UKF-NB-3r Doce sub lines 1 – 5. Both UKF-NB-3r Doce 1 and 4 show a consistent fold change and more so in UKF-NB-3 Doce 4 which also had the most consistent $IC_{50}$ values. UKF-NB-3r Doce 2 and 5 show an undulating response to the presence and absence of docetaxel and ultimately the cell lines were not possible to passage. UKF-NB-3r Doce 2 also indicates a period of consistent fold changes from week 37 – 57 but also failed in week 96.

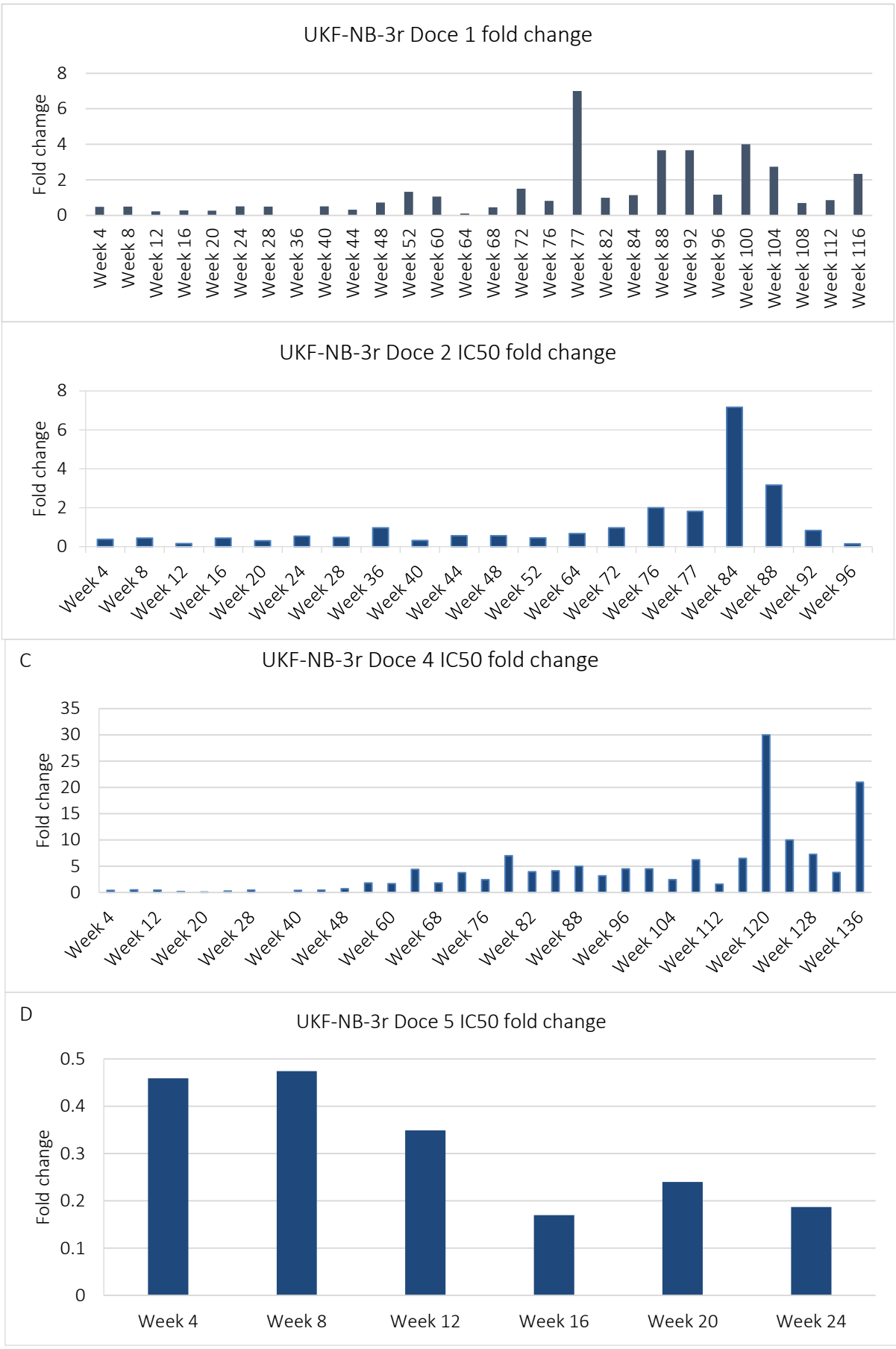


Figure 22: Fold change in $IC_{50}$ values calculated using 120hr MTT assays every 4 weeks when cell number was high enough for an MTT to be carried out. Only UKF-NB-3r Doce 1 and 4 have the highest fold changes than the >2-fold threshold to be deemed resistant with UKF-NB-3 Doce 4 showing the highest fold changes

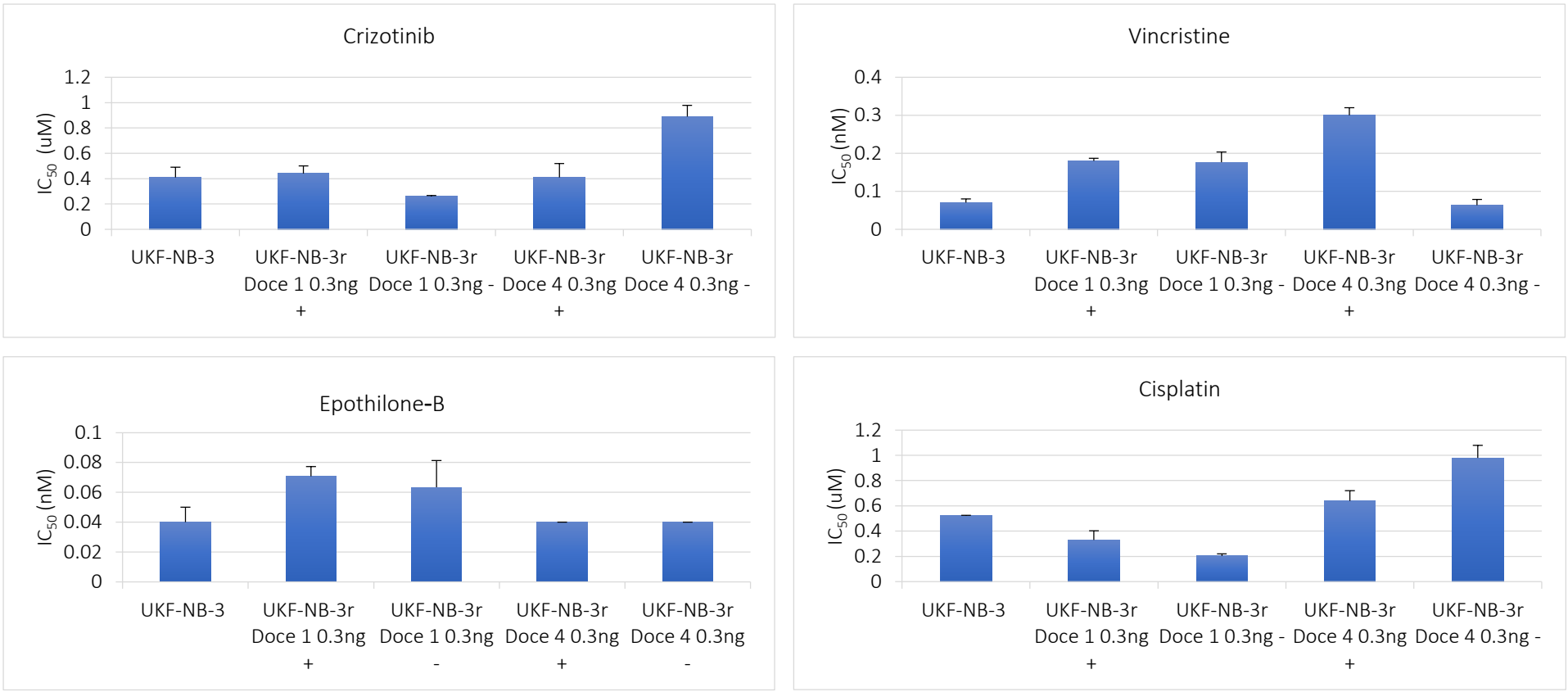


Figure 23: Cross resistance profiles for UKF-NB-3r Doce 1 and UKF-NB-3 Doce 4 in the presence and absence of drug when tested against crizotinib, vincristine, epothilone-B and cisplatin and compared with the parental UKF-NB-3 cell line. UKF-NB-3 Doce 4 was more resistant to both cisplatin and crizotinib in the presence and absence of docetaxel and only in the presence of drug when tested against vincristine. UKF-NB-3r Doce 1 was more resistant to epothilone-b for both conditions and more sensitive than the parental to cisplatin. (n=3)

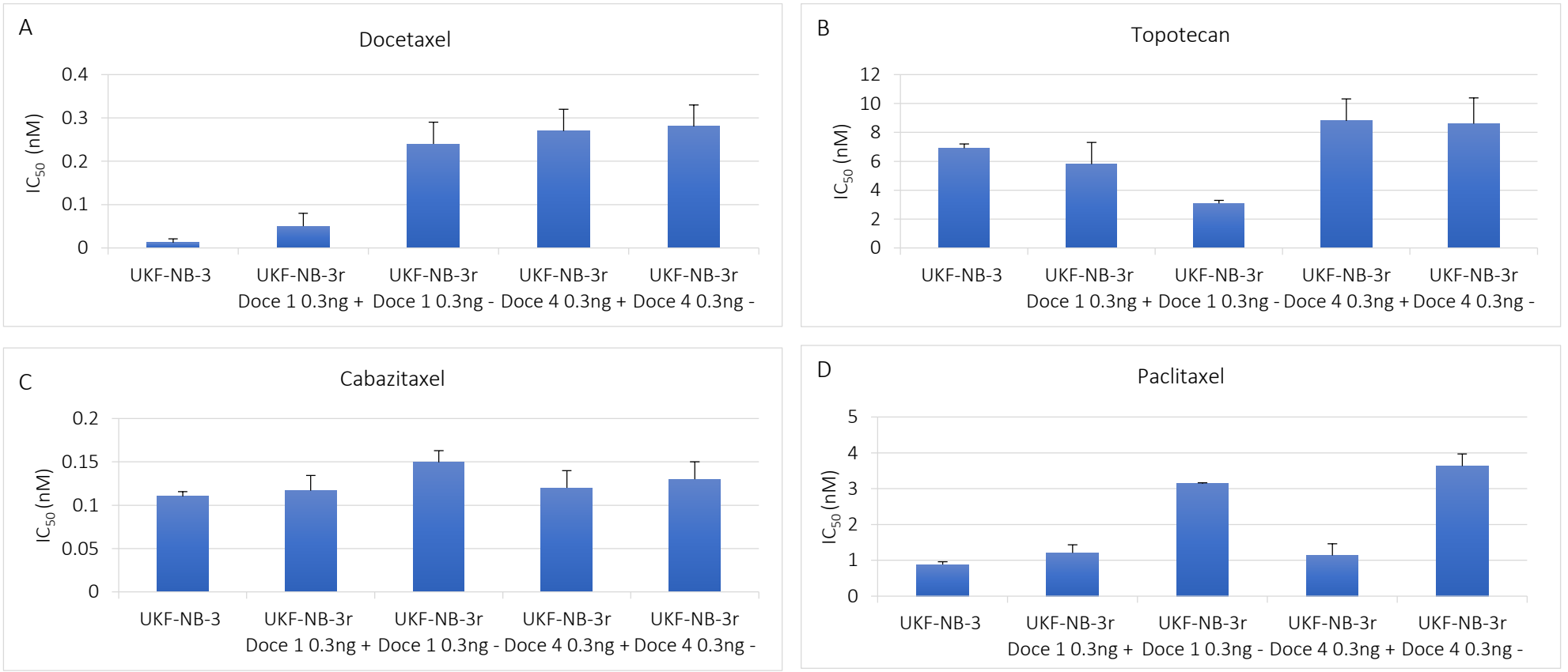


Figure 24: Cross resistance profiles for UKF-NB-3r Doce 1 and UKF-NB-3r Doce 4 in the presence and absence of docetaxel when tested against docetaxel, topotecan, cabazitaxel and paclitaxel and compared with the parental UKF-NB-3. UKF-NB-3r Doce 4 was more resistant to docetaxel, topotecan and paclitaxel than both UKF-NB-3r Doce 1 and UKF-NB-3 and slightly more sensitive to cabazitaxel. (n=3)

## 4.5 Discussion

Having chosen similar acting drugs and some within the same family this allowed us to investigate the clear differences highlighted in the protocol. A study to look into the differences in adapting sub-lines to certain drugs has not been done to this extent, where we have been able to closely monitor the growth pattern changes and map these to $IC_{50}$ values in routinely testing the cell lines monthly.

Using our standardised protocol, it can be concluded that when comparing the adaptation of UKF-NB-3 cell lines to study the development of acquired resistance to epothilone-B, cabazitaxel, docetaxel and paclitaxel, it is much easier to adapt cell lines to docetaxel and paclitaxel than to epothilone-B and cabazitaxel. This result is clearly shown in that epothilone-B and cabazitaxel sub-lines were not possible to continue passaging for as long as the other two drug adapted sub-lines. The adaptation of UKF-NB-3 to docetaxel and paclitaxel has been so successful in this project that the cell lines are still proliferating steadily in the presence and absence of drug and are continually showing resistance when compared to the parental.

Cabazitaxel is used effectively in the treatment of prostate cancer and interestingly is often prescribed after treatment with docetaxel, indicating that cabazitaxel is much more toxic than docetaxel and would also explain the difficulty in adapting cell lines to the drug (Pezaro, C.J, Omlin, A.G., Altavilla, A., Lorente, D., Ferraldeschi, R *et al* 2014; Oudard, S and Angelergues, A, 2014). Epothilone-B, another tubulin binding agent similar to the taxanes is a highly toxic therapeutic which is notorious for difficulty in adapting cell lines to but showed potency in the treatment of taxane-resistant cancer cell lines (Cheng, K.L, Bradley, T and Budman, D.R, 2008). This again would highlight the difficulty to adapt the sub-lines to this drug due to its efficacy in preventing cell growth and also explain the trend seen when the cell lines over time eventually cannot overcome the weeks having been in the presence of the drug. Finally, the UKF-NB-3r docetaxel adapted sub-line was the earliest cell line to show the development of acquired resistance with UKF-NB-3r Doce 4 indicating it was the most resistant from early stages in the protocol and indeed had the highest fold increase when compared to the parental as well as in the 8-drug panel where It is consistently has the highest IC50 fold changes in the majority of drugs. Makarovskiy, A.N, Siyaporn, E, Hixson, D.C and Akerley, W 2002, discuss an evaluation of docetaxel and paclitaxel effects on prostate cancer cell lines and report that when generating docetaxel resistant sub-lines, they too saw enhanced sensitivity to paclitaxel which occurs when the sub-lines investigated by this lab had been present in docetaxel. Taken together what is apparent is that the mechanisms underlying the resistance to paclitaxel and docetaxel are more effective than those in cabazitaxel and epothilone-B. This was a systematic approach to observe the cell lines over a long period of time and how they began to generate resistance. The remaining docetaxel and paclitaxel lines will be analysed with exome sequencing and for their growth kinetics using xCELLigence to better understand these findings.

# Chapter 5

# Investigation of intra-cell line heterogeneity in the neuroblastoma cell line UKF-NB-3

## 5.1 Introduction

The work carried out in this chapter covers the characterisation of 10 UKF-NB-3 single cell derived clones in order to investigate and study intra-cell line heterogeneity. The use of single-cell derived clones allows us to compare the findings back to the original parental cell line UKF-NB-3 and see any changes which have developed. This chapter has three sections which includes: fluorescence *in situ* hybridisation (FISH) of all 10 single cell derived clones and the UKF-NB-3 parental, cross-resistance profiles and doubling times.

## 5.2 Fluorescence *in situ* hybridisation (FISH) of UKF-NB-3 clones allowing full chromosomal analysis and characterisation of the whole cell genome

10 single-cell derived UKF-NB-3 clones were used for this project, with metaphases captured to allow analysis of chromosomal patterns seen across the cell lines. Each device allows identification of three chromosomes in each of the 8 squares using whole chromosome painting probes for three different chromosomes which each had three chromosomes in three different colour fluorophores; red, green and aqua. For this results chapter, each figure therefore identifies three chromosomes in the three fluorophores stated. All images captured were used to determine percentages of aberrations and translocations in the cell lines. Each metaphase is expected to contain two copies of each chromosome (diploidy) and so the expected appearance would be the presence of two clear fluorescent chromosomes for each colour investigated. FISH is an extensive tool, which has been used in several applications and is in development with other projects. FISH has been used to identify biomarkers in prostate cancer patients, which in turn would predict radiosensitivity of the cancers, which could be adapted for a variety of techniques in acquired resistance research (Beaton, L.A., Marro, L., Samiee, S., Malone, S., Grimes, S *et al* 2015).

The advantage of analyses such as FISH is that it is a non-invasive technique and could be repeated during the course of treatment to analyse progress and potential genomic changes. This is of important relevance as genomic instability occurs in rapidly dividing cells and can lead to the emergence of resistant outgrowths and the insensitivity to therapeutics. Wawrzyniak, E., Kotkowska, A., Blonski, J.Z., Siemieniuk-Rys, M., Ziolkowska, E., *et al* 2014 discuss the use of FISH to study changes in the progress of chronic lymphocytic leukemia (CLL), which can be used to identify patient outcome and to effectively monitor clonal evolution.

### 5.2.1 Results of chromosome 3, 15 and 17 in UKF-NB3 and 10 single cell derived clones

For each result shown, a minimum of 5 images of each square was taken in order to demonstrate the multiple number of times a metaphase may show the same result. Furthermore, in each of the figures the UKF-NB-3 single cell derived clones are compared with the UKF-NB3 parental. The first three shown are chromosome 3 in red, 15 with aqua and 17 with green which are highlighted in UKF-NB-3 parental in Figure 25A and the 10 UKF-NB-3 clones in Figure 25B.

In the UKF-NB-3 parental, the majority of metaphases displayed diploidy in chromosome 3 and this was also seen in UKF-NB-3 Clones 1, 3, 4, 7, 64 and 93. Differences were seen in UKF-NB-3 Clone 2 which had a variation of no chromosomes in 25% and 1 copy in 25% of the metaphases. This was similar to UKF-NB-3 clone 24 which had 50% with diploidy and 50% with only 1 chromosome highlighted. UKF-NB-3 Clone 56 and 80 indicated higher levels of heterogeneity with 75% of the metaphases showing an additional chromosome with the remaining metaphases containing no chromosome 3, a single or an extra copy.

Chromosome 15 in the UKF-NB-3 cell line displayed a high (90%) of very small multiple chromosomal translocations on various other chromosomes which is highlighted in Figure 25A. This was seen in the majority of metaphases of all UKF-NB-3 Clones except for clone 56 which had metaphases hard to distinguish. UKF-NB-3 Clone 3 had a higher majority of metaphases showing just two copies with no changes as shown in Figure 25B.

Chromosome 17 had a very clear single translocation seen in 70% of the UKF-NB-3 cell line which is highlighted in Figure 25A. When compared to the single cell derived clones in the figure 25B, the same translocation is seen in the UKF-NB-3 Clones 1, 2, 4, 7, 64, 80 and 93. UKF-NB-3 Clone 3 and 24 had a higher percentage of metaphases with no translocation. UKF-NB-3 Clone 56 had more varied results throughout the metaphases captured but there is a single translocation of chromosome 17 but with only one copy which is not seen in any other clones

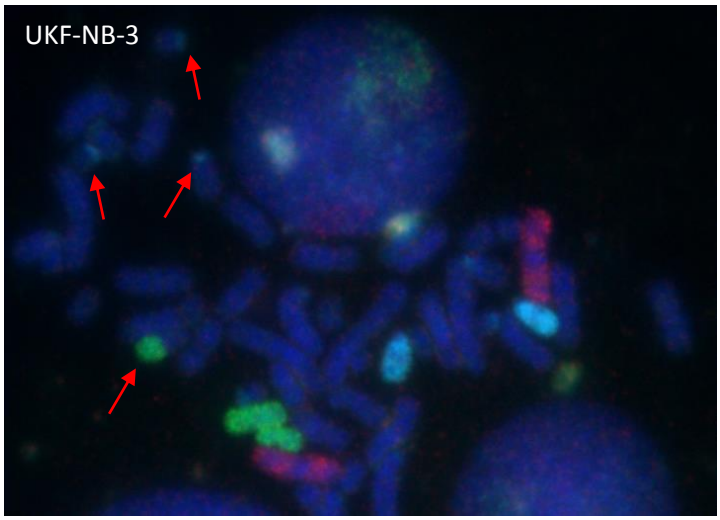


Figure 25A: UKF-NB-3 with chromosome 3 in red which displayed mainly diploid chromosomes, chromosome 15 in aqua which displayed multiple translocations shown by the red arrows and chromosome 17 stained with green which indicated a single translocation in 70% of the metaphases captured and is highlighted by the red arrow.

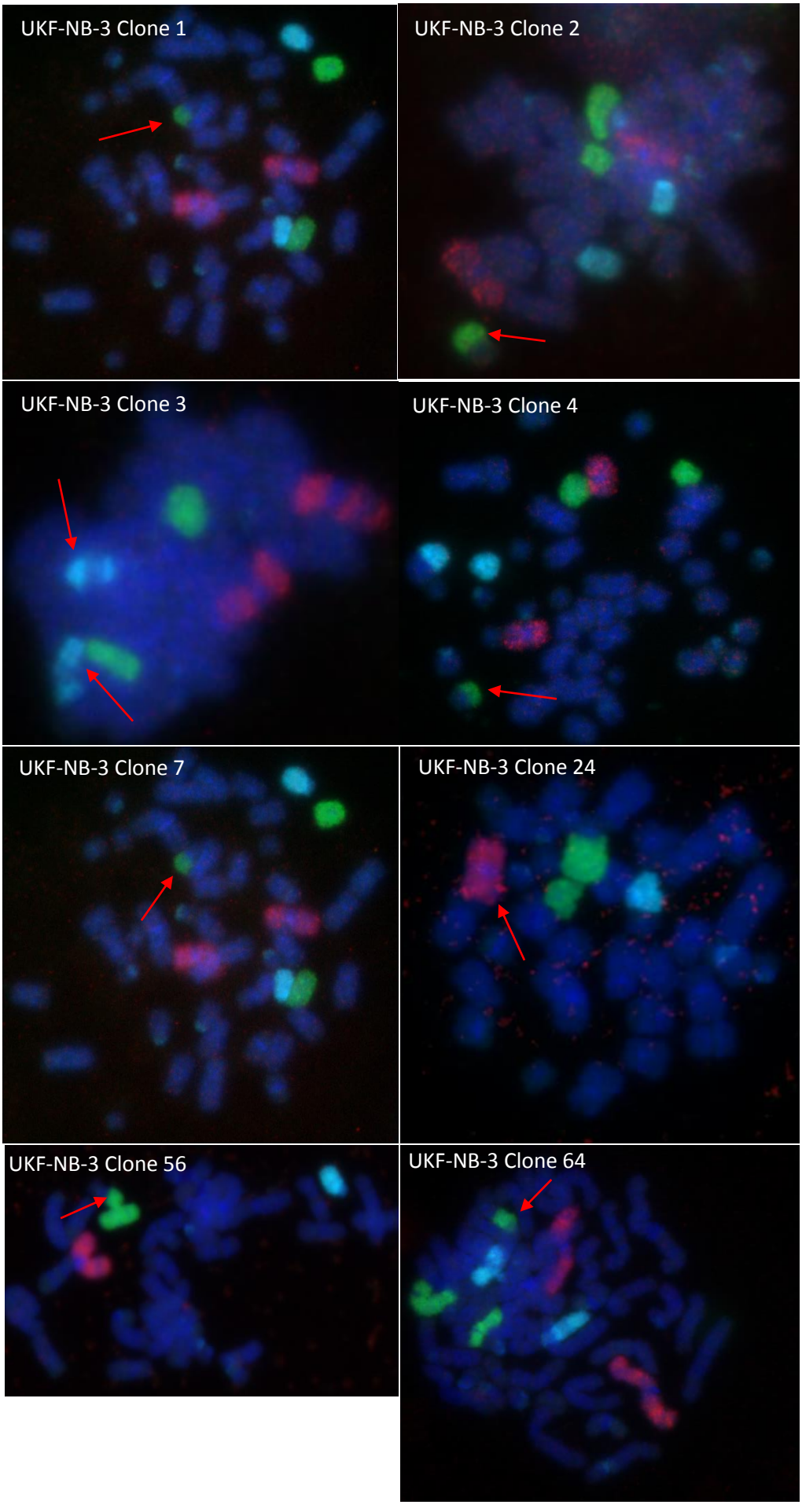
UKF-NB-3 Clone 1
UKF-NB-3 Clone 2
UKF-NB-3 Clone 3
UKF-NB-3 Clone 4
UKF-NB-3 Clone 7
UKF-NB-3 Clone 24
UKF-NB-3 Clone 56
UKF-NB-3 Clone 64

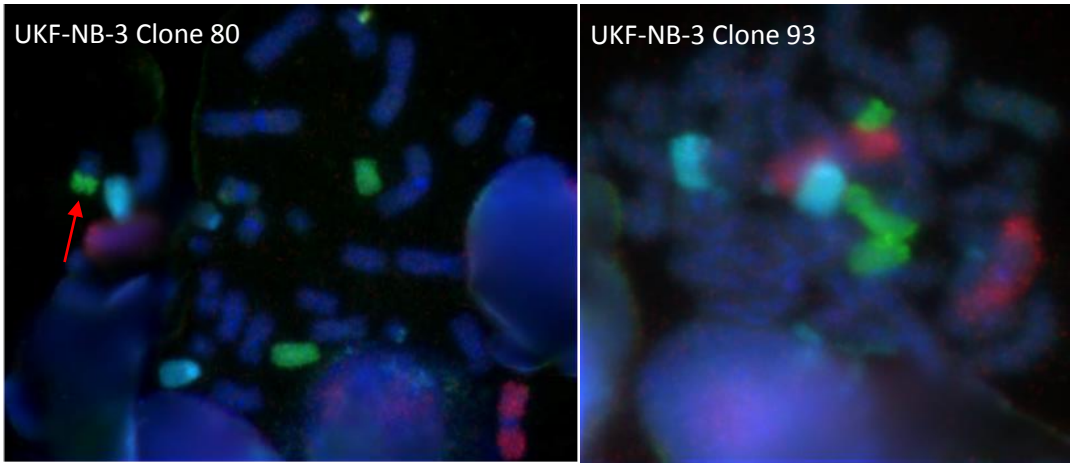


Figure 25B: All 10 UKF-NB-3 single-cell derived clones with chromosome 3 (red) which the majority of UKF-NB-3 clones displayed two copies of but some such as UKF-NB-3 Clone 24 had some images with only one copy as shown by the red arrow. Chromosome 15 (aqua) translocations were in a large majority of the clones but UKF-NB-3 clone 3 had two copies only. Chromosome 17 (green) had the same single translocation in the large majority of the clones and is highlighted in relevant images.

### 5.2.2 Results of chromosome 8, chromosome 12 and chromosome 21 in UKF-NB3 and 10 single cell derived clones

The next three chromosomes investigated on the second square of the device were 8 (red), 12 (aqua) and 21 (green). UKF-NB-3 parental had two copies of chromosome 8 in all metaphases captured and this was seen in all the UKF-NB-3 clones with no changes observed in any images.

In 85% of the metaphases taken of UKF-NB-3 there was a single translocation of chromosome 12 as shown in Figure 26A. Interestingly, a difference was observed from the parental as all the derived UKF-NB-3 clones all contained an extra chromosome 12 in the majority of metaphases as highlighted in Figure 26B. Except for UKF-NB-3 Clone 4 which was the only sub-line to contain the same mutation as the parental line in 100% of the metaphases.

Chromosome 21 in UKF-NB-3 had two copies in 70% of metaphases captured but the UKF-NB-3 clones had a great deal of variability as shown in Figure 26B. Clones 1, 2, 24 and 93 had multiple translocations of chromosome 21 in over 60% of the metaphases. Metaphases captured of UKF-NB-3 clones 3, 4 and 80 had multiple translocations in 100% of images taken. UKF-NB-3 Clone 7 had the same translocations in 90% of metaphases which only differed by the presence of one or two copies of the chromosome UKF-NB-3 56 had over 80% of metaphases displaying multiple translocations but the majority were with only one copy of chromosome 21. UKF-NB-3 Clone 64 had over 70% multiple translocations but as shown in Figure 26B the remaining metaphases showed either one or two copies.

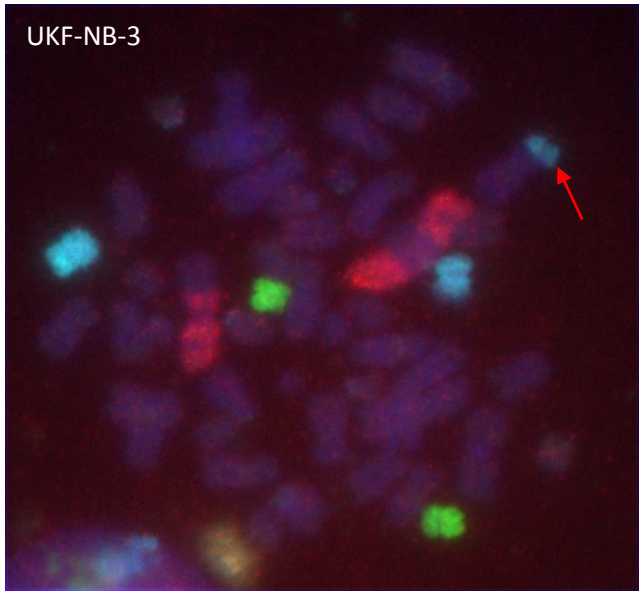


Figure 26A: UKF-NB-3 with chromosome 8 (red) with two copies as seen in all metaphases. Chromosome 12 (aqua) had a single translocation in 85% of images captured and is highlighted with the red arrow. Chromosome 21 (green) had two copies in 70% of metaphases.

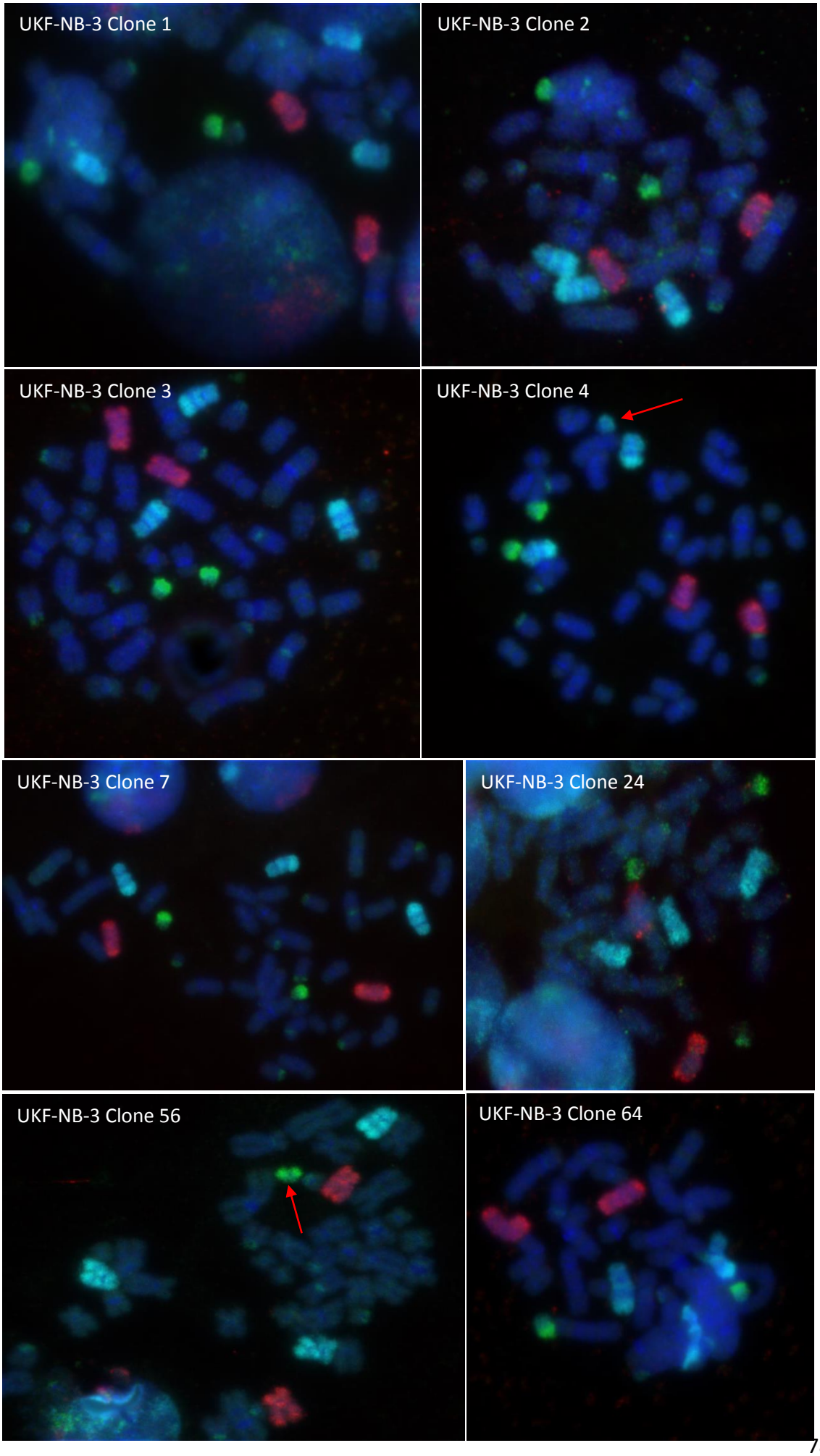
UKF-NB-3 Clone 1
UKF-NB-3 Clone 2
UKF-NB-3 Clone 3
UKF-NB-3 Clone 4
UKF-NB-3 Clone 7
UKF-NB-3 Clone 24
UKF-NB-3 Clone 56
UKF-NB-3 Clone 64

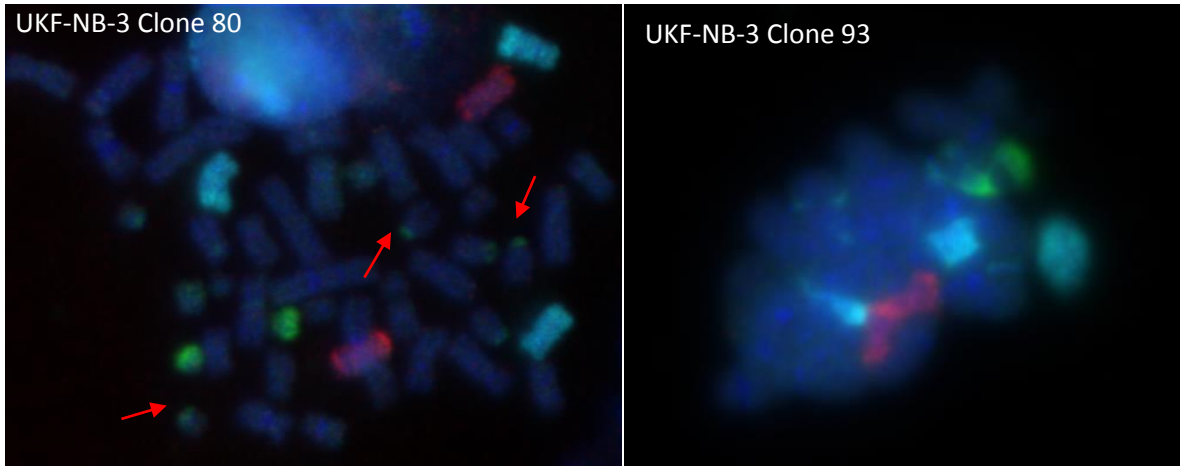


Figure 26B: All 10 UKF-NB-3 single-cell derived clones with chromosome 8 in red with two copies in all images captured of all clones. Chromosome 12 in aqua had an extra copy in all metaphases captured but only UKF-NB-3 Clone 4 had the same translocation as UKF-NB-3 as highlighted with the red arrow. Chromosome 21 in green had high variation in the UKF-NB-3 Clones with the majority displaying multiple translocations but UKF-NB-3 Clone 56 had only one copy of the chromosome alongside the translocations as highlighted.

### 5.2.3 Results of chromosome 1, chromosome 16 and chromosome 19 in UKF-NB3 and 10 single cell derived clones

UKF-NB-3 parental had two copies of chromosome 1 (red) in 100% of the metaphases captured as clearly shown in Figure 27A. This pattern was also replicated in UKF-NB-3 Clone 1 in 100% of the metaphases and UKF-NB-3 Clone 3 in 70% of images taken. UKF-NB-3 Clone 2 had a single translocation in 57% of the metaphases. UKF-NB-3 Clone 4 had 78% of metaphases indicating a single translocation of chromosome 1 alongside a single copy and UKF-NB-3 Clone 7 and 24 had the same result but in 90%. UKF-NB-3 Clone 56 had differences across all images captured with 40% showing two copies with the single translocation and 30% of metaphases the same as UKF-NB-3. UKF-NB-3 Clone 64 metaphases contained no evidence of a single translocation and displayed the same chromosome pattern as UKF-NB-3. UKF-NB-3 Clone 80 and 93 had metaphases showing a single translocation in 100% of the images but with varying copies of the chromosomes, UKF-NB-3 Clone 80 with two and UKF-NB-3 Clone 93 with one.

Chromosome 16 (aqua) had a varying degree of heterogeneity across the UKF-NB-3 cell line with 60% of the metaphases displaying an extra chromosome and 40% highlighted a single translocation as shown in Figure 27A. When compared with the findings from the UKF-NB-3 Clones the same single translocation but not an extra chromosome as shown in Figure 27B.

Chromosome 19 (green) was observed in UKF-NB-3 to have 60% of metaphases showing multiple translocations but only UKF-NB-3 Clone 80 had the same mutation as UKF-NB-3. All the remaining clones displayed two copies of chromosome 19 on the majority of metaphases captured.

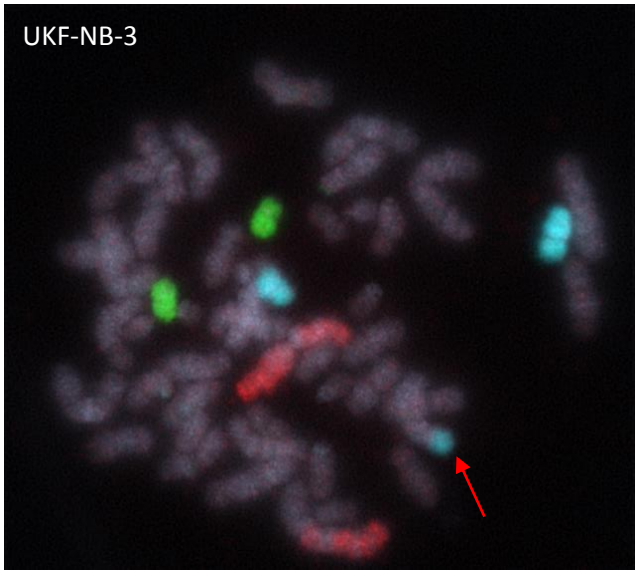


Figure 27A: Metaphase captured of UKF-NB-3, Chromosome 1 (red) had two copies in 100% of metaphases captured. The red arrow indicates the single translocation of chromosome 16 (aqua) seen in 60% of the metaphases captured. Chromosome 19 (green) had two copies in 40% of metaphases captured and 60% presented with multiple translocations.

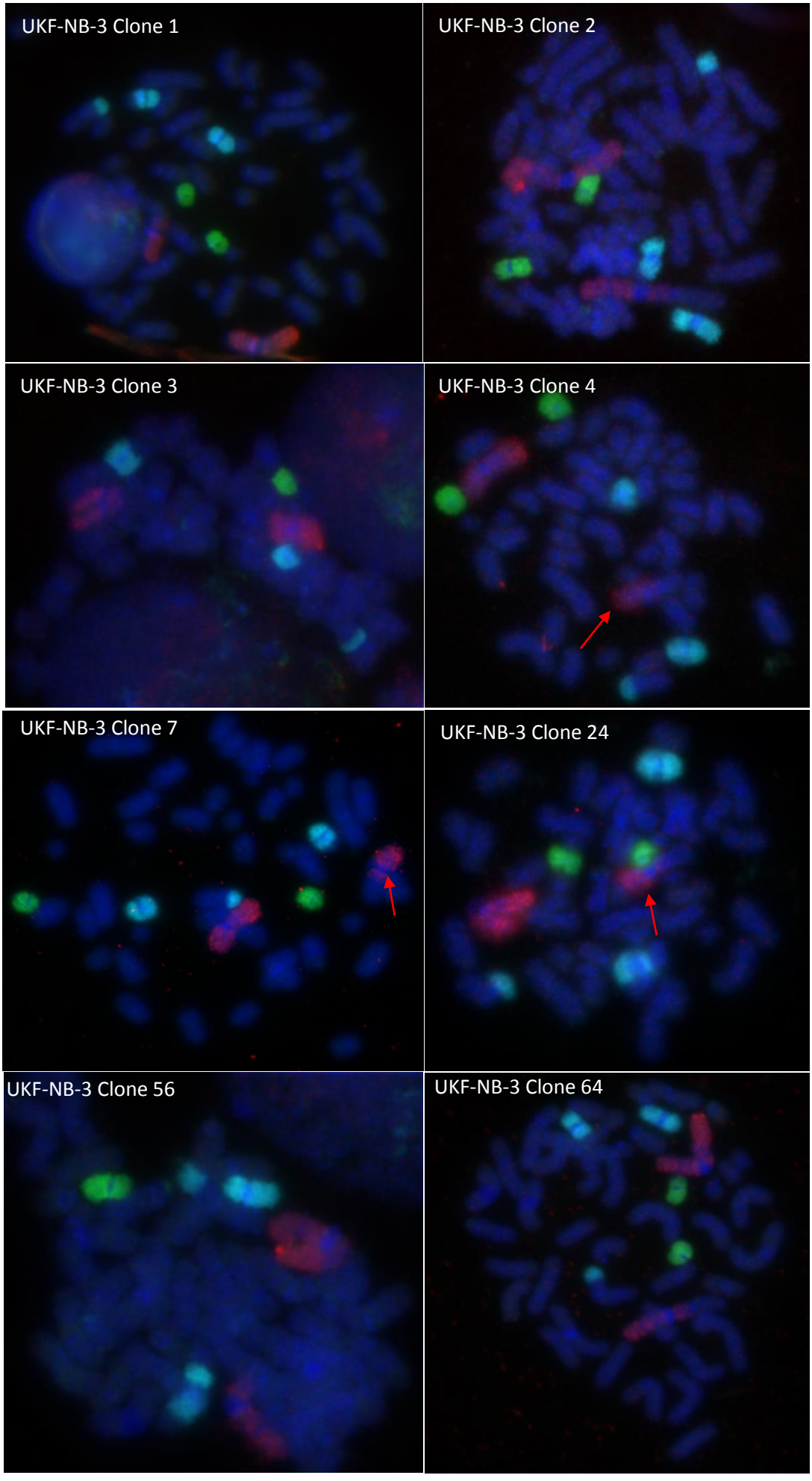
UKF-NB-3 Clone 1
UKF-NB-3 Clone 2
UKF-NB-3 Clone 3
UKF-NB-3 Clone 4
UKF-NB-3 Clone 7
UKF-NB-3 Clone 24
UKF-NB-3 Clone 56
UKF-NB-3 Clone 64

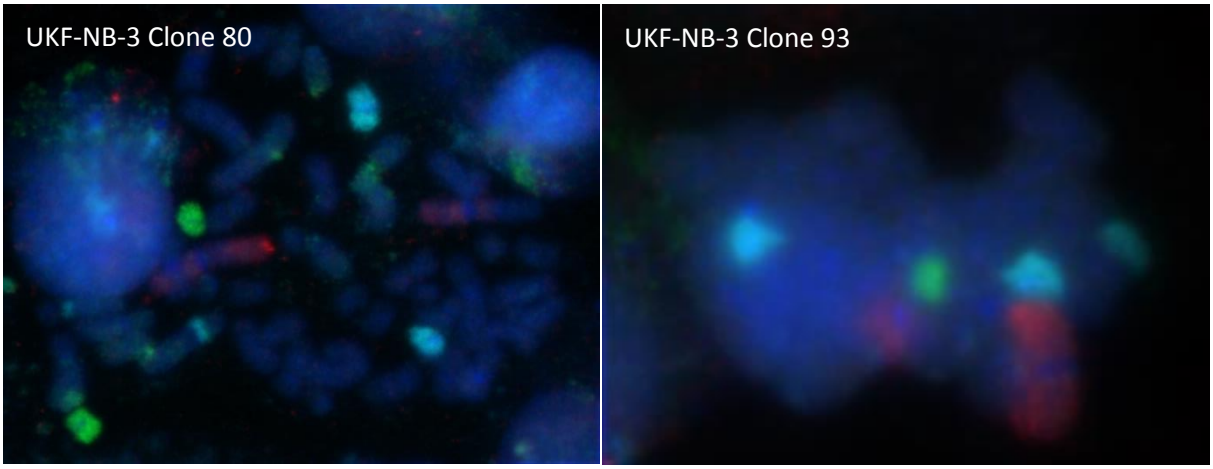


Figure 27B: Metaphases captured of all 10 UKF-NB-3 Clones. Chromosome 1 (red) had varied results throughout the clones with UKF-NB-3 Clone 1,3 and 64 displaying two copies but UKF-NB-3 Clone 4, 7 and 24 displayed a single translocation as highlighted. All clones contained a single translocation of chromosome 16 (aqua) clearly seen in each metaphase. Chromosome 19 (green) had two copies in all UKF-NB-3 clones except for UKF-NB-3 Clone 80 which displayed multiple translocations as highlighted.

### 5.2.4 Results of chromosome 2, chromosome 13 and chromosome 20 in UKF-NB3 and 10 single cell derived clones

UKF-NB-3 had a single translocation of chromosome 2 (red) in all metaphases captured with only the copy number differing with 70% showing two and 30% with one copy as shown in Figure 28A. Interestingly, in 90% of the images, separate translocations of chromosome 2 also attached to two copies of chromosome 13 (aqua) this was also seen in all the UKF-NB-3 Clones as shown in Figure 28B. 90% of UKF-NB-3 Clone 1 metaphases displayed multiple translocations of chromosome 2. All remaining clones had a higher percentage of metaphases containing the same single translocation (with different copy numbers) as the parental as well as some metaphases containing multiple translocations.

Chromosome 13 in UKF-NB-3 had multiple translocations seen in all metaphases captured of UKF-NB-3 but 20% of these contained only one chromosome. All UKF-NB-3 Clones had multiple translocations of chromosome 13 with no difference when compared to the UKF-NB-3 parental (Figure 28B).

Chromosome 20 (green) was observed with one extra chromosome in 90% of the UKF-NB-3 metaphases captured as shown in Figure 28A. The derived UKF-NB-3 clones all had the same mutation in the majority of metaphases as shown in Figure 28B with the exception of UKF-NB-3 Clone 56 which had a higher proportion of metaphases containing four copies of chromosome 20. UKF-NB-3 Clone 80 had the most variation in all the cell lines analysed with equal percentages of metaphases which displayed one to four copies of chromosome 20. UKF-NB-3 Clone 93 had a range of metaphase patterns with an equal amount presenting two and three copies of chromosome 20 and a single metaphase with no copies and just multiple translocations.

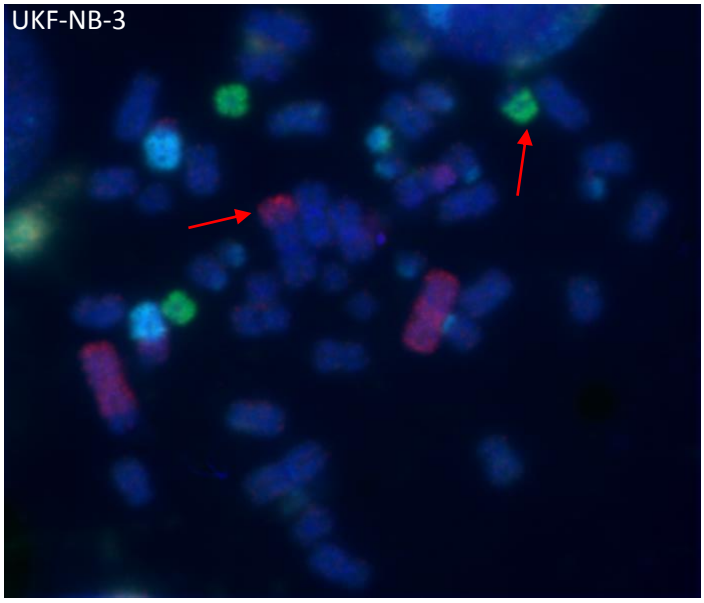


Figure 28A: Metaphase captured of UKF-NB-3 displaying a translocation of chromosome 2 (red) as highlighted. Multiple translocations of chromosome 13 (aqua) were observed with varying copy numbers. An extra chromosome 20 (green) was observed in 90% of images captured and is highlighted above.

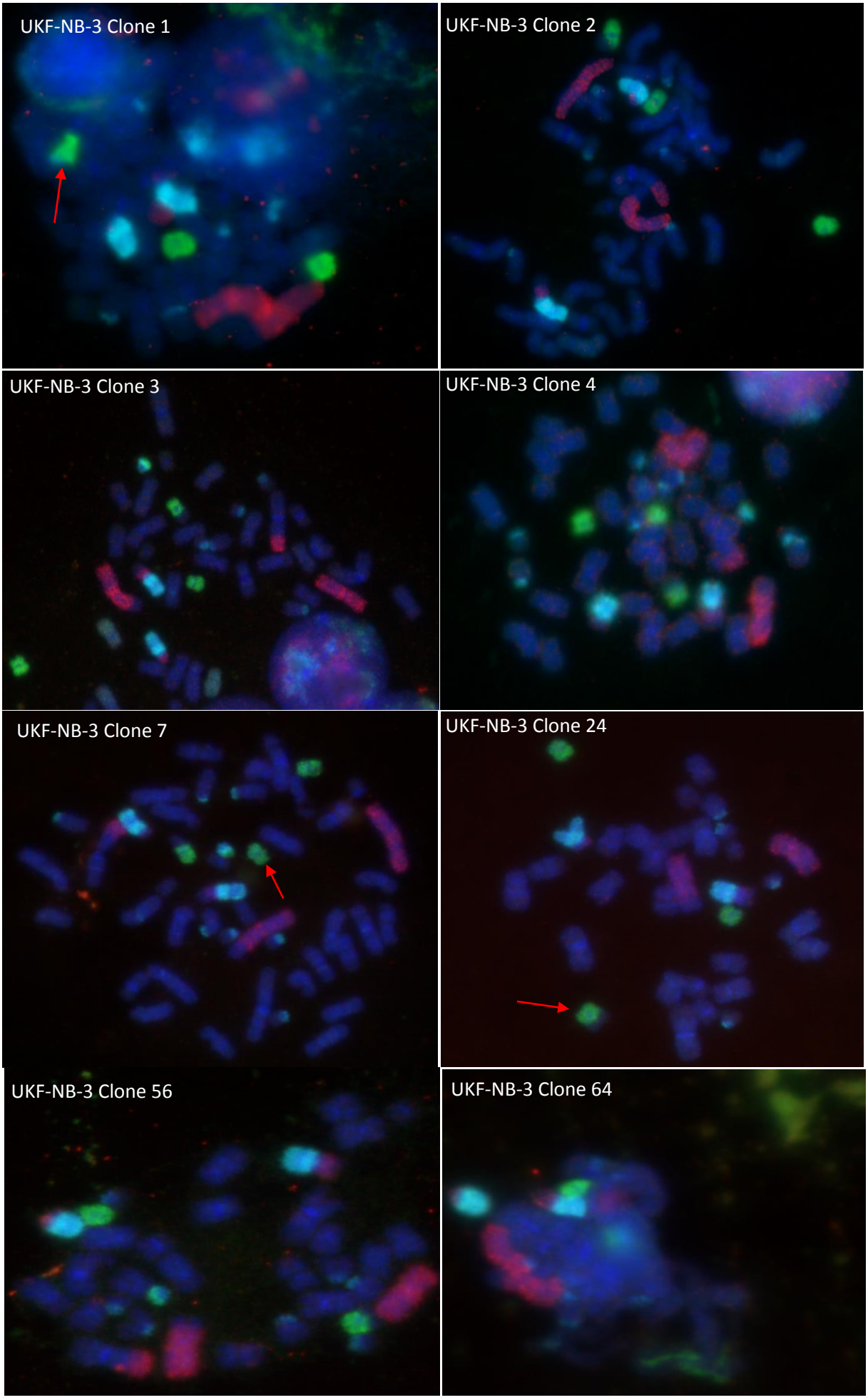
UKF-NB-3 Clone 1
UKF-NB-3 Clone 2
UKF-NB-3 Clone 3
UKF-NB-3 Clone 4
UKF-NB-3 Clone 7
UKF-NB-3 Clone 24
UKF-NB-3 Clone 56
UKF-NB-3 Clone 64

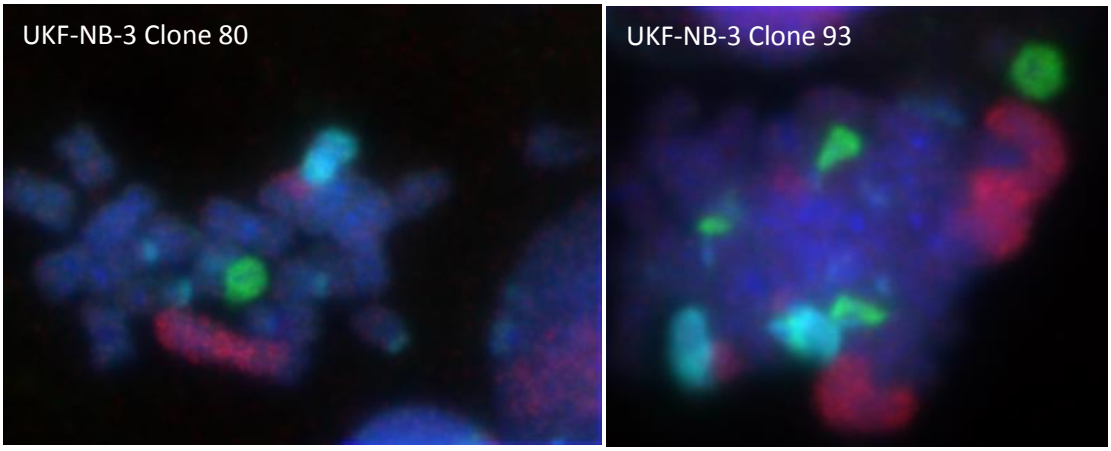


Figure 28B: Metaphases of all 10 UKF-NB-3 clones with chromosome 2 (red) attaching to two copies of chromosome 13 (aqua) in all clones but clearly shown in UKF-NB-3 Clone 3 and Clone 56 as highlighted as well as multiple translocations of chromosome 13. A high majority of the clones also presented with one extra chromosome 20 (green) as highlighted in UKF-NB-3 Clone 1, 7 and 24.

### 5.2.5 Results of chromosome 9, chromosome 11 and chromosome 22 in UKF-NB3 and 10 single cell derived clones

Chromosome 9 (red) in UKF-NB-3 had two copies in 100% of the metaphases captured as shown in Figure 29A and this was also replicated in UKF-NB-3 Clone 3, in 60% of the metaphases in UKF-NB-3 Clone 4 and Clone 64 and in 80% of UKF-NB-3 Clone 93. UKF-NB-3 Clone 1 had only one metaphase containing the same two copies and UKF-NB-3 Clone 2 differed from the parental with three copies of chromosome 9 as shown in Figure 29B. This was also seen in UKF-NB-3 Clone 56 in a lower percentage of images and some contained only one copy. UKF-NB-3 Clone 7 and 24 also differed from UKF-NB-3 with 100% of metaphases displaying a single translocation alongside two copies of the chromosome. Finally, UKF-NB-3 Clone 80 had only one copy of chromosome 9 and a single translocation. UKF-NB-3 had 80% metaphases that indicated two copies of chromosome 11 (aqua) with multiple translocations as shown in Figure 29A. UKF-NB-3 Clones 1, 2, 3, 4, 7, 64 and 93 al contained two copies of chromosome 11. UKF-NB-3 Clone 24 had an extra copy of in both metaphases captured, UKF-NB-3 Clone 56 had 40% of metaphases with one and two copies, but the remaining 20% contained multiple translocations as seen in UKF-NB-3.UKF-NB-3 Clone 80 had only one copy of the chromosome in 75% of images analysed.

UKF-NB-3 had two copies of chromosome 22 (green) and one clear single translocation in 100% of metaphases as shown in Figure 29A. UKF-NB-3 Clone 1, 3 and 64 all contained the same chromosomal pattern as the parental as shown in Figure 29B. UKF-NB-3 clones 4, 7, 24, 56, 80 and 93 all had two copies but multiple translocations of chromosome 22. UKF-NB-3 Clone 2 presented the same result but with one copy of the chromosome.

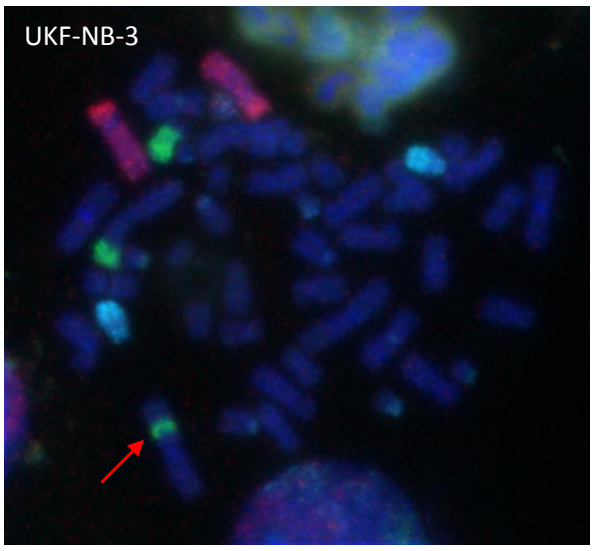


Figure 29A: Chromosome 9 (red), chromosome 11 (aqua) and chromosome 22 (green) in UKF-NB-3. There are two copies of chromosome 9 seen in 100% of metaphases as well as two copies of chromosome 11 with multiple translocations. The red arrow indicates the single translocation observed alongside two copies of chromosome 22 in 100% of images captured.

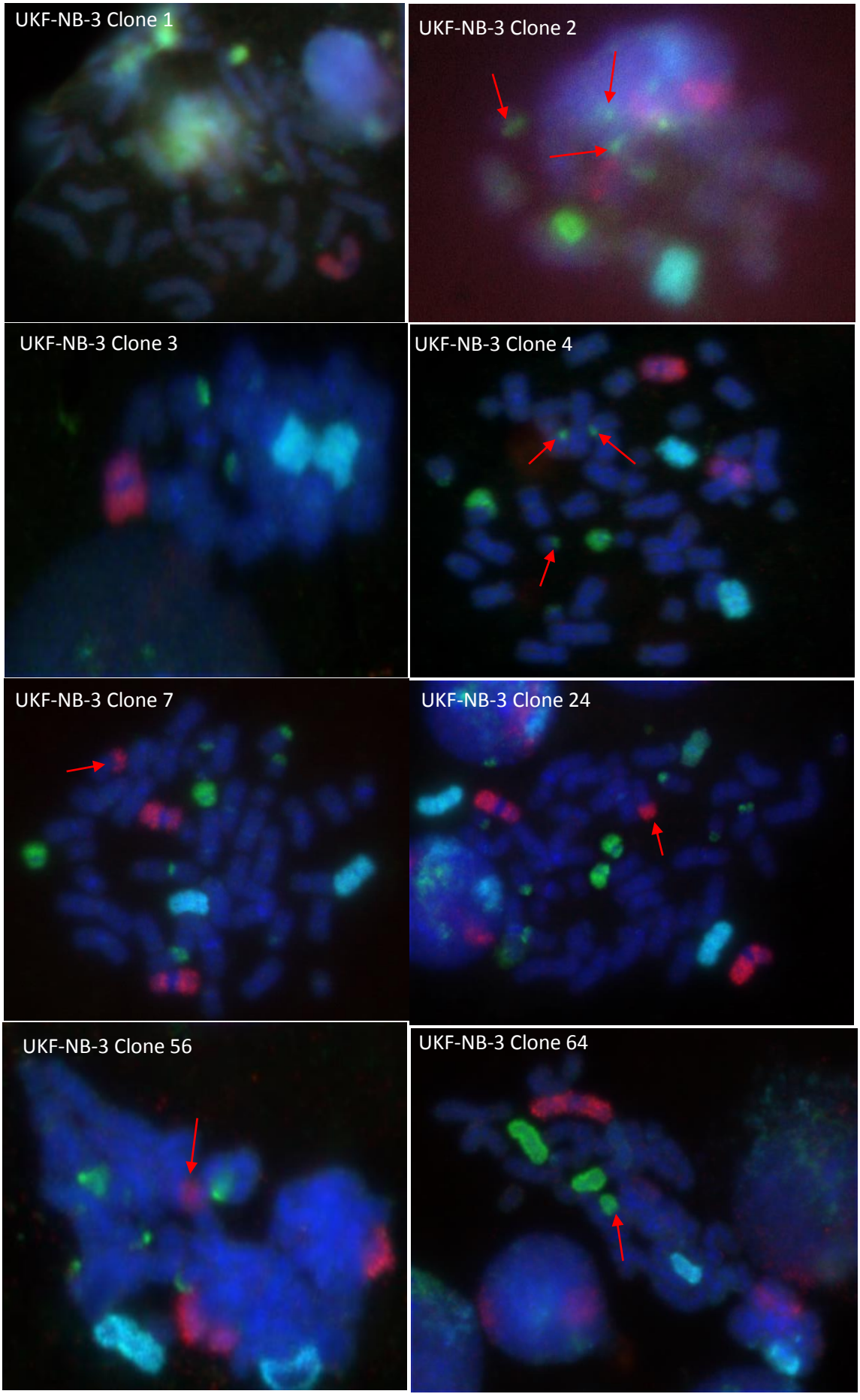
UKF-NB-3 Clone 1
UKF-NB-3 Clone 2
UKF-NB-3 Clone 3
UKF-NB-3 Clone 4
UKF-NB-3 Clone 7
UKF-NB-3 Clone 24
UKF-NB-3 Clone 56
UKF-NB-3 Clone 64

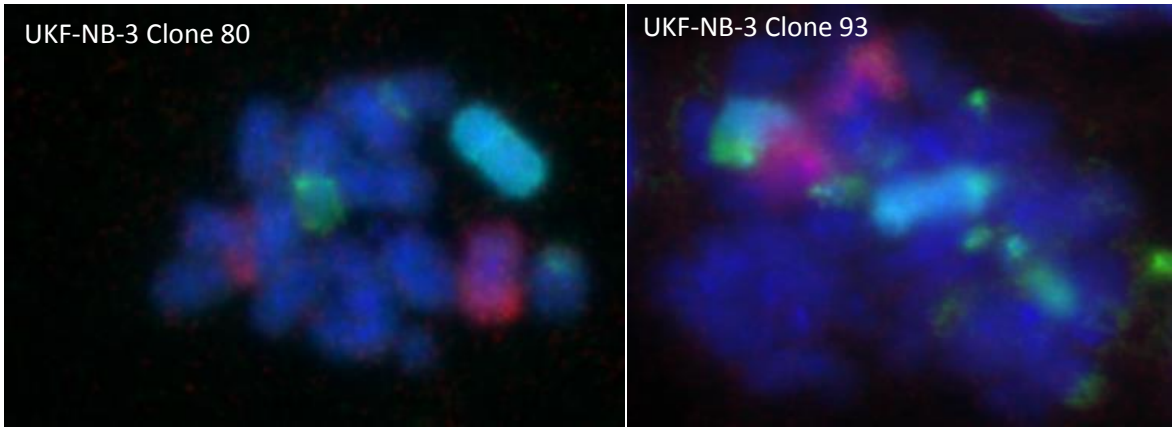


Figure 29B: Metaphases captured of all 10 UKF-NB-3 Clones. Chromosome 9 (red) had different patterns in the clones with UKF-NB-3 Clone 7, 24 and 56 expressing a translocation as highlighted and others such as UKF-NB-3 Clone 80 with just a single copy of the chromosome. Chromosome 11 (aqua) presented with two copies in the majority of the clones with some presenting an extra or single copy as seen in UKF-NB-3 Clone 80. Chromosome 22 (green) also differed with the majority of clones presenting multiple translocations seen in UKF-NB-3 Clone 2 and 4 but others such as UKF-NB-3 Clone 64 presenting with a single translocation.

### 5.2.6 Results of chromosome 4, chromosome 14 and chromosome 18 in UKF-NB3 and 10 single cell derived clones

UKF-NB-3 had two copies of chromosome 4 (red) in the majority of metaphases captured as shown in Figure 30A. In the single-cell derived clones a high percentage of all images contained the same two copies as shown in Figure 30B with only a few displaying only one copy. The only difference was observed in UKF-NB-3 Clone 2 which contained a single translocation in one metaphase captured.

UKF-NB-3 had two copies of chromosome 14 (aqua) in 100% of metaphases captured again highlighted in Figure 30A. There was a high amount of variability in comparison in the UKF-NB-3 Clones as shown in Figure 30B. UKF-NB-3 Clone 1, 7 and 56 had diploidy but alongside multiple translocations in over 80% of images. UKF-NB-3 Clones 2, 3 and 24 all had multiple translocation in 75% of the metaphases and 25% had the same mutation as the parental. UKF-NB-3 Clone 4 and 64 had 100% of metaphases indicating two copies and multiple translocations. UKF-NB-3 Clone 80 had multiple translocations in 50% of the metaphases and finally UKF-NB-3 Clone 93 was the only cell line to have the majority of images displaying diploidy with a single translocation.

Chromosome 18 (green) had high variation in UKF-NB-3 with 30% of images displaying diploid, 30% with two copies and a single translocation and the remainder with a single copy with one translocation as shown in Figure 30A. In UKF-NB-3 Clones 1, 2, 3, 56, 64, 80 and 93 the majority of metaphases indicated diploidy alongside a single translocation. Interestingly, a difference was observed in UKF-NB-3 Clone 4 with over 50% of metaphases presenting with only one copy of chromosome 18 and a single translocation. 100% of metaphases from UKF-NB-3 Clone 7 and 24 had two copies and a single translocation.

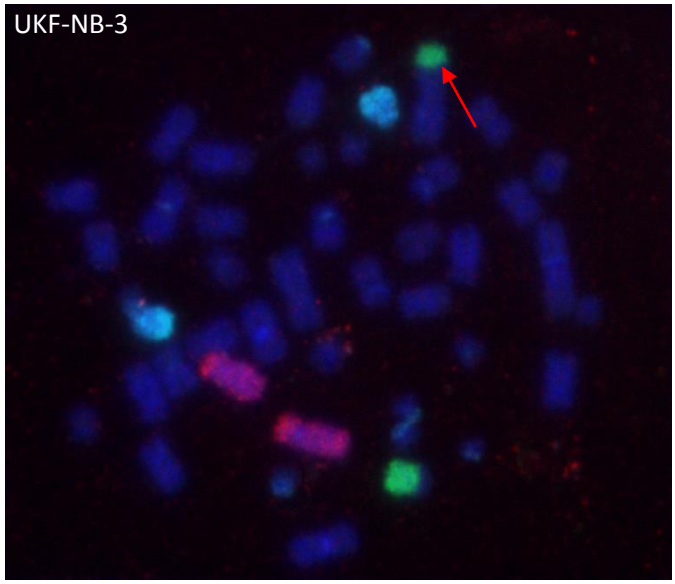


Figure 30A: Chromosome 4 (red), chromosome 14 (aqua) and chromosome 18 (green) in UKF-NB-3. There are two copies of chromosome 4 seen in the majority of metaphases as well as two copies of chromosome 14. The red arrow indicates a possible single translocation observed alongside one copy of chromosome 18 seen in 40% of images captured.

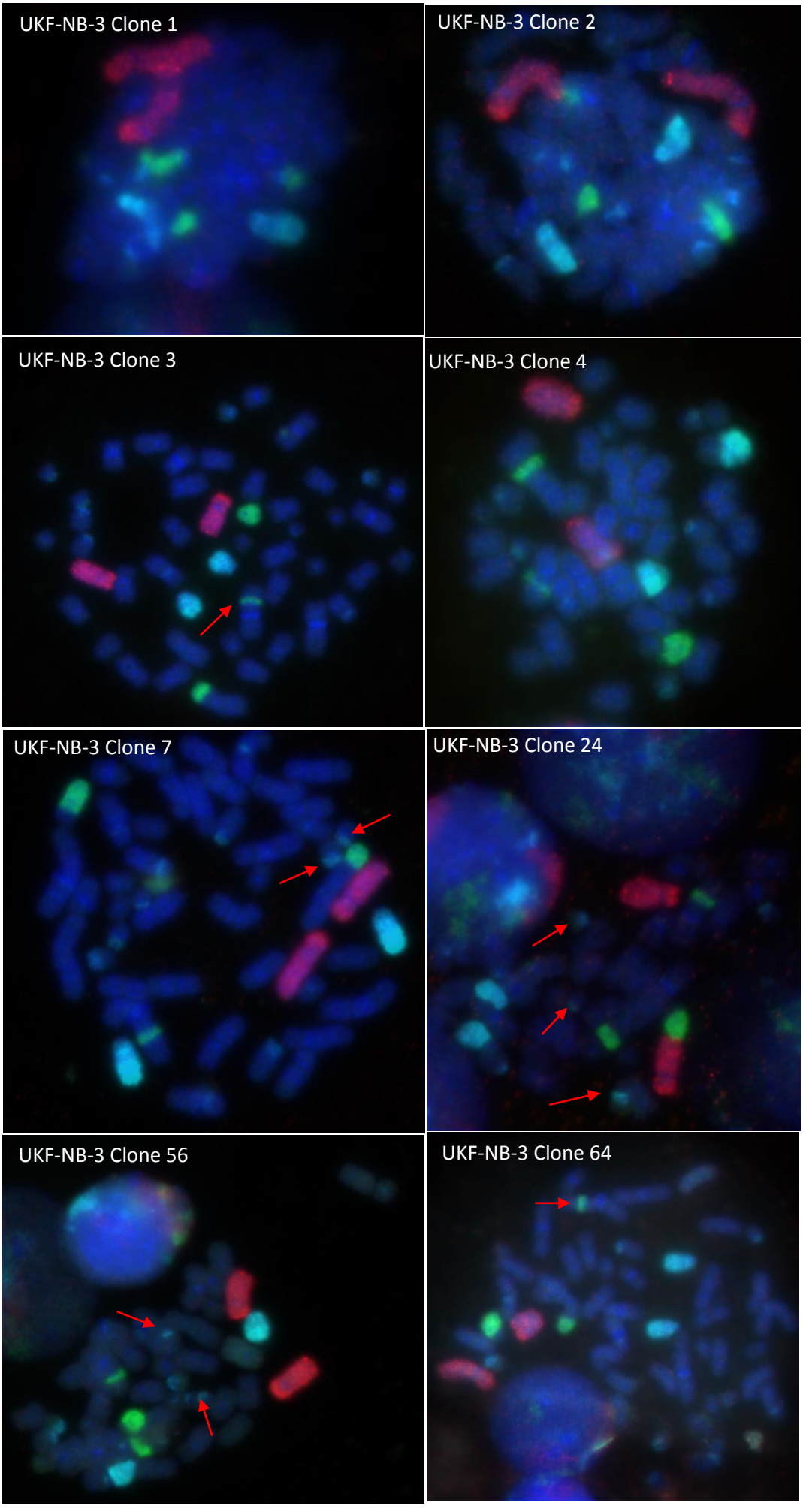
UKF-NB-3 Clone 1
UKF-NB-3 Clone 2
UKF-NB-3 Clone 3
UKF-NB-3 Clone 4
UKF-NB-3 Clone 7
UKF-NB-3 Clone 24
UKF-NB-3 Clone 56
UKF-NB-3 Clone 64

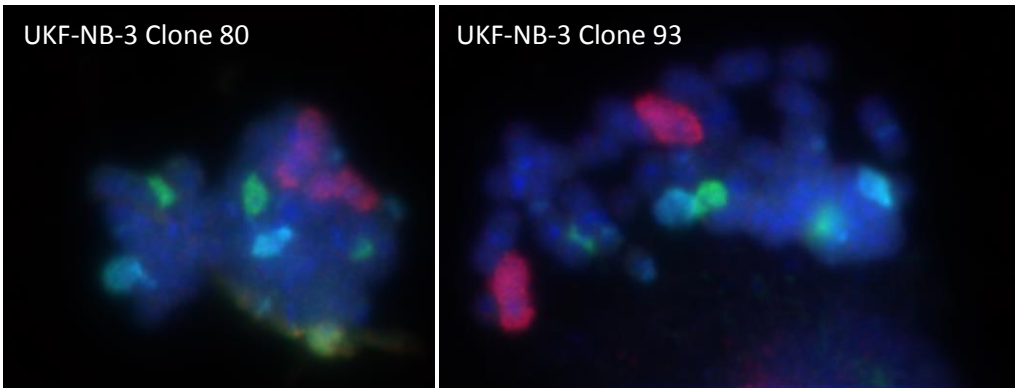


Figure 30B: All metaphases of the 10 UKF-NB-3 Clones with chromosome 4 (red) which all displayed two copies of the chromosome in the majority of images captured. Chromosome 14 (aqua) had mainly two copies in the majority of the UKF-NB-3 Clones with some presenting multiple translocations as seen in UKF-NB-3 Clone 7, 24 and 56. Chromosome 18 (green) displayed as two copies and a single translocation as shown in UKF-NB-3 Clone 3 and Clone 64 and in the majority of clones.

### 5.2.7 Results of chromosome 5, chromosome 10 and chromosome 7 in UKF-NB3 and 10 single cell derived clones

100% of images taken of UKF-NB-3 identified two copies of chromosome 5 (red) as shown in Figure 31A, which was seen in almost 100% of the metaphases taken of the UKF-NB-3 Clones with only very small percentages presenting just one copy. UKF-NB-3 Clone 7 and 56 also contained one extra chromosome in 20% and 30% respectively.

Chromosome 10 (aqua) displayed a single small translocation in 100% of the metaphases captured from UKF-NB-3. This was again seen in all the derived clones in very high percentages as shown in Figure 31B with only UKF-NB-3 Clone 93 containing no translocations and just two copies of chromosome 10.

In the UKF-NB-3 cell line, chromosome 7 (green) had two copies in over 90% of images taken as shown in Figure 31A. The UKF-NB-3 Clones all presented with similar results with two copies in the majority of metaphases captured. There was a translocation in UKF-NB-3 Clone 80 which is highlighted in Figure 31B.

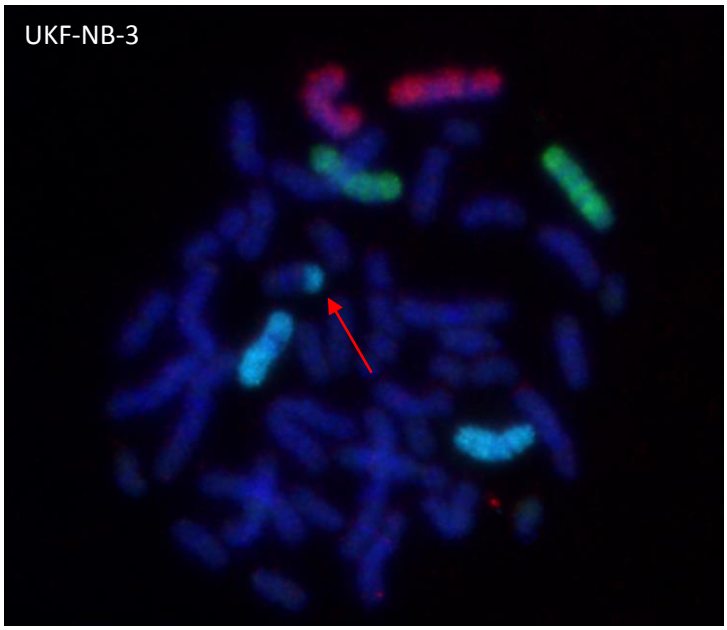


Figure 31A: Chromosome 5 (red), chromosome 10 (aqua) and chromosome 7 (green) in UKF-NB-3. There are two copies of chromosome 5 seen in the majority of metaphases. The red arrow indicates the single translocation observed alongside two copies of chromosome 10 seen in 100% of the images captured. Diploidy of chromosome 7 is also observed.

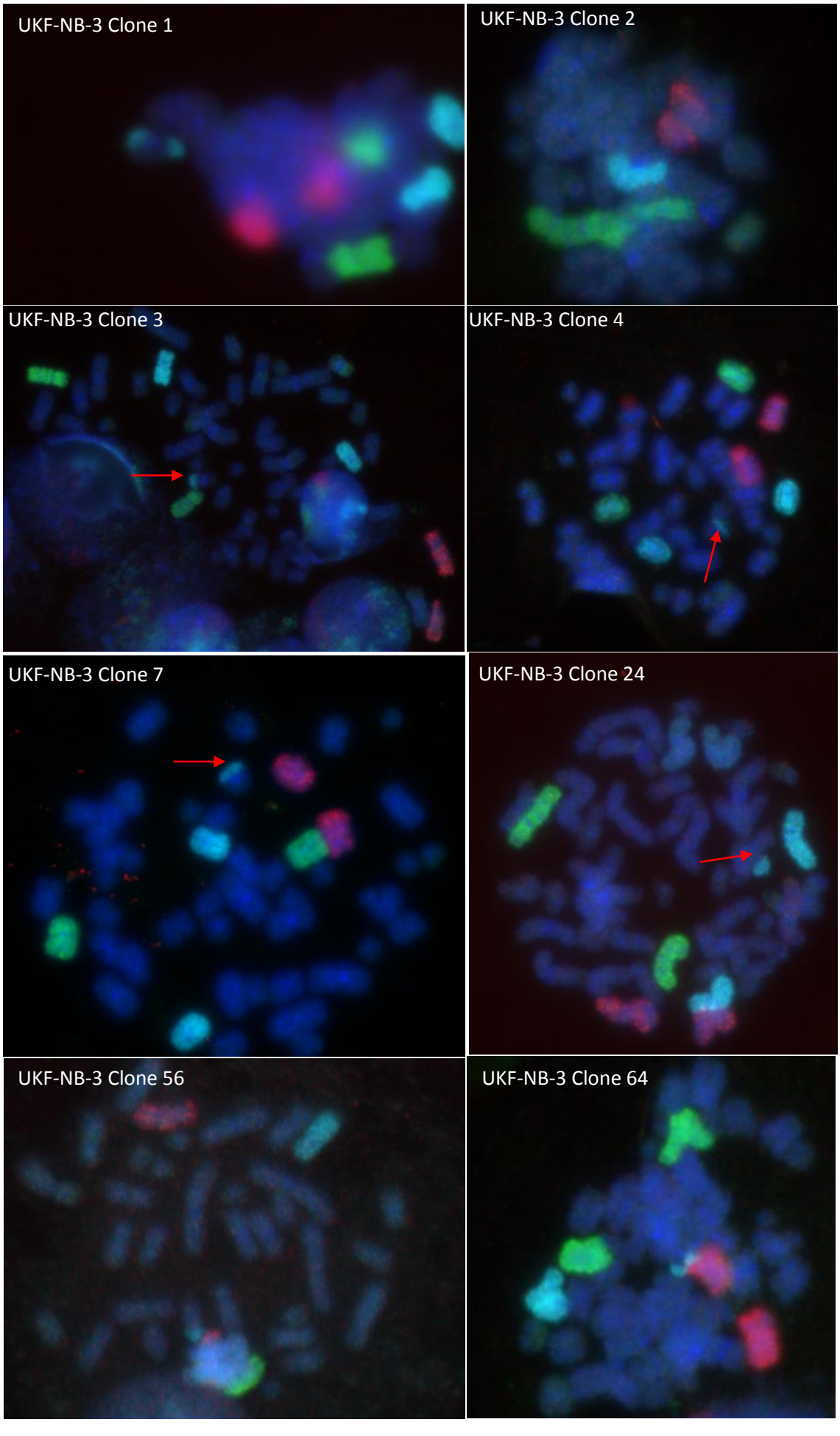
UKF-NB-3 Clone 1
UKF-NB-3 Clone 2
UKF-NB-3 Clone 3
UKF-NB-3 Clone 4
UKF-NB-3 Clone 7
UKF-NB-3 Clone 24
UKF-NB-3 Clone 56
UKF-NB-3 Clone 64

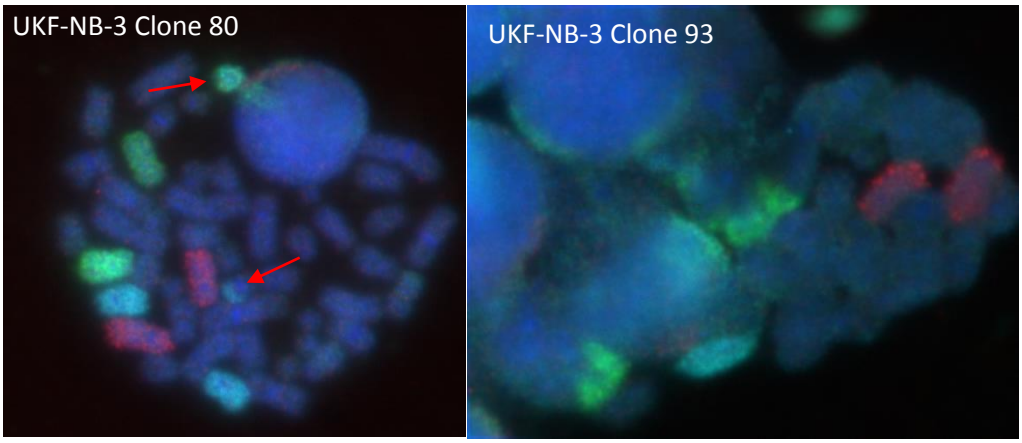


Figure 31B: All 10 UKF-NB-3 Clones with chromosome 5 (red) presenting with two copies in the high majority of metaphases captured. Chromosome 10 (aqua) displayed a single translocation in the majority of UKF-NB-3 Clones and is highlighted in the relevant metaphases. Chromosome 7 (green) has two copies in the majority of clones with some presenting different patterns such as UKF-NB-3 Clone 80 with a small translocation.

### 5.2.8 Results of chromosome X, chromosome 6 and chromosome Y in UKF-NB3 and 10 single cell derived clones

The X chromosome (red) in 100% of the metaphases captured in UKF-NB-3 had only one copy but this had small sections for the Y chromosome throughout the chromosome X as shown in Figure 32A this was result was also seen in all the UKF-NB-3 clones in Figure 32B.

Chromosome 6 (aqua) in the UKF-NB-3 line had two copies in 100% of the metaphases captured as shown in Figure 32A. The majority of all the UKF-NB-3 clones had diploidy with the exception of UKF-NB-3 Clone 1, 24 and 80 which all had a few metaphases containing only one copy.

The Y chromosome (green) was not detected clearly in all the metaphases taken but small translocations were seen in many images, in Figure 32A there is a small amount of FITC highlighted but this was only seen clearly in two images and not in others. This was similar in the UKF-NB-3 Clones as shown in Figure 32B with almost all showing no clear Y chromosome but some unidentified green fluorescence.

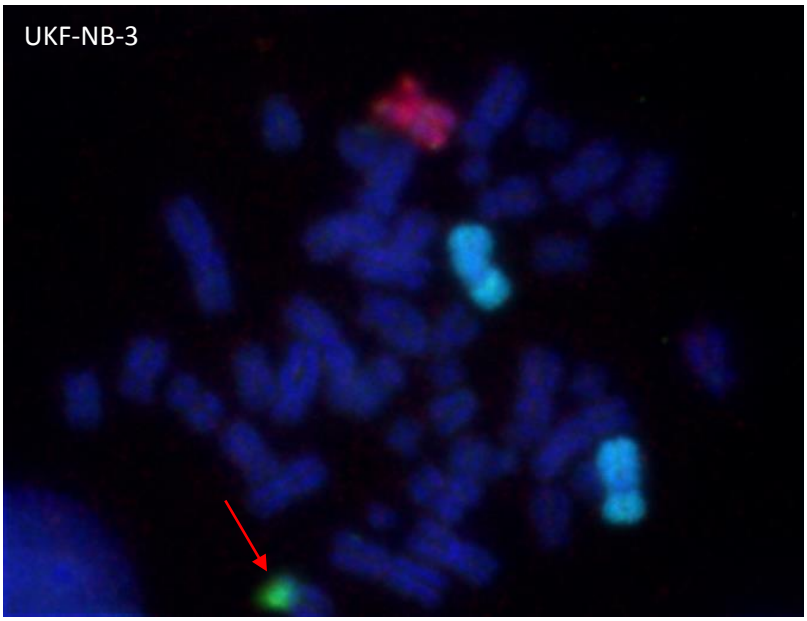


Figure 32A: Chromosome X (red), chromosome 6 (aqua) and chromosome Y (green) in UKF-NB-3. There are two copies of chromosome 5 seen in the majority of metaphases. The red arrow indicates the single translocation observed alongside two copies of chromosome 10 seen in 100% of the images captured. Diploidy of chromosome 7 is also observed.

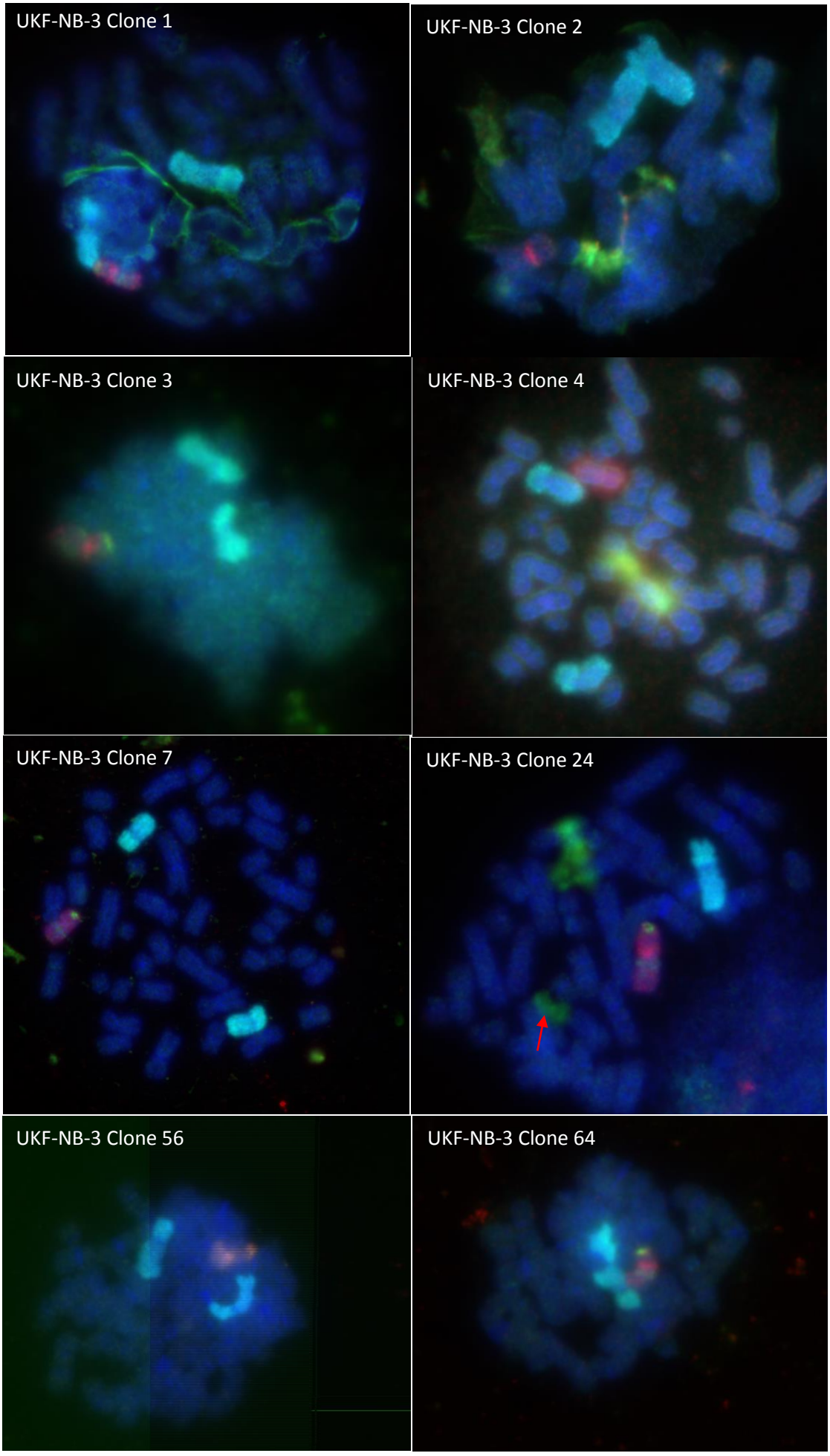
UKF-NB-3 Clone 1
UKF-NB-3 Clone 2
UKF-NB-3 Clone 3
UKF-NB-3 Clone 4
UKF-NB-3 Clone 7
UKF-NB-3 Clone 24
UKF-NB-3 Clone 56
UKF-NB-3 Clone 64

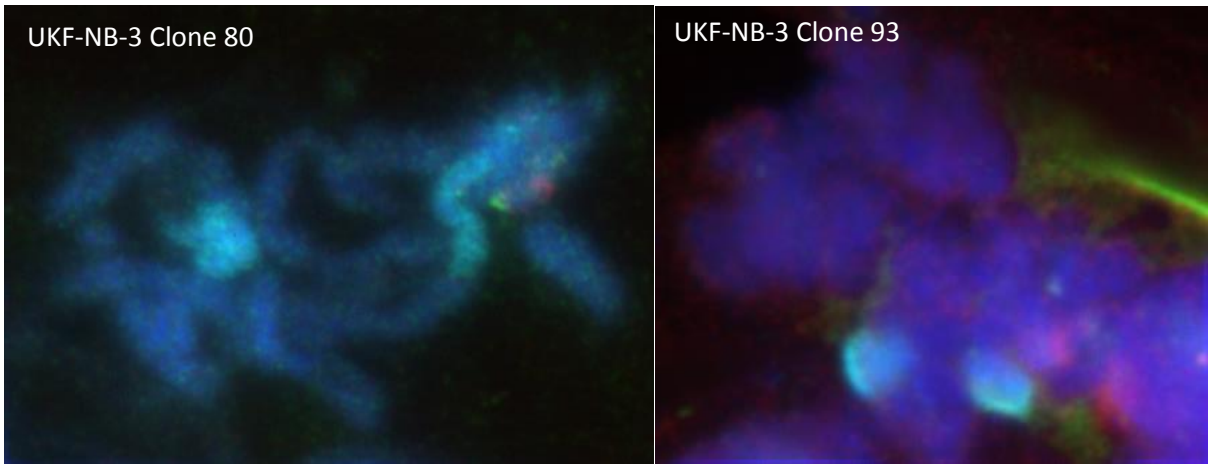


Figure 32B: All metaphases for all UKF-NB-3 Clones with the X chromosome (red) presented as one copy in the majority of metaphases captured. Chromosome 6 (aqua) was displayed as two copies in the metaphases captured with some such as UKF-NB-3 Clone 24 as highlighted. The Y chromosome (green) was not clearly defined in any of the metaphases.

### 5.3 Growth kinetics and doubling times of UKF-NB-3 Clones 1 – 93

To characterise the ten single cell derived UKF-NB-3 Clones further, we determined doubling times for each cell line. The doubling times ranged from 17.9 hours in UKF-NB-3 Clone 7 to 31.3 hours in UKF-NB-3 Clone 2. However, the differences did not reach statistical significance and results are shown in Figure 33.

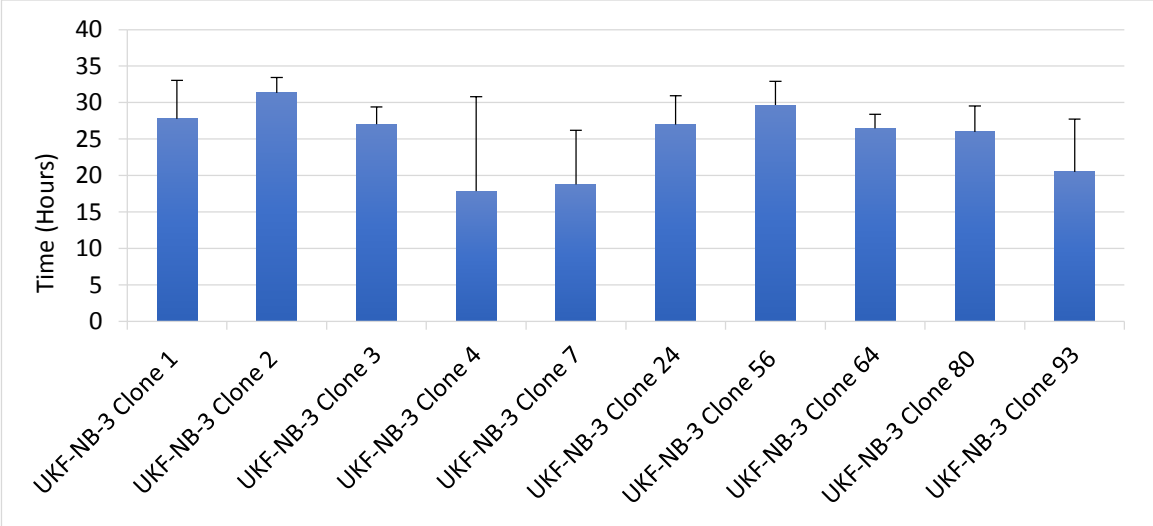


Figure 33: Doubling times of all UKF-NB-3 Clones 1-93 generated using the xCELLigence system and although there were differences between the cell lines none of them reached statistical significance n=3.

## 5.4 Drug sensitivity studies of UKF-NB-3 and 10 UKF-NB-3 single-cell derived clones against an 11-drug panel

We determined drug sensitivity profiles of UKF-NB-3 and the ten-single cell-derived UKF-NB-3 clones to a panel of drugs including: anaplastic lymphoma kinase (ALK) inhibitors (crizotinib and NVP-TAE684), tubulin-binding agents (docetaxel, epothilone-B, 2-methoxyestradiol, vincristine, vinblastine and combretastatin A4), the p38 inhibitor losmapimod and DNA damaging agents (doxorubicin and cisplatin). Notably, a previous lab member (Georgia Walden) had carried out the data analysis of UKF-NB-3 Clones 1 – 7 in the presence of all the drugs except for crizotinib, TAE-NVP-684, doxorubicin, losmapimod and cisplatin.

UKF-NB-3 and all clonal sub-lines displayed similar $IC_{50}$ and $IC_{90}$ values for the ALK inhibitors, crizotinib and NVP-TAE684 (Figure 36 and Figure 37). When tested for sensitivity against losmapimod (Figure 36) all the derived clones had a >2-fold increase when compared to the UKF-NB-3 parental except for UKF-NB-3 Clones 3 and 93. The majority of UKF-NB-3 clones had a higher sensitivity to doxorubicin (Figure 36) when compared to the parental but UKF-NB-3 Clones 56, 64 and 80 had a >2-fold increase in $IC_{50}$ value when compared to UKF-NB-3 Clones 1 and 3. All UKF-NB-3 Clones tested against cisplatin (Figure 35) had similar $IC_{50}$ values of around 0.5 μM with UKF-NB-3 Clone 3 and 80 with lower values. Vincristine, vinblastine and epothilone-B resulted in similar $IC_{50}$ values in all cell lines displaying a similar sensitivity to the parental line as shown in Figure 34. Docetaxel screening presented with a >2-fold increase seen only in UKF-NB-3 Clones 2 and 3 with all remaining clones displaying the same sensitivity as the parental Figure 35 2-methoxyestradiol $IC_{50}$ values in all UKF-NB-3 Clones were much higher than the parental with only UKF-NB-3 Clone 4 displaying a >2-fold increase (Figure 35). None of the UKF-NB-3 clones showed a >2-fold increase in combretastatin A4 when compared to the parental although clones 24-93 were higher in value than clones 1 – 7 as shown in Figure 37.

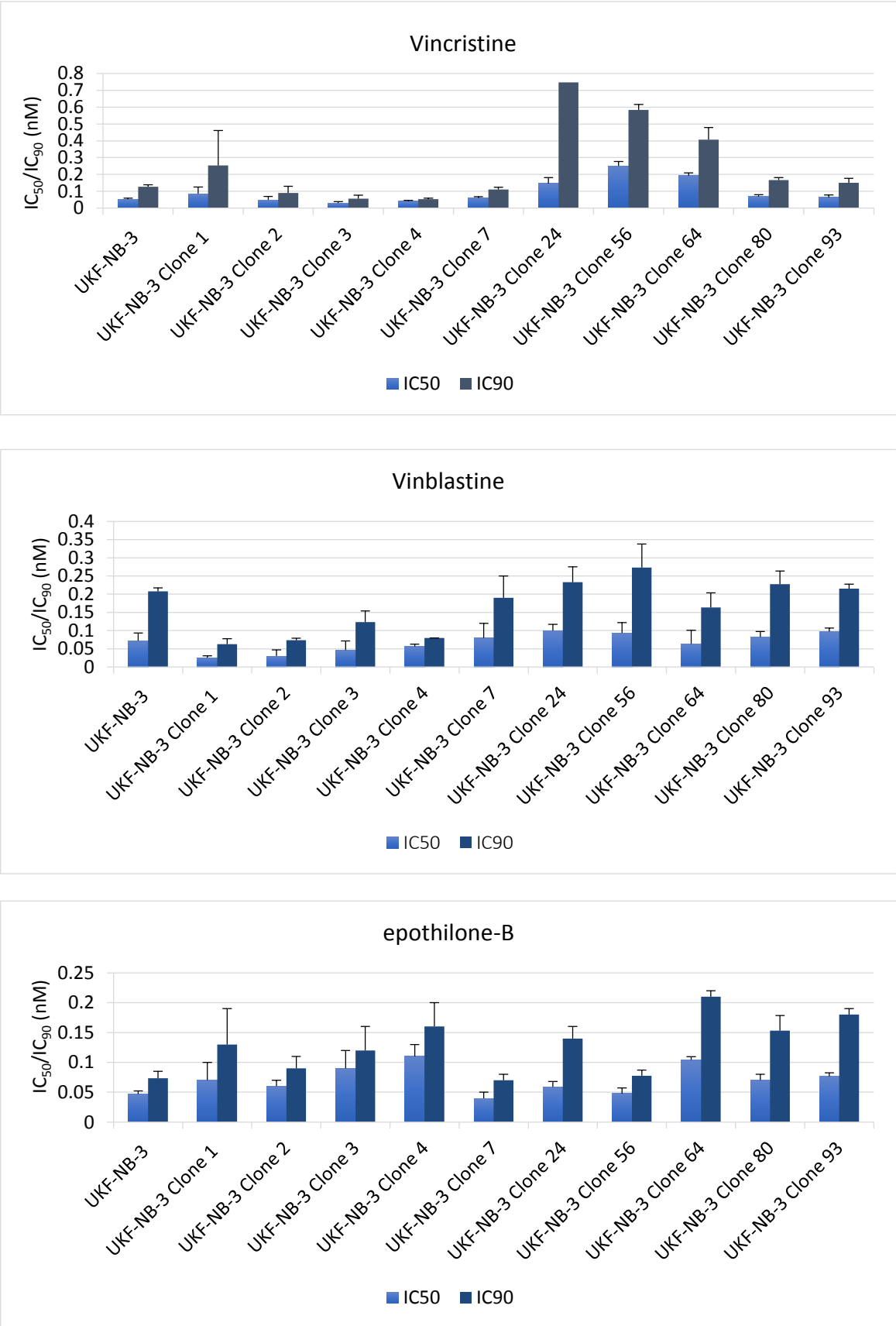


Figure 34: UKF-NB-3 and all 10 single cell derived UKF-NB-3 clones cross resistance profiles when tested against tubulin binding agents vincristine, vinblastine and epothilone-B. The majority of the UKF-NB-3 Clones displayed a similar sensitivity to UKF-NB-3 (n=3).

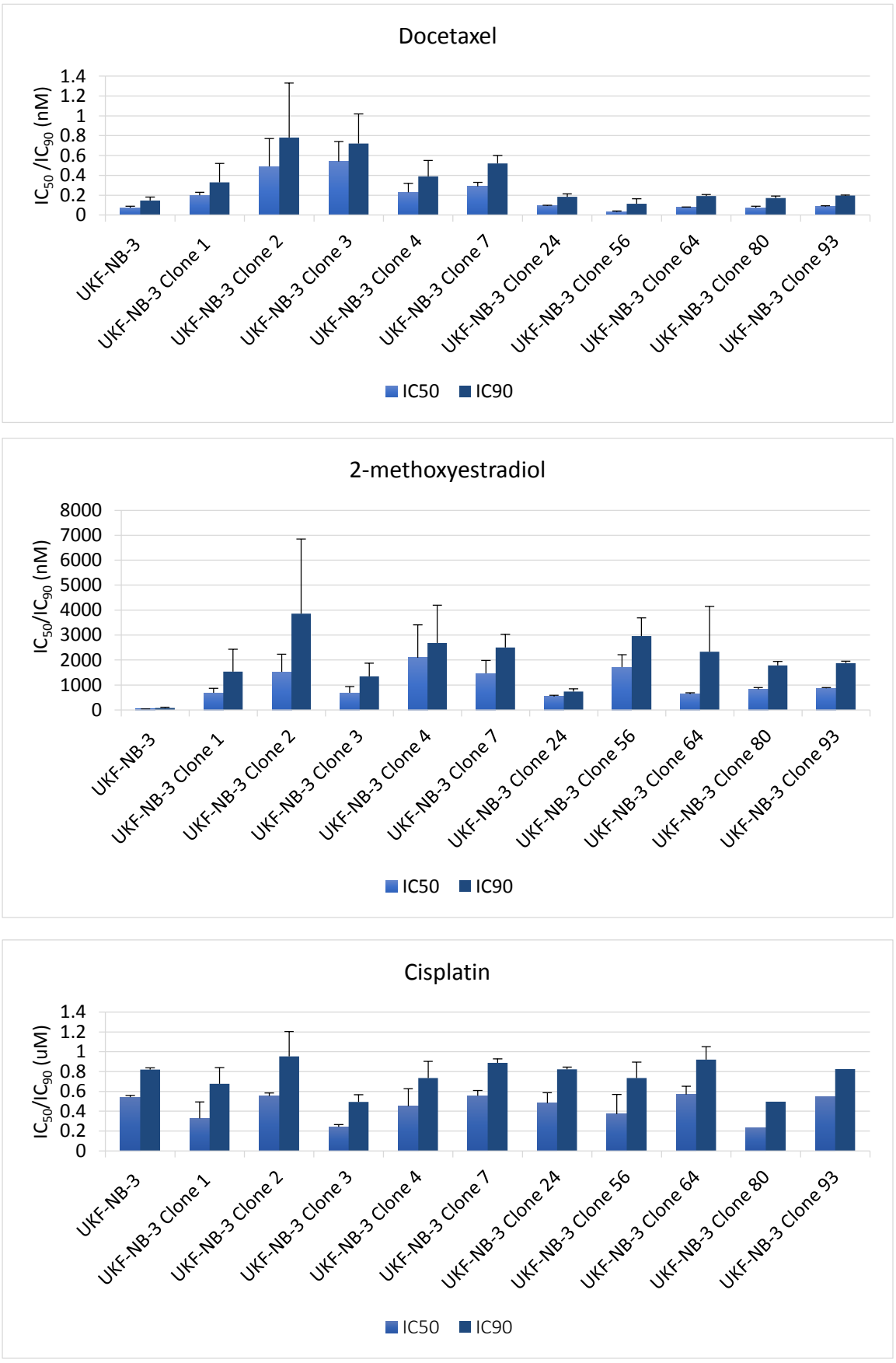


Figure 35: UKF-NB-3 and all 10 single-cell derived UKF-NB-3 clones cross resistance profiles tested against tubulin binding agents docetaxel which UKF-NB-3 Clone 2 and 3 displayed a > 2-fold increase and UKF-NB-3 Clone 4 indicating a > 2-fold increase against 2-methoxyestradiol. All clones had a similar $IC_{50}$ value for DNA damaging agent cisplatin (n=3)

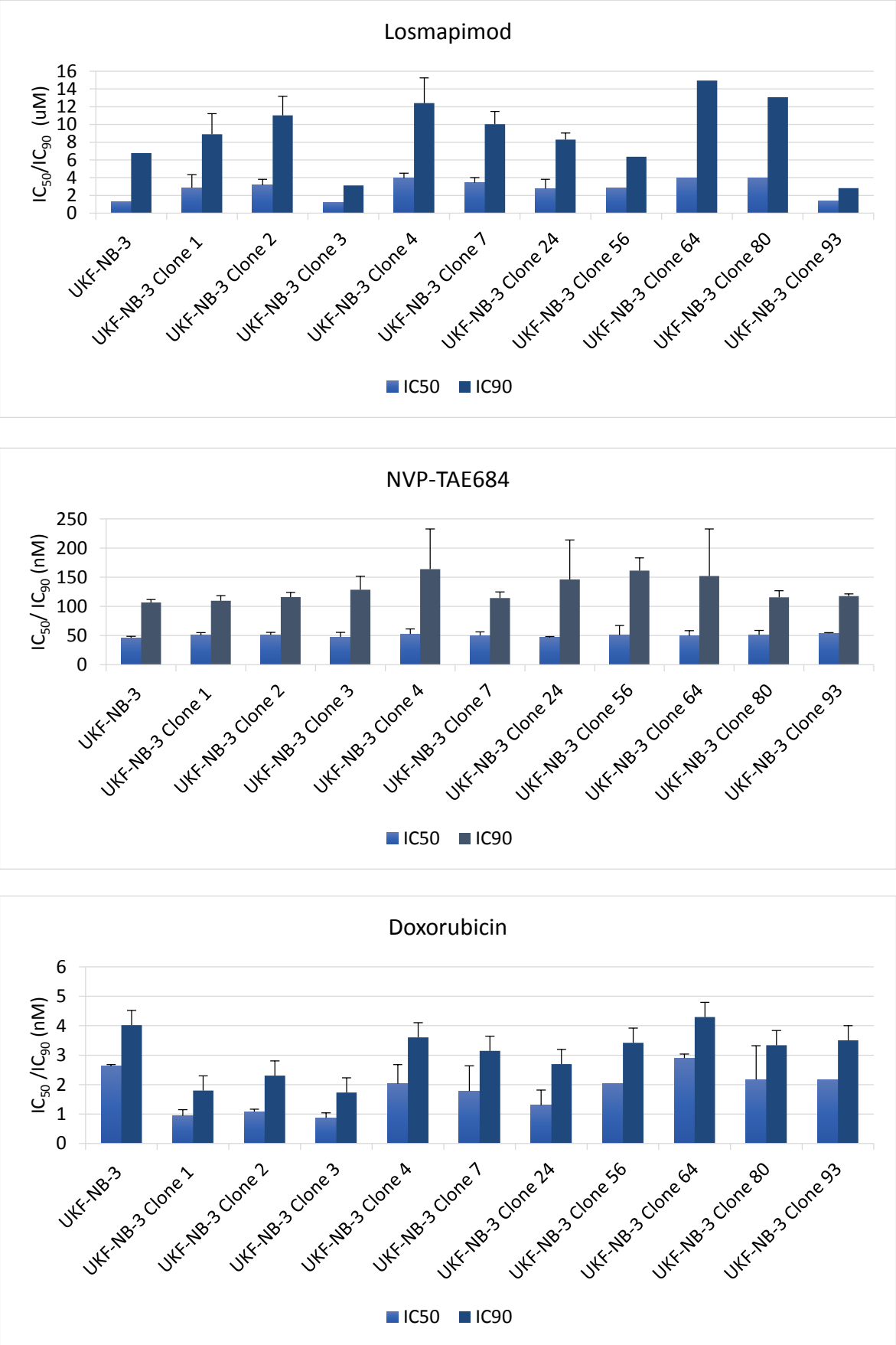


Figure 36: UKF-NB-3 and all 10 single-cell derived UKF-NB-3 clones cross resistance profiles tested against p38 inhibitor losmapimod where all UKF-NB-3 Clones had a >2-fold increase when compared to UKF-NB-3 except for UKF-NB-3 Clone 3 and 93. Resistance profiles against ALK inhibitor NVP-TAE684 were similar across all cell lines. UKF-NB-3 Clones were more sensitive to DNA damaging agent doxorubicin than UKF-NB-3 (n=3).

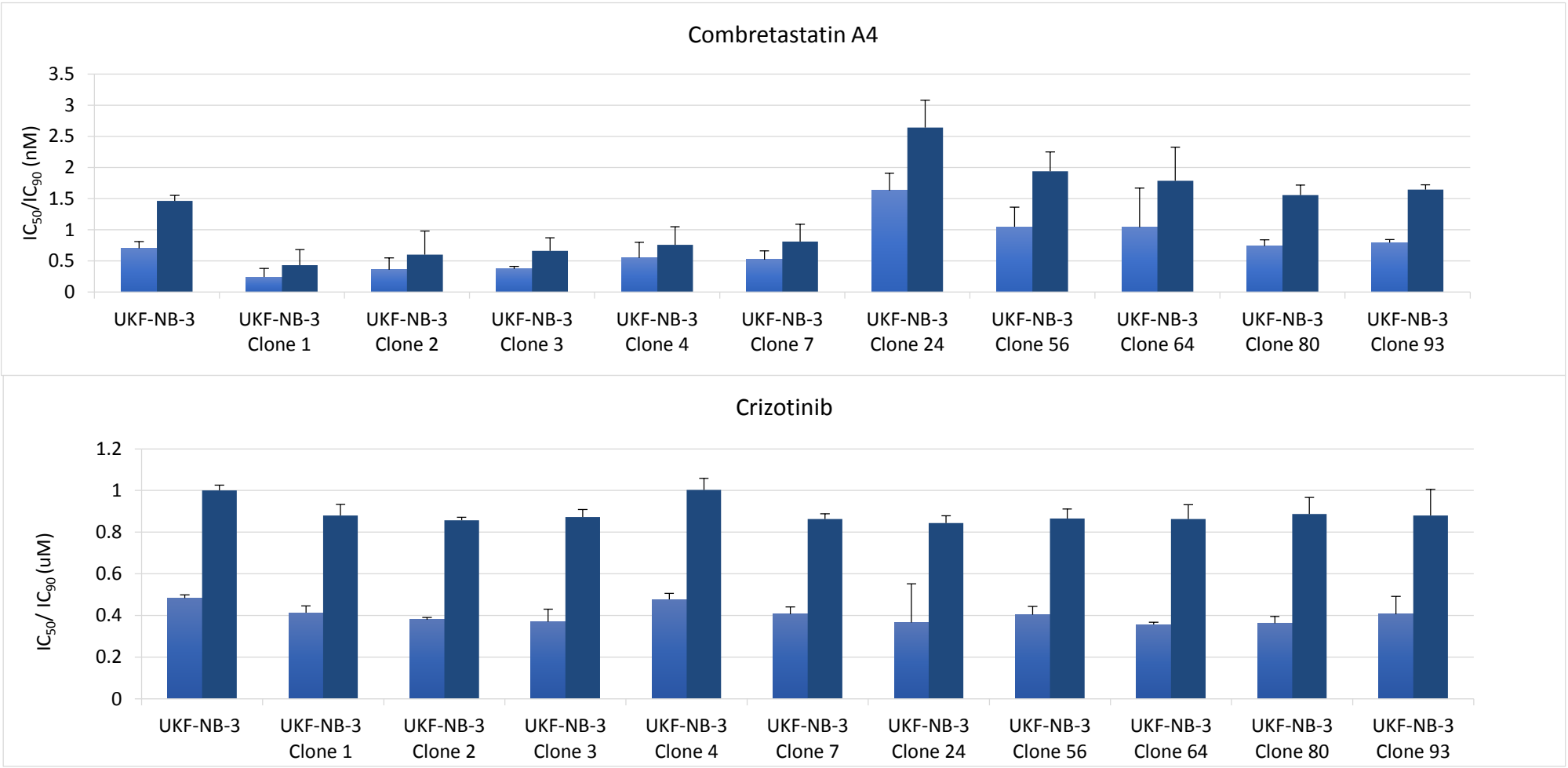


Figure 37: UKF-NB-3 and all 10 single-cell derived UKF-NB-3 Clones cross resistance profiles against tubulin binding agent combretastatin A4 where none of the cell lines had a >2-fold increase but UKF-NB-3 Clones 24-93 had higher values than UKF-NB-3 Clones 1-7. Against the ALK inhibitor crizotinib both the UKF-NB-3 and the UKF-NB-3 Clones displayed similar $IC_{50}$ value (n=3).

## 5.5 Discussion

It can be concluded that the use of FISH in the investigation of intra-cell line heterogeneity is an invaluable tool. It is clear to see changes between both the UKF-NB-3 parental line and the 10 UKF-NB-3 derived clones as well as variances between the clones. There are clear differences even between the metaphases taken of each clone and allow a huge range of analysis to be utilized.

UKF-NB-3 contained only two copies of chromosome 3 in every metaphase captured indicating no heterogeneity with this chromosome in the parental line. There was a difference in copy number of chromosome 3 within the UKF-NB-3 Clones with UKF-NB-3 Clone 56 containing the highest percentage (75%) of metaphases with an extra chromosome 3 with the other metaphases containing either one or no copies. Chromosome 15 had multiple translocations in both the UKF-NB-3 line and the clones, indicating that this mutation was passed on to all other cell lines except for UKF-NB-3 Clone 3 which contained a much lower percentage of metaphases with mutations. Chromosome 17 is well documented in neuroblastoma with the addition of the long arm of the chromosome indicative of poor outcome (Theissen, J., Oberthuer, A., Hombach, A., Volland, R., Hertwig, F., *et al* 2014). Chromosome 17 had a single mutation seen as a translocation in a 70% of the UKF-NB-3 cell line. Other metaphases indicated changes and almost all clones had exactly the same mutations except for UKF-NB-3 Clones 3 and 56, which indicated higher levels of intra-cell line heterogeneity with their metaphases displaying a variety of changes.

There were no changes in chromosome 8 between the UKF-NB-3 line and the UKF-NB-3 Clones with all metaphases displaying the same pattern, again indicating no intra-cell line heterogeneity. Chromosome 12 had an interesting change seen within the cell lines with the UKF-NB-3 line containing a majority of a single translocation but not in all metaphases captured. The amplification of aberrations in chromosome 12 is also well reported in Neuroblastoma, which correlates to tumour proliferation and development (Fransson, S.M., Kryh, H., Javanmardi, N., Ambros, I., Berbegall, A., *et al* 2015). In the UKF-NB-3 derived clones, UKF-NB-3 Clone 4 was the only cell line to contain the same mutation as the parental. The remaining nine clones actually displayed an extra chromosome instead of the translocation in the majority of metaphases captured. This is a direct difference from the UKF-NB-3 parental and indicates a further mutation, which has progressed from a single translocation but not in all clones.

UKF-NB-3 had various changes in the metaphases containing chromosome 21 but 70% displayed two copies with no aberrations indicating a small amount of heterogeneity in the cell line. The UKF-NB-3 Clones had a great deal of variability with all showing multiple translocations of the chromosome. UKF-NB-3 Clone 56 had the highest metaphases containing just one copy of the chromosome but alongside multiple translocations with copy number varying across many of the clones. This taken together indicates changes seen only within the clones and not identified in the parental. Chromosome 1 had two copies in all UKF-NB-3 metaphases indicating no heterogeneity in that cell line from the metaphases captured. Interestingly, all UKF-NB-3 Clones had a single

translocation of chromosome 1 in varying percentages, but this translocation was not observed in the parental line. The metaphases further differed with copy number of the chromosome with UKF-NB-3 Clone 56 with the highest level of intra-cell line heterogeneity with a range of changes in all metaphases captured. An interesting pattern of heterogeneity within UKF-NB-3 was seen with a larger majority of metaphases indicating an extra chromosome 16 with the remaining metaphases indicating just a single translocation. With the exception of UKF-NB-3 Clone 93 which retained the same mutation as the parental with three copies of the chromosome in the majority of the metaphases taken. Further changes were detected in UKF-NB-3 and the UKF-NB-3 derived clones with chromosome 19, with the parental line differing by presenting with multiple translocations but not in all metaphases taken indicating heterogeneity within the cell line. The clones contained no mutations of chromosome 19 as seen in the parental with the exception of UKF-NB-3 Clone 80. Chromosome 2 in all metaphases taken of UKF-NB-3 had a single translocation with only copy number differing, this was also observed to attach other translocations of each copy of chromosome 13. This same mutation was seen in all the UKF-NB-3 Clones with only the copy number differing with some metaphases within the clones containing multiple translocations of chromosome 2. The cell lines appeared to have very little intra-cell line heterogeneity with the mutational patterns of chromosome 2. This is perhaps to be expected due to *MYCN* and ALK genes, both prognosis markers in neuroblastoma are found on chromosome 2 (Morgenstern, D.A et al, 2014, Pandey, G.K and Kanduri, C, 2015).

Chromosome 13 presented with multiple translocations in UKF-NB-3 along with the small translocations of chromosome 2 seen on the copy of the chromosomes. This exact mutation was observed in the UKF-NB-3 Clones with very little variation between the cell lines and within the cell lines themselves. Chromosome 20 had more variation within the cell lines with UKF-NB-3 displaying one extra chromosome in almost all metaphases with only one presenting a difference. The UKF-NB-3 Clones appeared to carry the same mutations as the parental with UKF-NB-3 Clone 56 and UKF-NB-3 Clone 80 displaying an increase in chromosome copies. UKF-NB-3 Clone 93 had the highest amount of intra-cell line heterogeneity with the metaphases displaying different patterns of chromosome 20 and one with no copies and another with multiple translocations.

UKF-NB-3 Clones 7, 24 and 56 showed changes when compared with the parental with chromosome 9 and contained a single translocation but there was a great deal of heterogeneity within all cell lines with multiple differences. Chromosome 11 had a high number of multiple translocations in the UKF-NB-3 parental line with little change between intra-cell line metaphases, with almost all derived clones displaying two copies of the chromosome only. UKF-NB-3 Clone 56 had a high amount of intra-cell line heterogeneity with different metaphases presenting varying mutations, but a small percentage had the same mutations as the parental. Chromosome 22 presented with two copies and a single translocation in the UKF-NB-3 metaphases. The majority of UKF-NB-3 Clones also displayed the same mutation but some had multiple translocations. The UKF-

NB-3 Clones differed from the parental with chromosome 14 as only the UKF-NB-3 Clones displayed multiple translocations. Chromosome 18 had mutations seen in both the parental and the UKF-NB-3 Clones which was seen in all clones with only the copy number differing. A single translocation was noted in all cell lines and appeared in the high majority of parental metaphases and this mutation was in all single cell derived clones. All UKF-NB-3 Clones and UKF-NB-3 displayed a single translocation of chromosome 10 along with two copies seen in the majority of all metaphases. Chromosome 7 presented with two copies in the majority of metaphases of both UKF-NB-3 and UKF-NB-3 Clones. UKF-NB-3 Clone 56 had three copies in several metaphases as well as UKF-NB-3 Clone 80 and 93 which had differing mutations with a single translocation.

The use of FISH is clearly a useful tool in the visualization and investigation of intra-cell line heterogeneity with the technique presented all eleven full genomes of all UKF-NB-3 cell lines could be analysed. FISH is already used in the detection of known aberrations in chromosomes and subsequently used for diagnosis of diseases such as acute lymphoblastic leukemia (ALL) (Bishop, R., 2010). Further methods, which could be utilized alongside FISH, include chromosome-banding techniques, which could be used for both chromosome identification and abnormality detection (Bickmore, W.A., 2001). Further developments in the process would include identifying which chromosomes the translocations are locating to and analyse the mutations which are arising within the cell lines. With mutations that occur in UKF-NB-3 cell lines, specific FISH probes can be generated to give more precise information on the intra-cell line heterogeneity observed in the cell lines (Tucker, J.D., 2015). A great deal of research has been carried out on chromosomal aberrations in neuroblastoma and a recent publication from (Schramm, A., Koster, J., and Schulte, J.H 2015) observed in relapsed neuroblastomas when compared to primary tumours a much higher rate of *MYCN* using FISH probes which detected chromosome 2 and *MYCN*.

These uses of FISH as well as the investigation carried out to identify intra-cell line heterogeneity have huge promise in the understanding of clonal evolution and deeper understanding into the emergence of resistance mutations which may lead to relapsing and remission of tumours and ultimately treatment failure.

A drug-sensitivity screen of all 10 single–cell derived clones compared to the parental UKF-NB-3 line, highlighted that in the majority of the drugs tested, the cell lines responded fairly similarly. There were some variances within the cell lines possibly due to different mechanisms of action of the drugs investigated. When taken alongside the FISH analysis, results such as the ALK inhibitors (crizotinib and NVP-TAE684) response are very interesting. Almost all metaphases taken from each UKF-NB-3 Clone and the UKF-NB-3 parental all indicated translocation or aberration of chromosome 2 which is where the ALK gene is located (Hanna, M.G., Najfeld, V., Irie, H.Y., Tripodi, J and Nayak, A 2015). The tubulin-binding agents had a mixed response across all UKF-NB-3 clones but none showed a higher than 2-fold resistance and no UKF-NB-3 Clone had a consistently higher

$IC_{50}$ across all therapeutics. However, UKF-NB-3 Clone 24 had the highest $IC_{50}$ value when compared to parental and other clones at almost > 2-fold increase when tested against combretastatin A4.
But In therapeutics such as docetaxel UKF-NB-3 clone 2 and 3 displayed a much higher $IC_{50}$ value than the other UKF-NB-3 Clones and the parental cell line. This may indicate that the UKF-NB-3 Clones may possess more advantageous mutations to overcome the drug concentration such as a higher expression of ABCB1 transporters to effectively efflux the drug as seen in other cell lines (Hansen, S.N., Westergaard, D., Thomsen, M.B.H., Vistesen, M., Do, K.N *et al* 2015). Doxorubicin resulted in a varied response across the UKF-NB-3 clones with several displaying a lower sensitivity than the UKF-NB-3 parental and this indicated a good deal of intra-cell line heterogeneity across the cell lines as UKF-NB-3 Clones 4, 56, 64, 80 and 93 all had the same $IC_{50}$ value as the parental.
A more in-depth analysis of the UKF-NB-3 clones has been carried out by other lab members, including exome sequencing, which will further elucidate more differences within the clones. It is clear however, to see with both the drug sensitivity assays and FISH chromosomal analysis that there is a great deal of intra-cell line heterogeneity, as evidenced by the variability between the individual clones examined and more future work needed to uncover more information.

# Chapter 6

## Introduction of a novel SK-N-AS sub-line with acquired resistance to oxaliplatin

### 6.1 Introduction

Although there has been a great deal of progress in the diagnoses and treatment of cancer, patients with advanced metastatic disease continue to have five-year survival rates that remain low (Minguet, J., Smith., K.H and Bramlage, P., 2016). In order to increase these rates and improve patient prognosis, the development of more efficacious systemic treatments able to overcome drug resistance in tumours is imperative (Housman, G., Byler, S., Heerboth, S., Lapinska, K., Longacre, M *et al*., 2014). The development of drug resistance can intrinsic, where an untreated patient has no response to therapy from the beginning of treatment or acquired where a tumour will respond to therapy initially but eventually become resistant leading to relapse and treatment failure (Lippert, T.H., Ruoff, H.J and Volm, M., 2008). Acquired drug resistance is a major issue across a large majority of cancers and therefore it is important to understand the mechanisms underlying the development of resistance. Drug-adapted cancer cell lines are vital as model systems to understand the development of resistance and to mimic what is also seen in the clinic (Crystal, A.S., Shaw, A.T., Sequist, L.V., Friboulet, L., Niederst, M.J., *et al* 2014). For this project we used neuroblastoma as our model system as approximately half of patients diagnosed are high risk and overall survival rates are below 50% (Matthay, K.K., Reynolds, P.C., Seeger, R.C., Shimada, H., Adkins, E.S., *et al* 2009). Survival rates decrease even further to 10% in high-risk patients who develop acquired resistance following initial treatment (Basta, N.O., Halliday, G.C, Makin, G., Birch, J., Feltbower, R *et al*., 2016).

For this project we introduced and characterised a non-MYCN-amplified novel SK-N-AS sub-line with acquired resistance to oxaliplatin (SK-N-AS$^{r}$OXALI$^{4000}$). Oxaliplatin has indicated efficacy as a treatment for neuroblastoma with less toxicity than other platinum agents and is being trialled in several studies (Lam, C.G., Furman, W.L., Wang, C., Spunt, S.L., Wu, J.W *et al* 2015).

### 6.2 Results

#### 6.2.1 Cross resistance profiles of SK-N-AS, SK-N-AS$^{r}$OXALI$^{4000}$ and SK-N-AS$^{r}$OXALI$^{-4000}$

For the investigation of drug resistance profiles of the cell lines, I cultured, harvested and ran MTT assays alongside other project members as well as advising on starting concentrations of investigated drugs and $IC_{50}$ values. SK-N-AS, SK-N-AS$^{r}$OXALI$^{4000}$ and SK-N-AS$^{r}$OXALI$^{-4000}$ were tested against three platinum agents, oxaliplatin, cisplatin and carboplatin alongside two other DNA damaging agents. Doxorubicin, an anthracycline antibiotic which intercalates into DNA, disrupts the correct functioning of topoisomerase II and leads eventually to cell death (Thorn, C.F., Oshiro, C., Marsh, S., *et al* 2011). And gemcitabine (2',2'-difloruo 2'deoxycytidine, dFdC) a cytidine analogue, which following influx via nucleoside transporters converts to di and tri-phosphorylated (dFdCDP and dFdCTP) gemcitabine (Mini, E., Nobili, B., Caciagli, I., *et al* 2006). Once phosphorylated

gemcitabine cytotoxic effects include inhibition of DNA polymerase, inhibition of production of deoxyribonucleotides and the ability for dFdTCP to be hidden from DNA repair enzymes. (Mini, E., Nobili, B., Caciagli, I., et al 2006). As shown in Figure 38, SK-N-AS$^{r}$OXALI$^{4000}$ had an $IC_{50}$ value of 834-fold compared to SK-N-As when tested against oxaliplatin and an $IC_{90}$ value of 774-fold. SK-N-AS$^{r}$OXALI$^{-4000}$ cells grown in the absence of oxaliplatin had a lower $IC_{50}$ value than SK-N-AS$^{r}$OXALI$^{4000}$ but were still 487-fold higher than SK-N-AS. This indicates that resistance development does not depend on the continuous addition of oxaliplatin. When profiled against cisplatin and carboplatin, SK-N-AS had a lower $IC_{50}$ and $IC_{90}$ when compared to both SK-N-AS$^{r}$OXALI$^{4000}$ and SK-N-AS$^{r}$OXALI$^{-4000}$ but both drugs were lower in resistance when compared to oxaliplatin. When tested against doxorubicin, SK-N-AS$^{r}$OXALI$^{4000}$ and SK-N-AS$^{r}$OXALI$^{-4000}$ indicated a lower $IC_{50}$ and $IC_{90}$ value than SK-N-AS suggesting a higher sensitivity of both cell lines to doxorubicin. The same was true of gemcitabine with SK-N-AS presenting a higher $IC_{50}$ and $IC_{90}$ value when compared to SK-N-AS$^{r}$OXALI$^{4000}$ and SK-N-AS$^{r}$OXALI$^{-4000}$.

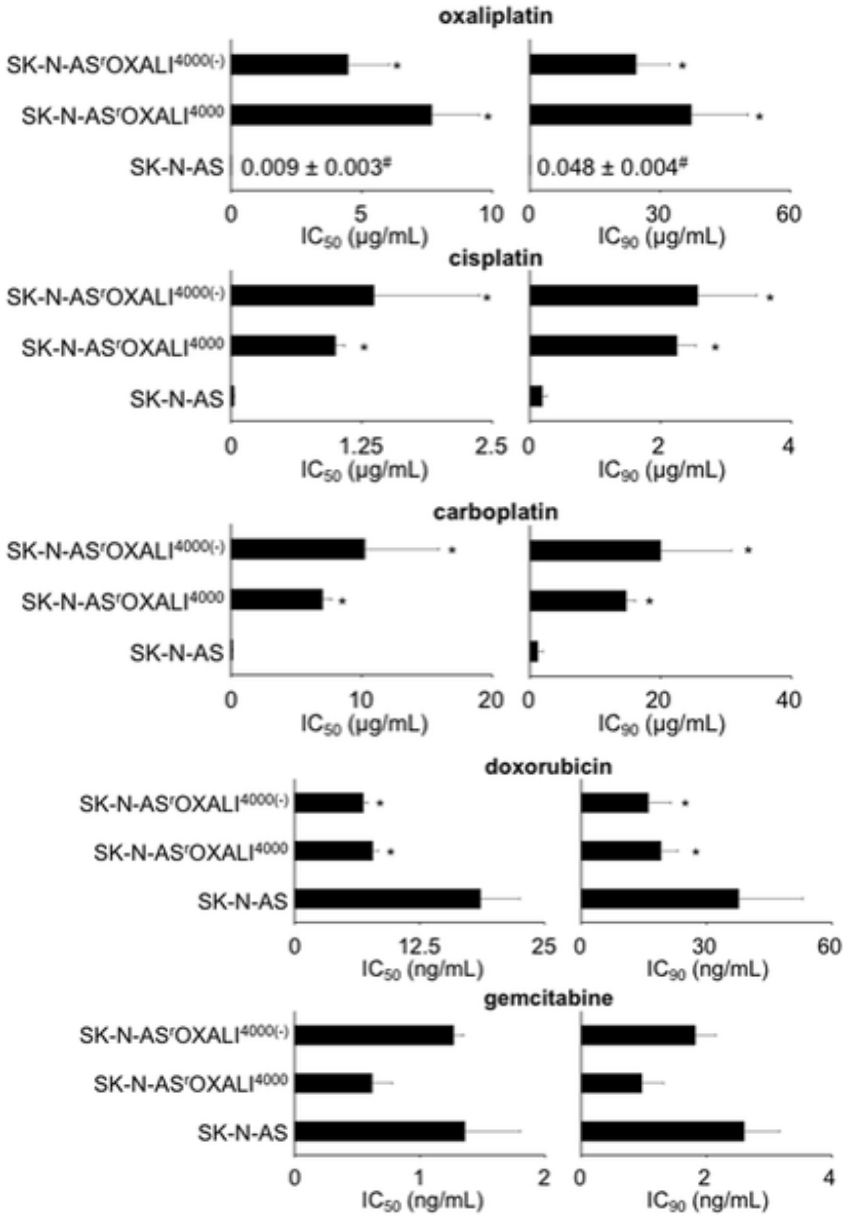


Figure 38: Viability of SK-NAS cell line, adapted to oxaliplatin (SK-N-AS$^{r}$OXALI$^{4000}$) and passaged in the absence of oxaliplatin for 10 weeks (SK-N-AS$^{r}$OXALI$^{-4000}$) when tested against DNA damaging agents using MTT assays.

For this characterisation I once again cultured, passaged and harvested the cell lines as well as advised on the protocol. As oncolytic viruses are in use as a potential treatment for neuroblastoma, cell lines were infected with Influenza A H1N1 strain A/WSN133 at different multiplicities of infection (MOIs).

As shown in Figure 39, following 48hr incubation using MTT assay with the infection there was no significant reduction in SK-N-AS cell viability up to three MOIs. SK-N-AS$^{r}$OXALI$^{4000}$ had reduced cell viability between MOIs of one to three and in SK-N-AS$^{r}$OXALI$^{-4000}$ at MOI of three. Additionally, when infected into *MYCN*-amplified UKF-NB-3, the cells were much more susceptible to infection with Influenza A than non-MYCN SK-N-AS cells.

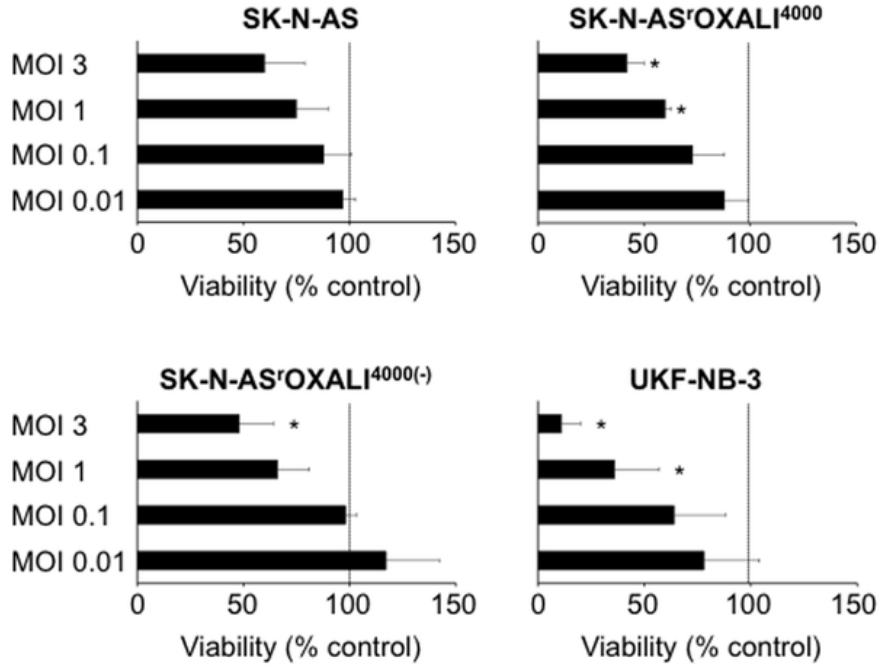


Figure 39: Effect of H1N1 influenza A virus infection on cell viability. Four cell lines were investigated to determine cell viability after 48hrs following infection with different multiplicities of infection and a non-treated control. Cell lines of interest included non-*MYCN*-amplified SK-N-AS, SK-N-AS$^{r}$OXALI$^{4000}$ and SK-N-AS$^{r}$OXALI$^{-4000}$ and *MYCN*-amplified UKF-NB-3. Viability of non-infected control cells is shown by the dotted line. *P < 0.05 relative to non-infected control cells.

### 6.2.2 Chromosomal analysis of cell lines

In order to analyse complete cell line genomes, cell lines were characterised using 24-chromosome fluorescence *in situ* hybridisation (FISH) as shown in Figure 40. Alongside harvesting, culturing and maintaining all cell lines I was actively involved in troubleshooting this analysis as well as perfecting the technique of capturing the highest concentration of metaphases in the samples needed for FISH. Figure 40 shows chromosomal aberrations in chromosomes 2, 12 and 8 in all three of the cell lines but notably less in the parental SK-N-AS compared to the oxaliplatin resistant sub-line SK-N-AS$^{r}$OXALI$^{4000}$ and the SK-N-AS$^{r}$OXALI$^{-4000}$ cell line (grown for a minimum of 10 passages without the addition of oxaliplatin). The percentage of two sets of chromosomes seen across the three cell lines

varied with SK-N-AS showing 50% diploidy and SK-N-AS$^{r}$OXALI$^{4000}$ and SK-N-AS$^{r}$OXALI$^{-4000}$ with lower values of 34% and 38% respectively.

Figure 40 shows chromosome number 2, 12 and 8 as an example of chromosomal comparison across all three of the investigated cell lines. As seen in SK-N-AS there is diploidy seen across all three sets of chromosomes with two signals clearly detected in texas red for the cell lines. When compared to SK-N-AS$^{r}$OXALI$^{4000}$ there are more than two chromosomes with partial labelling seen in chromosome 12. Interestingly, when oxaliplatin is removed from the cell line in SK-N-AS$^{r}$OXALI$^{-4000}$ the chromosomal pattern is very similar to SK-N-AS$^{r}$OXALI$^{4000}$.

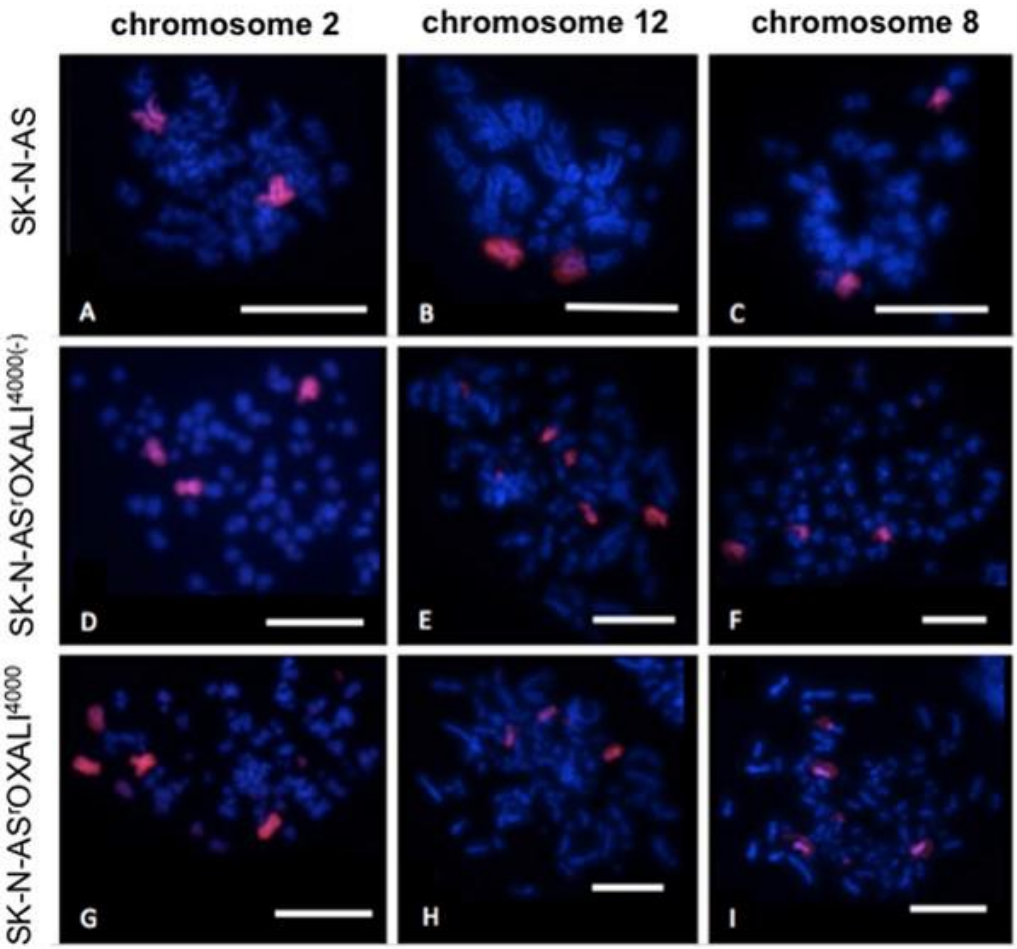


Figure 40: Chromosomes 2, 12 and 8 shown in SK-N-AS, SK-N-AS$^{r}$OXALI$^{4000}$ and SK-N-AS$^{r}$OXALI$^{-4000}$ (whereby oxaliplatin had been omitted for a minimum of 10 passages). The figure shows the presence of more chromosomal abnormalities including partial labelling and higher diploidy in SK-N-AS$^{r}$OXALI$^{4000}$ and SK-N-AS$^{r}$OXALI$^{-4000}$ than in SK-N-AS.

### 6.2.3 Receptor Tyrosine Kinase phosphorylation

For this project I was involved in the passaging, harvesting and preparation of cell lines throughout the investigation. Phosphorylation status of the cell lines was investigated, and 49 receptor tyrosine kinases were analysed using a commercial kit (Proteome Profiler Human Phos-Pho- RTK Array Kit, Abingdon, UK). Using ImageJ software, phosphorylation status was determined both visually and

densitometrically. In order to be counted as phosphorylated, receptor tyrosine kinases spots had to be visible and fold change spot density/ density control membrane to be greater than 2.5.

Eight of the 49 receptor tyrosine kinases: EGFR, INSR, IGF1R, PDGFRB, AXL, EPHA10, DDR2, and RYK were phosphorylated in one of the three cell lines as shown in Figure 41A. DDR2 and EPHA10 receptor tyrosine kinase phosphorylation was > 2-fold reduced in SK-N-AS$^{r}$OXALI$^{4000}$ vs SK-N-AS but not in SK-N-AS$^{r}$OXALI$^{-4000}$. SK-N-AS$^{r}$OXALI$^{-4000}$ compared to SK-N-AS showed increased phosphorylation of PDGFRB and IGF1R but no difference was seen in SK-N-AS$^{r}$OXALI$^{4000}$ vs SK-N-AS. In both oxaliplatin resistant cell lines SK-N-AS$^{r}$OXALI$^{4000}$ and SK-N-AS$^{r}$OXALI$^{-4000}$ phosphorylation of INSR had a > 2-fold increase. Figure 41B shows that all three cell lines had a similar phosphorylation levels of EGFR, AXL and RYK as there were no fold changes smaller than 2.

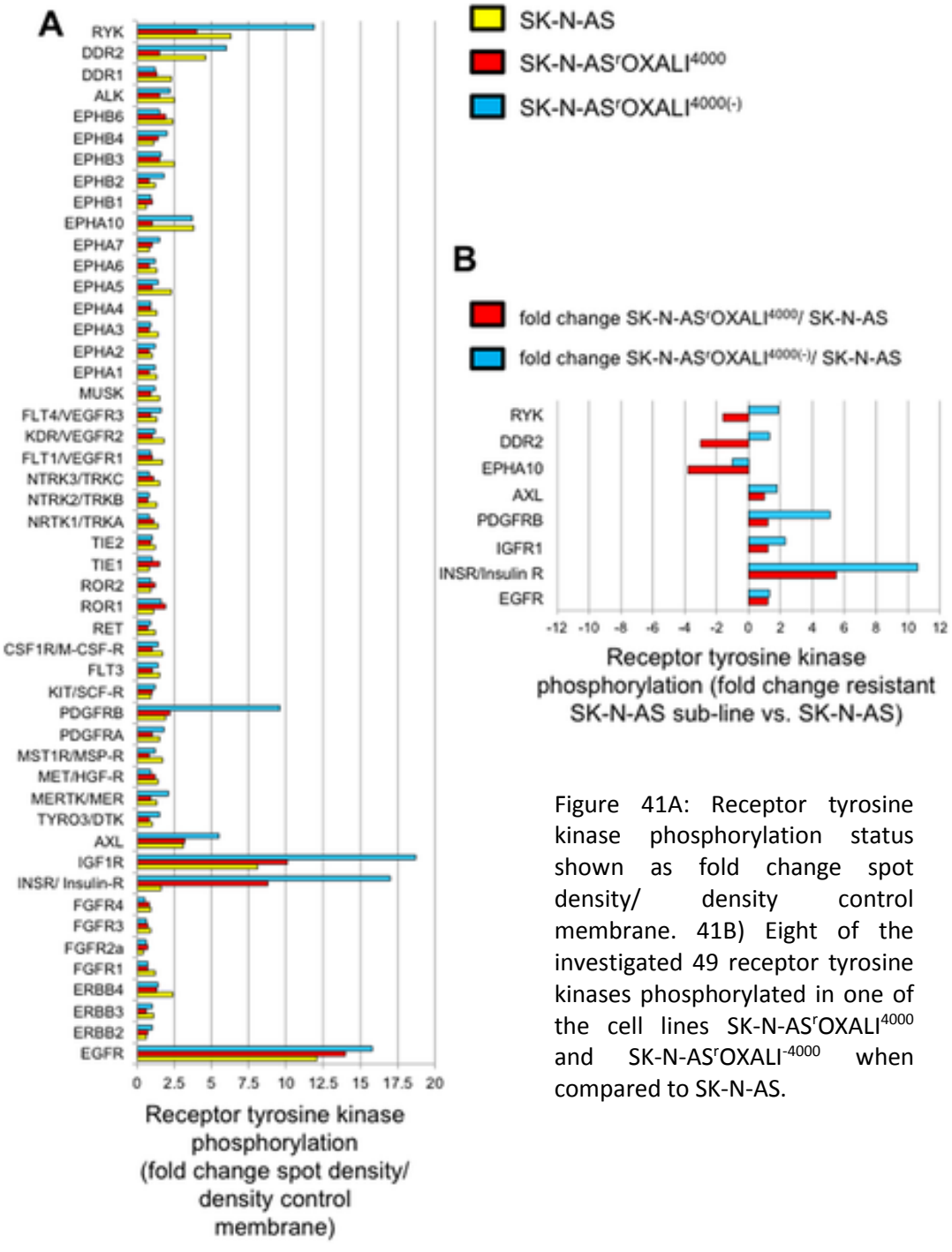


Figure 41A: Receptor tyrosine kinase phosphorylation status shown as fold change spot density/ density control membrane. 41B) Eight of the investigated 49 receptor tyrosine kinases phosphorylated in one of the cell lines SK-N-AS$^{r}$OXALI$^{4000}$ and SK-N-AS$^{r}$OXALI$^{-4000}$ when compared to SK-N-AS.

### 6.2.4 Oxygen consumption by SK-N-AS and SK-N-AS$^{r}$OXALI$^{4000}$ cells

For this section of the project I passaged and harvested the cell lines for the experiments. Following investigation using respirometry experiments both SK-N-AS and SK-N-AS$^{r}$OXALI$^{4000}$ show functional mitochondria and subsequently functional oxidative phosphorylation. Furthermore, it is indicated that the cell lines do not display a Warburg metabolism due to oligomycin reducing and FCCP enhancing oxygen consumption as shown in Figure 42. Using the evidence of the results taken together it appears that oxaliplatin resistance formation is not associated with cancer cell metabolism alterations in this cell line.

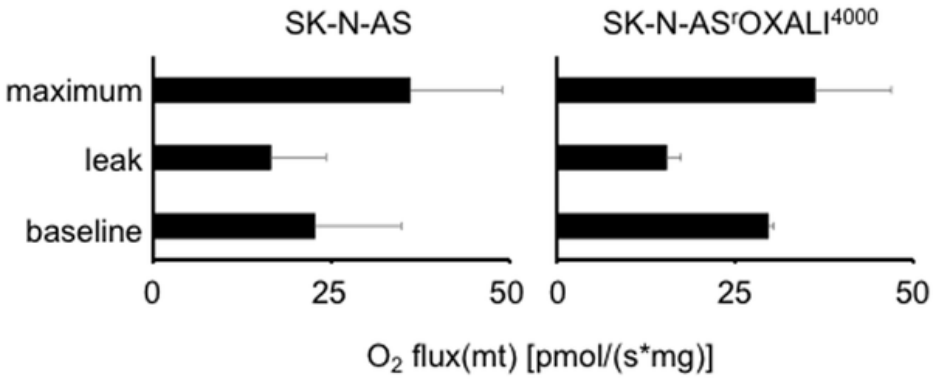


Figure 42: Oxygen consumption was investigated using intact cells in the absence of either oligomycin (8µg/mL) or FCCP (10 µM) for the baseline. And then shown in response to oligomycin, an inhibitor of ATP synthase causing a leak of protons resulting in inhibition of respiration (leak). Finally, investigated with intact cells in response to FCCP which detaches the electron transport chain and results in oxidative phosphorylation (maximum).

### 6.2.5 Cell sensitivity to ultraviolet C (UVC)-induced DNA damage

For this experiment I advised on the protocol for MTT assays, constructed the UV chamber alongside fellow students and harvested and cultured cell lines.

It is well documented that platinum drugs such as cisplatin, carboplatin and oxaliplatin cause induced DNA damage and therefore the nucleotide excision repair (NER) pathway may determine sensitivity to these agents. In order to assess this, we observed the NER response in SK-N-AS and SK-N-AS$^{r}$OXALI$^{4000}$ when treated with UVC radiation, which induces DNA damage repaired by the NER pathway.

Using 120hr MTT assays to test radiation doses, SK-N-AS$^{r}$OXALI$^{4000}$ displayed a higher sensitivity to UVC than SK-N-AS as shown in Figure 43. A further colony formation assay shown in Figure 43B highlights the increased number of colonies in SK-N-AS following radiation than in SK-N-AS$^{r}$OXALI$^{4000}$. Taken together, these results indicate that increased nucleotide excision repair is not indicative of oxaliplatin resistance in SK-N-AS$^{r}$OXALI$^{4000}$.

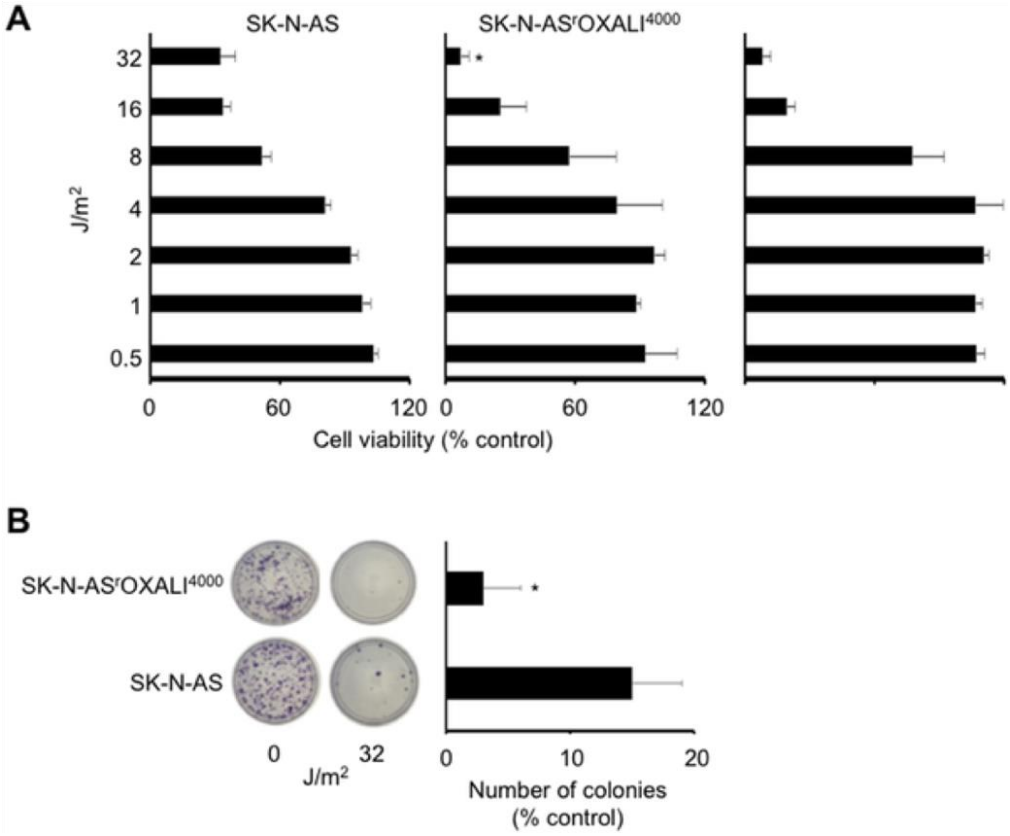


Figure 43: A) MTT assay results after 5 days following exposure depicting dose-dependent effects of UVC on SK-N-AS and SK-N-AS$^{r}$OXALI$^{4000}$. B) Quantification of SK-N-AS and SK-N-AS$^{r}$OXALI$^{4000}$ colony formation following 11 days exposure to UVC (32 J/m$^2$) when compared to non-irradiated control.

## 6.3 Discussion

For this project we characterised and introduced a sub line of the non-*MYCN*-amplified neuroblastoma cell line SK-N-AS, SK-N-AS$^{r}$OXALI$^{4000}$ with acquired resistance to oxaliplatin, a DNA damaging agent. These cells exhibited clear resistance to oxaliplatin when compared to the sensitive parental SK-N-AS cells. This was further compounded when the SK-N-AS$^{r}$OXALI$^{4000}$ were cultured for 10 passages without the addition of oxaliplatin and the cells still displayed enhanced resistance when compared to the parental line indicative of a stable resistance phenotype. Alongside cisplatin and carboplatin, oxaliplatin also belongs to the class of platinum-based chemotherapeutics. The mechanism of action of oxaliplatin is as a DNA-interacting agent forming adducts which in turn disrupts DNA replication and transcription (Martinez-Balibera, E., Martinez-Cardus, A., Gines, A, Ruiz de Porras, V., Moutinho, C *et al* 2015). Cisplatin and carboplatin have similar modes of action but due to higher cytotoxicity oxaliplatin is a more favourable treatment option (Woynarowski, J.M., Faivre, S., Herzig, M.C., Arnett, B., Chapman, W.G., *et al* 2000). In the cross-resistance profiles carried out initially in this project the SK-N-AS$^{r}$OXALI$^{4000}$ cells exhibited considerable cross-resistance to both cisplatin and carboplatin but oxaliplatin resistance was highest of the three tested. When the viability of SK-N-AS$^{r}$OXALI$^{4000}$ was tested against doxorubicin they did not show cross resistance nor to gemcitabine which was of interest as both of these drugs induce DNA damage by different mechanisms to the platinum agents. Doxorubicin is an

anthracycline which has several mechanisms in cancer cells including cross linking DNA, disruption of DNA replication and inhibition of topoisomerase II (Peng, X., Chen, B, Lim C.C and Sawyer, D.B 2005). Interestingly, the SK-N-AS$^{r}$OXALI$^{4000}$ cells were more sensitive to doxorubicin than the parental SK-N-AS and it is unclear as to why this is the case and there is very little documented on the sensitivity to doxorubicin in platinum drug-adapted cell lines. When tested against gemcitabine, a nucleoside analogue which inhibits DNA synthesis (Cavalcante, L.d.S and Monteiro, G 2014), cell lines SK-N-AS and SK-N-AS$^{r}$OXALI$^{4000}$ exhibited similar sensitivity.

Oncolytic viruses are used as anti-cancer therapies by regressing tumours through two main mechanisms of action: direct killing of tumour cells by replication dependent apoptosis and an anti-tumour response (Graaf, J.F. de., Vor, L.de., Fouchier, R.A.M and Hoogen, B.G. van den, 2018). One example of a promising treatment is the modified herpes simplex virus-1, talimogene laherparepvec (T-VEC) successfully used to treat patients with melanoma (Andtbacka, R.H.I., Kaufman, H.L., Collichio, F., Amatruda, T., Senzer, N., *et al* 2015). For this project approach we used Influenza A H1N1 strain A/WSN133 and interestingly SK-N-AS$^{r}$OXALI$^{4000}$ cells exhibited higher sensitivity to the viral infection when compared to SK-N-AS parental cells. The mechanism behind this sensitivity is unknown and further work would need to be carried out to determine the cause. However, as (Dayaram, T and Marriot, S.J 2008) discuss a common target of transforming viruses are cyclin-dependent kinase (CDK) inhibitor genes which can drive cell cycle progression and subsequently viral replication. As CKIs are often mutated in cancer this could explain the sensitivity in cancer cell lines to certain viruses, but this remains unclear and was not investigated in SK-N-AS$^{r}$OXALI$^{4000}$ to identify if this was the mechanism.

Following full chromosomal characterisation of the cell lines SK-N-AS$^{r}$OXALI$^{4000}$ cells when compared to SK-N-AS cells displayed more chromosomal abnormalities shown as rearrangements and aneuploidy. This is somewhat to be expected as the chromosomal irregularities correspond with as oxaliplatin being DNA damaging agent.

49 receptor tyrosine kinases were investigated as part of the project eight of which were phosphorylated in a minimum of one cell line. However, the RTKs: DDR2, EPHA10, PDGFRB, IGF1R and INSR were found to be of interest due to the difference in phosphorylation between the parental SK-N-AS and resistant SK-N-AS$^{r}$OXALI$^{4000}$ cells. The results highlighted that phosphorylation of DDR2 and EPHA10 were lower in SK-N-AS$^{r}$OXALI$^{4000}$ cells when compared with SK-N-AS and higher in SK-N-AS$^{r}$OXALI$^{-4000}$. These results could indicate that the difference is present because of the addition of oxaliplatin continuously during passaging rather than a mechanism which remains with the removal of oxaliplatin. DDR2 is a tyrosine kinase receptor which binds collagen and has been reported to promote several cellular processes including cell migration, proliferation and survival, all of which can be exploited in cancerous cells (Hammerman, P.S., Sos, M.L., Ramos, A.H., Xu, C *et al* 2011). However, its role in a response to platinum drugs is unknown. Our findings demonstrated that phosphorylation of DDR2 was lower in SK-N-AS$^{r}$OXALI$^{4000}$ cells when compared with SK-N-AS

and higher in SK-N-AS$^{r}$OXALI$^{-4000}$. EPHA10 is a member of the Eph RTK family and is involved in transduction via two-way signalling (Li, Y., Ye, F., Ma, Q., Yang, Z., Liu, D *et al* 2017). EPHA10 is highly expressed in breast cancer tissue and is used as a tumour marker but further understanding of its role is needed (Zang, X., Ding, H., Zhao, X., Li, X., Du, Z., *et al* 2016).

SK-N-AS$^{r}$OXALI$^{-4000}$ cells showed an increased phosphorylation of IGF1R and PDGFRB when compared to SK-N-AS, but this was not seen when comparing SK-N-AS$^{r}$OXALI$^{4000}$ to the parental.

IGF1R is a signalling molecule which is overexpressed in cancer cells leading to effects such as apoptosis inhibition and cell motility (Bahr, C and Groner, B., 2004). Studies with IGF1R have shown that it may also have a role in drug efflux pumps such as multidrug-resistance-associated protein 2 (MRP-2) (Denduluri, S.K., Idowu, O., Wang, Z., Liao, Z., Yan, Z., *et al* 2015). PDGFRB is another established anti-cancer drug target and interestingly cisplatin was shown to deplete its expression in neuroblastoma cell lines (Wetterskog, D., Moshiri, A., Ozaki, T., Uramoto, H., Nakagawara, A *et al* 2009). Therefore, it may be that the addition of oxaliplatin in SK-N-AS$^{r}$OXALI$^{4000}$ cells caused the difference in phosphorylation seen in SK-N-AS$^{r}$OXALI$^{-4000}$ cells when compared to the parental.

Finally, both SK-N-AS$^{r}$OXALI$^{4000}$ and SK-N-AS$^{r}$OXALI$^{-4000}$ cells had increased phosphorylation of INSR when compared to SK-N-AS, this may be due to a direct result of oxaliplatin resistance. As INSR has so far resulted in limited clinical success due to targeting IGF1R it is unclear as to the role of the RTK in acquired resistance (Singh, P., Alex, J.M and Bast F., 2013).

Experiments to test oxygen consumption by SK-N-AS and SK-N-AS$^{r}$OXALI$^{4000}$ cells using respirometry tests showed that there was no difference in oxidative phosphorylation. This indicated that the SK-N-AS$^{r}$OXALI$^{4000}$ cells were not showing a Warburg phenotype. This is of interest as platinum-drug resistance has previously indicated that a Warburg metabolism may prevent damage caused by the therapeutic (Zhao, Y, Butler, E.B and Tan, M., 2013).

When inducing DNA damage through irradiation with UVC, surprisingly the SK-N-AS$^{r}$OXALI$^{4000}$ cells displayed a higher sensitivity than the SK-N-AS parental line. It was assumed initially that SK-N-AS$^{r}$OXALI$^{4000}$ cells would show a lower sensitivity to the DNA damage caused by UVC, particularly as damage caused by both oxaliplatin and UVC is repaired by nucleotide excision repair (Sancar, A., Lindsey-Boltz, L.A, Unsal-Kacmaz, K and Linn, S., 2004). However, there are a multitude of mechanisms which contribute to platinum drug resistance and with further examination it may be possible to uncover more findings regarding the sensitivity to UVC.

In conclusion, it appears that oxaliplatin resistant mechanisms are not directly associated with an increase in DNA repair capacity and further experimentation and investigation is needed to understand the complex underlying resistance mechanisms. As the focus for platinum drug investigation has primarily focused on cisplatin and carboplatin resistance which have similar if not the same mode of action it is imperative to also focus on models of oxaliplatin resistance.

# Chapter 7

## Conclusions and future work

This project has provided insight into the use of drug-adapted cancer cell lines in research and where they can be utilised. The main cause of treatment failure is the emergence of drug resistance in cancer cells whereby the tumour cells are no longer sensitive to the therapeutics given. This is a major issue in cancers such as pancreatic, breast and high-risk neuroblastoma, which was the model used in this study. It is very difficult to analyse a tumour throughout treatment and to track changes as it is not always feasible or ethical to take continued biopsies. Therefore, the use of cancer cell lines is crucial in detecting changes in response to chemotherapeutics and the development of multidrug resistance.

The first issue addressed in this work was the authentication of cell lines, the misidentification of which is a problem across all research. We propose the use of MALDI-TOF, which has shown huge impact clinically in the identification of bacteria through the generation of a known sample database (Angeletti, S 2017), as a method to identify cell lines of the same genetic origin. This method has shown great promise for differentiating between parental and resistant sub-lines and different drug-adapted cell lines. Further work in this project is to generate a mass spec fingerprint for each of the cell lines and then to generate a database, this would allow for routine testing to confirm authentication and as a means of detecting further differences between cell lines if applicable. Coupled with further whole genome and exome sequencing of each of the cell lines a full characterisation could be achieved to look at deeper differences between the samples (Diede, S.J., 2014).

This project established a standardised drug adaptation protocol allowing for an in-depth analysis of drug adaptation of cell lines when comparing drugs with the same target. Our extensive findings indicate, as expected, that it is much harder to induce resistance to cabazitaxel and epothilone-B than to docetaxel and paclitaxel. A study of the differences in adapting sub-lines has not been done to this extent and the project is still ongoing. The main conclusion is that this systematic approach allowed us to observe that UKF-NB-3 cells become resistant to docetaxel and paclitaxel much more easily than to the other therapeutics. Further work in this area will be to investigate the remaining two docetaxel sub-lines UKF-NB-3 Doce 1 and 4 through exome sequencing, further drug sensitivity assays and an in-depth analysis of the ABCB1 transporter. This could include testing against cabazitaxel, which interestingly may have an anti-cancer effect in ABCB1 upregulated cells (Duran, G.E., Derdau, V., Weitz, D., Philippe, N., Blankenstein, J et al 2018). Another area which might have been interesting to investigate is the role of miRNAs in resistance with interesting findings reported with miR-27b promoting docetaxel resistance in NSCLC (Armstrong, C.M., Liu, C., Lou, W., Lombard, A.P., Evans, C.P *et al* 2017). Given more time it would have been interesting to have exposed the resistant sub-lines to higher doses of docetaxel and to remove weeks without drug added

altogether to see if the resistant phenotype remained. These findings taken together demonstrate that cancer cells can develop resistance much easier to certain drugs, with others they are unable to overcome the drug's effects. This information could be used for understanding underlying mechanisms of resistance with repeated MTT analysis to generate $IC_{50}$ values to monitor resistance formation. Another method for monitoring resistance and studying heterogeneity is through circulating tumour DNA (ctDNA) which allows the tracking of alterations of a tumour throughout treatment. Jacob, C.J., Simmons, A.D., Lovejoy, A.F., Esfahani, M.S., Newman, A.M 2016 discuss detecting resistance markers such as the EGFR C797S mutation in NSCLC using ctDNA.

Through the use of intensive FISH chromosomal analysis, we have demonstrated it is an effective tool for investigating intra-cell line heterogeneity. The chromosomal aberrations detected changes between the UKF-NB-3 clones and the parental cell line they are derived from as well as variances between the clones. A direct difference between the UKF-NB-3 parental and the majority of the clones was observed with chromosome 12 which had an extra copy in all the UKF-NB-3 clones but a single translocation in the parental. Amplification of chromosome 12 is well documented in neuroblastoma as well as potential targets from regions 12q13-14 and 12q15 (Fransson, S.M., Kryh, H., Javanmardi, N., Ambros, I., Berbegall, A *et al* 2015). Our finding present that the chromosomal changes are seen in the majority of single cell derived clones from UKF-NB-3 indicative of the intra-cell line heterogeneity within neuroblastoma. One other interesting finding was chromosome 2 translocations attaching to chromosome 13 in all the UKF-NB-3 clones and this is something we would have investigated further, as there appears to be no further research into such a finding. *MYCN* location at chromosome 2 is very well documented and is a criteria in the diagnosis of neuroblastoma (Williams, R.D., Chagtai, T., Alcaide-German, M., Apps, J., Wegert, J *et al* 2015) this additional finding could indicate an unknown factor associated with the addition of chromosome 13. In addition to whole genome analysis we also performed drug sensitivity assays which detected more differences as well as similarities. This may be due to differing mechanisms of action of drugs investigated but ALK inhibitors crizotinib and NVP-TAE-684 were of particular interest due to aberrations seen in chromosome 2 where ALK is located in all the UKF-NB-3 clones. Further work in this area would be to investigate ABCB1 in the UKF-NB-3 Clones to identify if some are expressing higher levels than others to explain some of the results seen in the drug sensitivity screen. Additionally, conducting FISH on a selection of resistant sub-lines to compare to the parental once again may indicate further chromosomal changes which could be developed as potential candidates for drug targeting. With more time a FISH probe could be generated to look for specific chromosomal aberrations which appear frequently in cell lines and tested against drug sensitivity assays to determine if there is a link between alteration and acquired drug resistance. DNA FISH probes have been used extensively in breast cancer (Magnani, L., Frige, G., Gadaleta, R.M., Corleone, G., Fabris, S *et al* 2017) and leukemia (Hu, L., Ru, K., Zhang, L., Huang, Y., Zhu, X *et al* 2014) among many others. Finally, full karyotyping to establish where the chromosomal aberrations are

moving was a next step in the project, to determine which chromosomes the translocations were occurring at and to look for patterns within the cell lines and in resistant sub-lines.

This project established a novel neuroblastoma sub line SK-N-AS$^{r}$OXALI$^{4000}$ with acquired resistance to oxaliplatin. Oxaliplatin has a much lower cytotoxicity than cisplatin and carboplatin but a favourable treatment outcome making it a valid anti-cancer agent to investigate further. SK-N-AS$^{r}$OXALI$^{4000}$ did not exhibit cross resistance to DNA damaging agent's gemcitabine or doxorubicin indicating that the resistance mechanisms differ between different chemotherapeutics targeting the DNA. Further work could be carried out here as there is little documentation on the effect of doxorubicin and gemcitabine of platinum resistant sub-lines. Interestingly, recent studies have used bevacizumab alongside doxorubicin and other chemotherapy agents to treat platinum resistance in ovarian cancer and this has significantly improved progression free survival (Poveda, A.M., Selle, F., Hilpert, F., Reuss, A., Savarese, *et al* 2015). Further characterisation of SK-N-AS$^{r}$OXALI$^{4000}$ including treatment relative to the phosphorylation data would be another step to elucidate resistance mechanisms further with potential drug targets. Examples include EPHA10 and IGF1R which need further examination and cross resistance assays using relevant chemotherapeutics to uncover more information. Finally, the discovery that SK-N-AS$^{r}$OXALI$^{4000}$ cells had a higher sensitivity to UVC radiation may also impact treatment options to oxaliplatin resistance. Further examination of this finding is crucial to understanding the mechanisms underlying the changes seen when compared to the sensitive SK-N-AS parental and more experiments to investigate DNA damage.

Overall, the work carried out in this thesis is to validate the use of drug-adapted cell lines in cancer research and how the findings can uncover resistance mechanisms without the repeated biopsies of patients as well as identifying favourable treatment options and sensitivity to certain therapeutics. Translating findings in cell lines into a clinical setting is another step which was limited in this project, but the evidence found can influence treatment options by predicting and hopefully preventing multidrug resistance and treatment failure in patients.

## Bibliography


Abdi, H, Williams, L.J and Valentin, D 2013 Multiple factor analysis: principal component analysis for multitable and multiblock data sets *WIREs computational statistics* **5** 149-179

Allison, K.H. and Sledge, G.W. 2014 Heterogeneity and cancer *Oncology* **28** 772-8

Andtbacka, R.H.I., Kaufman, H.L., Collichio, F., Amatruda, T., Senzer, N., *et al* 2015 Talimogene Laherparepvec Improves Durable Response Rate in Patients with Advanced Melanoma *Journal of Clinical Oncology* **33** 1-9

Angeletti, S 2017 Matrix assisted laser desorption time of flight mass spectrometry (MALDI-TOF MS) in clinical microbiology *Journal of Microbiological Methods* **138** 20-29

Armstrong, C.M., Liu, C., Lou, W., Lombard, A.P., Evans, C.P *et al* 2017 MicroRNA-181a promotes docetaxel resistance in prostate cancer cells *Prostate* **77** 1020-1028

Attiyeh, E.F., London, W.B., Mosse, Y.P., Wang, Q., Winter, C., *et al* 2005 Chromosome 1p and 11q deletions and outcome in Neuroblastoma *New England Journal of Medicine* **353** 2243-2253

Azarova, A.M., Gautam, G and George, R.E 2011 Emerging importance of ALK in Neuroblastoma *Seminars in Cancer Biology* **21** 267-275

Bahr, C and Groner, B., 2004 The insulin like growth factor-1 receptor (IGF-1R) as a drug target: novel approaches to cancer therapy *Growth Hormone & IGF Research* **14** 287-295

Barone, G., Anderson, J., Pearson, A.D.J., Petrie, K and Chesler, L 2013 New strategies in Neuroblastoma: Therapeutic targeting of MYCN and ALK *Clinical Cancer Research* **19** 5814-21

Basta, N.O., Halliday, G.C, Makin, G., Birch, J., Feltbower, R et al., 2016 Factors associated with recurrence and survival length following relapse in patients with Neuroblastoma *British Journal of Cancer* **115** 1048-1057

Beaton, L.A., Marro, L., Samiee, S., Malone, S., Grimes, S *et al* 2015 Investigating chromosome damage using fluorescent in situ hybridization to identify biomarkers of radiosensitivity in prostate cancer patients *International Journal of Radiation Biology* **89** 1087-1093

Beretta, G.L., Benedetti, V., Cossa, G., Assaraf, Y.G., Bram, E *et al* 2010 Increased levels and defective glycosylation of MRPs in ovarian carcinoma cells resistant to oxaliplatin *Biochemical Pharmacology* **79** 1108-1117

Bickmore, W.A., 2001 Karyotype Analysis and Chromosome Banding *Encyclopedia of Life Sciences* 1-7

Bishop, R., 2010 Applications of fluorescence *in situ* hybridization (FISH) in detecting genetic *aberrations of medical significance Bioscience Horizons: The International Journal of Student Research* **3** 85-95

Bogen, D., Brunner, C., Walder, D., Ziegler, A., Abbasi, R *et al* 2016 The genetic tumor background is an important determinant for heterogeneous *MYCN-amplified* neuroblastoma *International Journal of Cancer* **139** 153-163

Brodeur, G.M 2003 Neuroblastoma: Biological insights into a clinical enigma *Nature Reviews Cancer* **3** 203-216

Burrell, R.A, McGranahan, N, Bartek, J and Swanton, C 2013 The causes and consequences of genetic heterogeneity in cancer evolution *Nature* **501** 338-345

Caldas, C 2012 Cancer sequencing unravels clonal evolution *Nature Biotechnology* **30** 408-410

Callaway, E 2013 Deal done over HeLa cell line *Nature* **500** 132- 133

Cancer Statistics for the UK *Cancer research UK* https://www.cancerresearchuk.org/health-professional/cancer-statistics-for-the-uk. Last accessed February 2019

Capes-Davis, A., Theodosopoulos, A.G., Drexler, H.G., Kohara, A., MacLeod, R.A., *et al* 2010Check your cultures! A list of cross-contaminated or misidentified cell lines *International Journal of Cancer* **127** 1-8

Carter, L., Rothwell, D.G., Mesquita, B., Smowton, C., Leong, H.S *et al.,* 2017 Molecular analysis of circulating tumor cells identifies distinct copy-number profiles in patients with chemosensitive and chemorefractory small-cell lung cancer *Nature Medicine* **23** 114-19

Cavalcante, L.d.S and Monteiro, G 2014 Gemcitabine: Metabolism and molecular mechanisms of action, sensitivity and chemoresistance in pancreatic cancer *European Journal of Pharmacology* **741** 8-16

Chabon, J.J., Simmons, A.D., Lovejoy, A.F., Esfahani, M.S., Newman, A.M 2016 Circulating tumour DNA profiling reveals heterogeneity of EGFR inhibitor resistance mechanisms in lung cancer patients *Nature Communications* **7** 11815

Chapman, P.B., Hauschild, A., Robert, C., Haanen, J.B., Ascierto, P *et al*., 2011 Improved survival with vemurafenib in melanoma with BRAF V600E mutation *New England Journal of Medicine* **364** 2507-16

Chaturvedi, N.K., McGuire, T.R., Coulter, D.W., Shukla, A., McIntyre, E.M *et al* 2016 Improved therapy for neuroblastoma using a combination approach: superior efficacy with vismodegib and topotecan *Oncotarget* **7** 15215-15229

Cheng, K.L, Bradley, T and Budman, D.R, 2008 Novel microtubule-targeting agents – the epothilones *Biologics: Targets and therapy* 4 789 – 811

Cheung, N-K. V., and Dyer, M.A 2013 Neuroblastoma: Developmental Biology, Cancer Genomics, and Immunotherapy *Nature Reviews Cancer* **13** 397-411

Clement, V, et al 2010 Retracted: Marker-independent identification of glioma-initating cells *Nature Methods* **7** 224-228

Cohn, S.L., Pearson, A.D.J., London, W.B., Monclair, T., Ambros, P.F *et al* 2009 The International Neuroblastoma Risk Group (INRG) Classification System: An INGR Task Force Report *Journal of Clinical Oncology* **27** 289-297

Cole, S.P., Bhardwaj, G., Gerlach, J.H., Mackie, K.E., Grant, C.E *et al.,* 1992 Overexpression of a transporter gene in a multidrug-resistant human lung cancer cell line *Science* **258** 1650-4

Croce, C.M 2008 Oncogenes and Cancer *New England Journal of Medicine* **358** 502-511

Crystal, A.S., Shaw, A.T., Sequist, L.V., Friboulet, L., Niederst, M.J., *et al* 2014 Patient-derived models of acquired resistance can identify effective drug combinations for cancer *Science* **346** 1480-6

Dagogo-Jack, I and Shaw, A.T., 2017 Tumour heterogeneity and resistance to cancer therapies *Nature Reviews Clinical Oncology* **15** 81-94

Davies, H., Glodzik, D., Morganella, S., Yates, L.R., Staaf, J *et al* 2017 HRDetect is a predictor of BRCA1 and BRCA2 deficiency based on mutational signatures *Nature Medicine* **23** 517-525

Dayaram, T and Marriot, S.J 2008 Effect of Transforming Viruses on Molecular Mechanisms Associated with Cancer *Journal of Cellular Physiology* **216** 309-314

De Sousa E Melo, F, Vermeulen, L, Fessler, E *et al* 2013 Cancer heterogeneity – a multifaceted view *EMBO reports* **14** 686-695

Delbridge, A.R.D., Grabow, S., Strasser, A and Vaux, D.L 2016 Thirty years of BCL-2: translating cell death discoveries into novel cancer therapies *Nature Reviews Cancer* **16** 99-109

Denduluri, S.K., Idowu, O., Wang, Z., Liao, Z., Yan, Z., *et al* 2015 Insulin-like growth factor (IGF) signaling in tumorigenesis and the development of cancer drug resistance *Genes & Diseases* **2** 13-25

Diede, S.J 2014 spontaneous regression of metastatic cancer: learning from Neuroblastoma *Nature Reviews Cancer* **14** 71-72

Doebele, R.C., Pilling, A.B., Aisner, D.L., Kutateladze, T.G, Le, A.T et al 2012 Mechanisms of resistance to crizotinib in patients with ALK gene rearranged in non-small cell lung cancer *Clinical Cancer Research* **18** 1472-1482

Domingo-Domenech, J., Vidal, S.J., Rodriguez-Bravo, V., Castillo-Martin, M., Quinn, S.A *et al* 2012 Suppression of acquired docetaxel resistance in prostate cancer through depletion of notch- and hedgehog-dependent tumor-initiating cells *Cancer Cell* **22** 373-88

Drexler, H.G., Dirks, W.G., MacLeod, R.A and Uphoff, C.C., 2017 False and mycoplasma-contaminated leukemia-lymphoma cell lines: time for a reappraisal *International Journal of Cancer* **140** 1209-1214

Dumontet, C. and Jordan, M.A., 2010 Microtubule-binding agents: a dynamic field of cancer therapeutics *Nature Reviews Drug Discov*ery **9** 790-803 Review. Erratum in: *Nature Reviews Drug Discov*ery 2010 **9** 897

Duran, G.E., Derdau, V., Weitz, D., Philippe, N., Blankenstein, J et al 2018 Cabazitaxel is more active than first-generation taxanes in *ABCB1*(+) cell lines due to its reduced affinity for P-glycoprotein *Cancer Chemotherapy and Pharmacology* 81 1095-1103

Eleveld, T., Oldridge, D.A., Bernard, V., Koster, J., Daage, C *et al* 2015 Relapsed neuroblastomas show frequent RAS-MAPK pathway mutations *Nature Genetics* **48** 864-71

Engelman, J.A., Zejnullahu, K., Mitsudomi, T., Song, Y., Hyland, C *et al* 2007 MET amplification leads to gefitinib resistance in lung cancer by activating ERBB3 signaling *Science* **316** 1039-43

Esposito, A., Criscitiello, C., Locatelli, M., Milano, M., Curigliano, G 2016 Liquid biopsies for solid tumors: Understanding tumor heterogeneity and real time monitoring of early resistance to targeted therapies *Pharmacology & Therapeutics* **157** 120-4

Fletcher, J.I., Haber, M., Henderson, M.J. and Norris, M.D 2010 ABC transporters in cancer: more than just drug efflux pumps *Nature Reviews Cancer* **10** 147-158

Fransson, S.M., Kryh, H., Javanmardi, N., Ambros, I., Berbegall, A., *et al* 2015 Amplification of chromosomal regions 12q13-14 and 12q15 defines a distinct subgroup of high-risk neuroblastoma patients and is associated with atypical clinical features *American Association for Cancer Research* **75**

Freedman, L.P., Gibson, M.C., Ethier, S.P., Soule, H.R., Neve, R.M., *et al* 2015 Reproducibility: changing the policies and culture of cell line authentication *Nature Methods* **12** 493-497

Fresno Vara, J.A., Casado, E., de Castro, J., Cejas, P., Belda-Iniesta, C *et al* 2004 P13K/Akt signaling pathway and cancer *Cancer Treatment Reviews* **30** 193 - 204

Gillet, J.-P and Gottesman, M.M 2009 Mechanisms of Multidrug Resistance in Cancer. *Methods in Molecular Biology* **596** 47-76

Gollner, S., Oellerich, T., Agrawal-Singh, S., Schenk, T., Klein, H.U *et al* 2017 Loss of the histone methyltransferase EZH2 induces resistance to multiple drugs in acute myeloid leukemia *Nature Medicine* **23** 69-78

Goodspeed, A., Heiser, L.M., Gray, J.W and Costello, J.C 2016 Tumor-Derived Cell Lines as Molecular Models of Cancer Pharmacogenomics *Molecular Cancer Research* **14** 3-13

Gottesman, M.M 2002 Mechanisms of Cancer Drug Resistance *Annual Review of Medicine* **53** 615-627

Graaf, J.F. de., Vor, L.de., Fouchier, R.A.M and Hoogen, B.G. van den, 2018 Armed oncolytic viruses: A kick-start for anti-tumor immunity *Cytokine and Growth Factor Reviews* **41** 28-39

Greaves, M and Maley, C.C 2012 Clonal evolution in cancer *Nature* **481** 306-313

Groner, A.C., Cato, L., Tribolet-Hardy, J.d., Bernasocchi, T., Janouskova, H et al 2016 TRIM24 Is an Oncogenic Transcriptional Activator in Prostate Cancer *Cancer cell* **6** 846-858

Hadjuk, J., Matysiak, J and Kokot, Z.J 2016 Challenges in biomarker discovery with MALDI-TOF MS *Clinica Chimica Acta* **458** 84-98

Hammerman, P.S., Sos, M.L., Ramos, A.H., Xu, C *et al* 2011 Mutations in the DDR2 Kinase Gene Identify a Novel Therapeutic Target in Squamous Cell Lung Cancer *Cancer Discovery* 77-87

Hanahan, D and Weinberg, R.A 2011 Hallmarks of cancer: the next generation **144** 646-674

Hanna, M.G., Najfeld, V., Irie, H.Y., Tripodi, J and Nayak, A 2015 Analysis of ALK genes in 133 patients with breast cancer revealed polysomy of chromosome 2 and no ALK amplification *Springer plus* **439**

Hansen, S.N., Westergaard, D., Thomsen, M.B.H., Vistesen, M., Do, K.N *et al* 2015 Acquisition of docetaxel resistance in breast cancer cells reveals upregulation of *ABCB1* expression as a key mediator of resistance accompanied by discrete upregulation of other specific genes and pathways *Tumor Biology* **36** 4327 – 4338

Hata, A.N., Niederst, M.J., Archibald, H.L., Gomez-Caraballo, M., *et al* 2016 Tumor cells can follow distinct evolutionary paths to become resistant to epidermal growth factor receptor inhibition *Nature Medicine* **22** 262-9

Holla, V.R., Elamin, Y.Y., Bailey, A.M., Johnson, A.M., Litzenburger, B.C et al 2017 ALK: a tyrosine kinase target for cancer therapy *Molecular Case studies* **3** 1-20

Housman, G., Byler, S., Heerboth, S., Lapinska, K., Longacre, M *et al*., 2014 Drug resistance in Cancer: An Overview *Cancers* **6** 1769-1792

Housman, G., Byler, S., Heerboth, S., Lapinska, K., Longacre, M., Snyder, N *et al* 2014 Drug resistance in Cancer: An Overview *Cancers* **6** 1769-1792

Howlader, N., Altekruse, S.F., Li, C.I., Chen, V.W., Clarke, C.A *et al* 2014 US incidence of breast cancer subtypes defined by joint hormone receptor and HER2 status *Journal of the National Cancer Institute* **106** 1-8

Hu, L., Ru, K., Zhang, L., Huang, Y., Zhu, X *et al* 2014 Fluorescence in situ hybridization (FISH): an increasingly demanded tool for biomarker research and personalized medicine *Biomarker Research* **2** 1-13

Iorio, F., Knijnenburg, T.A., Vis, D.J., Bignell, G.R., Menden, M.P *et al.*, 2016 A landscape of Pharmacogenomic Interactions in Cancer *Cell* **166** 740-754

Jager, W., Horiguchi, Y., Shah, J., Hayashi, T., Awrey, S., Gust, K.M *et al*., 2013 Hiding in plain view: Genetic profiling reveals decades old cross-contamination of bladder cancer cell line KU7 with HeLa *Journal of Urology* **190** 1404-1409

James, C.R., Quinn, J.E., Mullan, P.B., Johnston, P.G and Harkin, D.P., 2007 BRCA1, a potential predictive biomarker in the treatment of breast cancer *Oncologist* **12** 142-150

Jolliffe, I.T, 2002 Principal Component Analysis *Springer* **2** 1-488

Joseph, J.D., Lu, N., Qian, J., Sensintaffar, J., Shao, G *et al* 2013 A clinically relevant androgen receptor mutation confers resistance to second-generation antiandrogens enzalutamide and ARN-509 *Cancer Discovery* **3** 1020-9

Joshi, G 2016 Biomarkers in cancer *International Research Journal of Pharmaceutical and Biosciences* **3** 29-44

Juliano, R.L and Ling, V., 1976 A surface glycoprotein modulating drug permeability in Chinese hamster ovary cell mutants *Biochim Biophys Acta* **455** 152-62

Jung, J., Lee, J.S., Dickson, M.A., Schwartz, G.K., Le Cesne, A *et al* 2016 TP53 mutations emerge with HDM2 inhibitor SAR405838 treatment in de-differentiated liposarcoma *Nature Communications* **7** 12609

Kamisawa, T., Wood, L.D., Itoi, T and Takaori, K 2016 Pancreatic Cancer *The Lancet* **388** 73-85

Kaneko, M., Tsuchida, Y., Mugishima, H., Ohnuma, N., Yamamoto, K *et al* 2002 Intensified chemotherapy increases the survival rates in patients with stage 4 neuroblastoma with MYCN amplification *Journal of Pediatric Haematology and Oncology* **24** 613-21

Katayama, K., Noguchi, K and Sugimoto, Y 2014 Regulations of P-Glycoprotein/ ABCB1/MDR1 in Human Cancer Cells *New Journal of Science* **2014** *1-10*

Kavallaris, M., 2010 Microtubules and resistance to tubulin binding agents *Nature Reviews Cancer* **10** 194-204

Kelland, L 2007 The resurgence of platinum-based cancer chemotherapy *Nature Reviews Cancer* **7** 573–584

Khan, O and Protheroe, A 2007 Khan, O and Protheroe, A 2007 Testis cancer *Postgrad Medical Journal* **83** 624-632

Kilari, D., Guancial, E and Kim, E.S 2016 Role of copper transporters in platinum resistance *World Journal of Clinical Oncology* **7** 106 -113

Kim, J.J and Tannock, I.F 2005 Repopulation of cancer cells during therapy: an important cause of treatment failure *Nature Reviews Cancer* **5** 516 – 525

Korpal, M., Korn, J.M., Gao, X., Rakiec, D.P., Ruddy, D.A *et al* 2013 An F876L mutation in androgen receptor confers genetic and phenotypic resistance to MDV3100 (enzalutamide) *Cancer Discovery* **3** 1030-43

Kotchetkov, *R et al* 2005 Increased malignant behavior in neuroblastoma cells with acquired multi-drug resistance does not depend on P-gp expression *International Journal of Oncology* **27** 1029-37

Kriegsmann, J., Kriegsmann, M and Casadonte, R 2014 MALDI-ToF imaging mass spectrometry in clinical pathology: A valuable tool for cancer diagnostics *International Journal of Oncology* **46** 1893-906

Kumar, T., Chaudhary, K., Gupta, S., Singh, H., Kumar, S *et al* 2013 CancerDR: Cancer Drug Resistance Database *Scientific Reports* **2** 1-6

Lam, C.G., Furman, W.L., Wang, C., Spunt, S.L., Wu, J.W et al 2015 Phase I Clinical Trial of Ifosfamide, Oxaliplatin and Etoposide (IOE) in Pediatric Patients with Refractory Solid Tumours *Journal of Pediatric Haematology and Oncology* **37** 13-18

Lam, S.W., Jimenez, C.R., and Boven, E 2013 Breast cancer classification by proteomic technologies: Current state of knowledge *Cancer Treatment Reviews* **40** 129-138

Lawrence, R.T, Perez, E.M., Hernandez, D., Miller, C.P., Haas, K.M *et al* 2015 The proteomic landscape of Triple-Negative Breast Cancer *Cell Reports* **11** 630-644

Li, Y., Ye, F., Ma, Q., Yang, Z., Liu, D *et al* 2017 Isoform expression patterns of EPHA10 protein mediate breast cancer progression by regulating the E-Cadherin and ß-catenin complex *Oncotarget* **8** 30344 – 30356

Liang, X-J., Mukherjee, S., Shen, D-W., and Maxfield, F.R 2006 Endocytic Recycling Compartments Altered in Cisplatin-Resistant Cancer Cells *Cancer Research* **66** 2346-2353

Lippert, T.H., Ruoff, H.J and Volm, M., 2008 Intrinsic and acquired drug resistance in malignant tumors. The main reason for therapeutic failure *Drug Research* **56** 261-264

Loschmann, N., Michaelis, M., Rothweiler, F., Voges, Y., Balonova, B *et al*., 2016 ABCB1 as predominant resistance mechanism in cells with acquired SNS-032 resistance *Oncotarge*t **6** 58051-58064

Loschmann, N., Michaelis, M., Rothweiler, F., Zehner, R., Cinatl, J., *et al* 2013 Testing of SNS-032 in a panel of Human Neuroblastoma Cell lines with Acquired Resistance to a Broad Range of Drugs *Translational Oncology* **1** 685-96

Louis, C.U and Shohet, J.M 2014 Neuroblastoma: Molecular Pathogenesis and Therapy *Annual Review of Medicine* **66** 49-63

Magnani, L., Frige, G., Gadaleta, R.M., Corleone, G., Fabris, S *et al* 2017 Acquired CYP19A1 amplification is an early specific mechanism of aromatase inhibitor resistance in ERα metastatic breast cancer *Nature Genetics* **49** 444-450

Makarovskiy, A.N, Siyaporn, E, Hixson, D.C and Akerley, W 2002 Survival of docetaxel-resistant prostate cancer cells in vitro depends on phenotype alterations and continuity of drug exposure *Cellular and Molecular Life Sciences* **59** 1198-1211

Mansoori, B., Mohammadi, A., Davudian, S., Shirjang, S and Baradaran, B 2017 The Different Mechanisms of Cancer Drug Resistance: A Brief Review *Advanced Pharmaceutical Bulletin* 7 339-348

Maris, J.M 2010 Recent advances in Neuroblastoma *New England Journal of Medicine* **362** 2202-2011

Marjanovic, N.D., Weinberg, R.A and Chaffer, C.L 2013 Cell Plasticity and Heterogeneity in Cancer *Clinical Chemistry* **59** 168-179

Martinez-Balibera, E., Martinez-Cardus, A., Gines, A, Ruiz de Porras, V., Moutinho, C *et al* 2015 Tumor-Related Molecular Mechanisms of Oxaliplatin Resistance *Molecular Cancer Therapeutics* **14** 1767-76

Marusyk, A.V and Polyak, K 2013 Cellular heterogeneity and molecular evolution in cancer *Annual Review of Pathology* **8** 277 – 302

Masters, J.A., Thomson, J.A., Daly-Burns, B., Reid, Y.A., Dirks, W.G., *et al* 2001 Short tandem repeat profiling provides an international reference standard for human cell lines *PNAS* **98** 8012-8017

Masters, J.R. 2012 End the scandal of false cell lines *Nature* **492** 186

Masters, J.R.W., 2010 Cell line misidentification *Nature Reviews Cancer* **10** 441-448

Matthay, K.K., Reynolds, P.C., Seeger, R.C., Shimada, H., Adkins, E.S., *et al* 2009 Long-Term Results for Children with High-Risk Neuroblastoma Treated on a Randomized Trial of Myeloablative Therapy Followed by 13-*cis*-Retinoic Acid: A Children's Oncology Group Study *Journal of Clinical Oncology* **27** 1007-1013

Mehra N, Lorente, D and de Bono, J.S.,2015 What have we learned from exceptional tumour responses?: Review and perspectives *Current Opinion in Oncology* **27** 267-75

Michaelis, M., Agha, B., Rothweiler, F., Loschmann, N., Voges, L *et al.,* 2015 Identification of flubendazole as potential anti-Neuroblastoma compound in a large cell line screen *Scientific Reports* **5** 8202

Michaelis, M., Matousek, J., Vogel, J.U., Slavik, T., Langer, K *et al* 2000 Bovine seminal ribonuclease attached to nanoparticles made of polylactic acid kills leukemia and lymphoma cell lines in vitro *Anticancer Drugs* **5** 369-76

Michaelis, M., Rothweiler, F., Agha, B., Barth, S., Voges, Y *et al* 2012 Human neuroblastoma cells with acquired resistance to the p53 activator RITA retain functional p53 and sensitivity to other p53 activating agents *Cell Death & Disease* **3** e294

Michaelis, M., Rothweiler, F., Barth, S., Cinatl, J., van Rikxoort, M *et al* 2011 Adaptation of cancer cells from different entities to the MDM2 inhibitor nutlin-3 results in the emergence of p53-mutated multi-drug-resistant cancer cells *Cell Death & Disease* **2** e243

Minguet, J., Smith., K.H and Bramlage, P., 2016 Targeted therapies for treatment of non-small cell lung cancer – Recent advances and future perspectives *International Journal of Cancer* **138** 2549 – 2561

Mini, E., Nobili, B., Caciagli, I., *et al* 2006 Cellular pharmacology of gemcitabine *Annals of Oncology* **17** 7-12

Miranda, M.B., Lauseker, M., Kraus, M-P., Proetel, U., Hanfstein, B *et al*., 2016 Secondary malignancies in chronic myeloid leukemia patients after imatinib-based treatment: long term observation in CML Study IV *Leukemia* **30** 1255-1262

Mitri, Z., Constantine, T and O'Regan, R., 2012 The HER2 Receptor in Breast Cancer: Pathophysiology, Clinical Use, and New Advances in Therapy *Chemotherapy Research and Practice* **2012** 1-7

Morgenstern, D.A et al, 2014, Pandey, G.K and Kanduri, C, 2015 Metachronous Neuroblastoma in an Infant with Germline Translocation Resulting in Partial Trisomy 2p: A role for ALK? *Journal of Pediatric Oncology* **36** 193-196

Mosmann, T 1983 Rapid colorimetric assay for cellular growth and survival: application to proliferation and cytotoxicity assays *Journal of Immunological Methods* **16** 55-63

Mosse, Y.P., Laudenslager, M., Longo, L., Cole, K.A., Wood, A., *et al* 2008 Identification of ALK as a major familial Neuroblastoma predisposition gene *Nature* **455** 930 – 935

Nazarian, R., Shi, H., Wang, Q., Kong, X., Koya, R.C *et al* 2010 Melanomas acquire resistance to B-RAF(V600E) inhibition by RTK or N-RAS upregulation *Nature* **468** 973-7

Ngan, E.S-W 2015 Heterogeneity of neuroblastoma *Oncoscience* **2** 837-838

Normanno, N., Denis, M.G., Thress, K.S., Ratcliffe, M and Reck, M 2017 Guide to detecting epidermal growth factor receptor (EGFR) mutations in ctDNA of patients with advanced non-small-cell lung cancer *Oncotarget* **8** 12501-12516

Nowell, Peter 1976 The clonal evolution of tumour cell populations *Science* **194** 23-28

O'Connor, J.P.B., Rose, C.J., Waterton, J.C., Carano, R.A.D., Parker, G.J.M et al 2014 Imaging Intratumor Heterogeneity: Role in Therapy Response, Resistance, and Clinical Outcome *Clinical Cancer Research* **21** 249-257

Oberthuer, A., Skowron, M., Spitz, R., Kahlert, Y., Westermann, F., *et al* 2005 Characterization of a complex genetic alteration on chromosome 2p that leads to four alternatively spliced fusion transcripts in the Neuroblastoma cell lines IMR-5, IMR-5/75 and IMR-32 *Gene* **19** 41-50

Okayama, H., Kohno, T., Ishii, Y., Shimada, Y., Shiraishi, K *et al* 2012 Identification of Genes Upregulated in ALK-Positive and EGFR/KRAS/ALK-Negative Lung Adenocarcinomas *Molecular and Cellular Pathobiology* **72** 100-111

Oldridge, D.O., Wood, A.C., Maris, J.M., 2015 Genetic predisposition to neuroblastoma mediated by a LMO1 super-enhancer polymorphism *Nature* **528** 418-421

Oudard, S and Angelergues, A, 2014 Cabazitaxel – the taxane of choice in the new mCRPC landscape *Nature Reviews Urology* **11** 370 – 372

Padovan-Merhar, O.M., Raman, P., Ostrovnaya, I., Kalletla, K., Rubnitz, K.R *et al* 2016 Enrichment of targetable mutations in the relapsed Neuroblastoma genome *PLOS Genetics* **12** 1-13

Pathania, S., Bhatia, R., Baldi, A., Singh, R and Rawal, R.K 2018 Drug metabolizing enzymes and their inhibitors' role in cancer resistance *Biomedicine & Pharmacotherapy* **105** 53-65

Peng, X., Chen, B, Lim C.C and Sawyer, D.B 2005 The Cardiotoxicology of Anthracycline Chemotherapeutics: Translating molecular mechanism into preventative medicine *Molecular Interventions* **5** 163-171

Pezaro, C.J, Omlin, A.G., Altavilla, A., Lorente, D., Ferraldeschi, R *et al* 2014 Activity of Cabazitaxel in Castration-resistant Prostate Cancer Progressing After Docetaxel and Next-generation Endocrine Agents *European Urology* **66** 459-465

Pisco, A.O, Jackson, A.D and Huang, S 2014 Reduced Intracellular Drug Accumulation in Drug-Resistant Leukemia Cells is Not Only Solely Due to MDR-Mediated Efflux but also to Decreased Uptake *Frontiers in Oncology* **4** 1-9

Poulikakos, P.L., Persaud, Y., Janakiraman, M., Kong, X., Ng, C *et al* 2011 RAF inhibitor resistance is mediated by dimerization of aberrantly spliced BRAF (V600E) *Nature* **480** 387-90

Poveda, A.M., Selle, F., Hilpert, F., Reuss, A., Savarese, *et al* 2015 Bevacizumab Combined with Weekly Paclitaxel, Pegylated Liposomal Doxorubicin, or Topotecan in Platinum-Resistant Recurrent Ovarian Cancer: Analysis by Chemotherapy Cohort of the Randomized Phase III AURELIA Trial *Journal of Clinical Oncology* **33** 3836 – 3839

Povey, J.F., O'Malley, C.J., Root, T., Martin, E.B., Montague, G.A *et al*, 2014 Rapid high-throughput characterisation, classification and selection of recombinant mammalian cell line phenotypes using intact cell MALDI-ToF mass spectrometry fingerprinting and PLS-DA modelling *Journal of Biotechnology* **184** 84-93

Rebouissou, S., Zucman-Ross, J., Moreau, R., Qui, Z and Hui, L 2017 Note of caution: contaminations of hepatocellular cell lines *Journal of Hepatology* **17** 32206-7

Regales, L., Gong, Y., Shen, R., de Stanchina, E., Vivanco, I *et al* 2009 Dual targeting of EGFR can overcome a major drug resistance mutation in mouse models of *EGFR* mutant lung cancer *Journal of Clinical Investigation* **119** 3000-3010

Rodrigo, M.A.M., Zitka, O., Krizkova, S., Moulick, A., Adam, V., *et al* 20142014 MALDI-TOF MS as evolving cancer diagnostic tool: A review *Journal of Pharmaceutical and Biomedical Analysis* **95** 245-255

Rubakhin, S.S and Sweedler, J.V 2007 Characterising peptides in individual mammalian cells using mass spectrometry *Nature Protocols* **2** 1987-1997

Russo, M., Misale, S., Wei, G., Siravenga, G., Crisafulli, G., *et al*., 2016 Acquired resistance to the TRK inhibitor Entrectinib in Colorectal Cancer *Cancer Discovery* **6** 36-44

Rybinksi, B and Yun, K 2016 Addressing intra-tumoural heterogeneity and therapy resistance *Oncotarget* **7** 72322-72342

Sancar, A., Lindsey-Boltz, L.A, Unsal-Kacmaz, K and Linn, S., 2004 Molecular mechanisms of mammalian DNA repair and the DNA damage checkpoints *Annual Review of Biochemistry* **73** 39-85

Sawyers, C.L 2008 The cancer biomarker problem *Nature* **452** 548-552

Sawyers, L., Ferguson, M., Ihrig, B., Young, H., Chakravarty, P *et al* 2014 Glutathione *S*-transferase P1 (*GSTP1*) directly influences platinum drug chemosensitivity in ovarian tumour cell lines *British Journal of Cancer* **111** 1150-1158

Schneider, C., Oellerich, T*.,* Baldauf, H.M., Schwartz, S.M., Thomas, D., *et al* 2017 SAMHD1 is a biomarker for cytarabine response and a therapeutic target in acute myeloid leukemia *Nature Medicine* **23** 250-5

Schone, C, Hofler, H and Walch, A 2013 MALDI imaging mass spectrometry in cancer research: Combining proteomic profiling and histological evaluation *Clinical Biochemistry* **46** 539-545

Schramm, A., Koster, J., and Schulte, J.H 2015 Mutational dynamics between primary and relapse neuroblastomas *Nature Genetics* **47** 872-877

Schrijver, W., Schuurman, K., van Rossum., A., Droog, M., Jeronimo, C et al 2018 FOXA1 levels are decreased in pleural breast cancer metastases after adjuvant endocrine therapy, and this is associated with poor outcome *Molecular Oncology* **12** 1884 – 1894

Seeger, R.C Immunology and immunotherapy of neuroblastoma 2011 *Seminars in Cancer Biology* **21** 229-237

Seeley, E.H and Caprioli, R.M 2012 3D Imaging by Mass Spectroscopy: A New Frontier *Analytical Chemistry* **84** 2105-2110

Seng, P., Drancourt, M., Gouriet, F., La Scola, B., Fournier, P.E *et al* 2009 Ongoing Revolution in Bacteriology: Routine Identification of Bacteria by Matrix-Assisted Laser Desorption Ionization Time-of-Flight Mass Spectroscopy *Clinical Infectious Diseases* **49** 543-451

Sever, R and Brugge, J.S. 2015 Signal transduction in cancer *Cold Spring Harbor Perspectives Medicine* **5** 1-21

Sharma, S.V., Haber, D.A and Settleman, J 2010 Cell line-based platforms to evaluate the therapeutic efficacy of candidate anticancer agents *Nature Reviews Cancer* **10** 241-253

Singh, P., Alex, J.M and Bast F., 2013 Insulin receptor (IR) and insulin-like growth factor receptor 1 (IGF-1R) signaling systems: novel treatment strategies for cancer *Medical Oncology* **31** 805

Somaschini, A., Amboldi, N., Nuzzo, A., Scacheri, E., Ukmar, G *et al.,* 2013 Cell line identity finding by fingerprinting, an optimized resource for short tandem repeat profile authentication *Genetic Testing and Molecular Biomarkers* **17** 254-259

Song, M.S., Salmena, L and Pandolfi, P.P 2012 The functions and regulation of the PTEN tumour suppressor *Molecular Cell Biology 13 283-296*

Sottoriva, A, Barnes, C.P and Graham, T.A 2017 Catch my drift? Making sense of genomic intra-tumour heterogeneity *Reviews on Cancer* **1867** 95-10

Swiatly, A., Horala, A., Hadjuk, J., Matysiak, J., Nowak-Markwitz, E *et al* 2017 MALDI-TOF-MS analysis in discovery and identification of serum proteomic patterns of ovarian cancer *BMC Cancer* **17** 1-9

Swift, C.C., Eklund, M.J., Kraveka, J.M. and Alazraki, A.L 2018 Updates in Diagnosis, Management, and Treatment of Neuroblastoma *Pediatric Imaging* **38** 566-580

Szakacs, G., Paterson, J.K., Ludwig, J.A., Boothe-Genthe, C., and Gottesman, M.M 2006 Targeting multidrug resistance in cancer *Nature Reviews Drug Discovery* **5** 219-234

Taieb, J., Pointet, A.L., Van Laethem, J.L., Laquente, B., Pernot, S *et al* 2017 What treatment in 2017 for inoperable pancreatic cancers? *Annals of oncology* **28** 1473-1483

Theissen, J., Oberthuer, A., Hombach, A., Volland, R., Hertwig, F., *et al* 2014 Chromosome 17/17q Gain and Unaltered Profiles in High Resolution Array-CGH are Prognostically Informative in Neuroblastoma *Genes, Chromosomes & Cancer* **53:** 639-649

Thorn, C.F., Oshiro, C., Marsh, S. Hernandez-Boussard, T., McLeod, H., Klein, T.E., *et al* 2011 Doxorubicin pathways: pharmacodynamics and adverse effects *Pharmacogenet Genomics* **21** 440-446

Tonini, G.P 2017 Growth progression and chromosome instability of Neuroblastoma: a new scenario of tumorigenesis *BMC Cancer* **17** 1-6

Torgovnick, A and Schumacher, B 2015 DNA repair mechanisms in cancer development and therapy *Frontiers in Genetics* **6** 1-15

Tucker, J.D., 2015 Reflections on the development and application of FISH whole chromosome painting *Mutation Research* **763** 2-14

Tyanova, S., Albrechtsen, R., Kronqvist, P., Cox, J., Mann, M *et al* 2016 Proteomic maps of breast cancer subtypes *Nature Communications* **7** 1-11

Vaidyanathan, A., Sawyers, L., Gannon, A.L., Chakravarty, P., Scott, A.L 2016 ABCB1 (MDR1) induction defines a common resistance mechanism in paclitaxel- and olarparib-resistant ovarian cancer cells *British Journal of Cancer* **115** 431-441

Vallo, S., Michaelis, M., Rothweiler, F., Bartsch, G., Gust, K.M *et al* 2015 Drug-Resistant Urothelial Cancer Cell Lines Display Diverse Sensitivity Profiles to Potential Second-Line Therapeutics *Translational Oncology* **8** 210-6

Vogues, Y., Michaelis, M., Rothweiler, F., Schaller, T., Schneider, C., *et al.,* 2016 Effects of YM155 on survivin levels and viability in Neuroblastoma cells with acquired drug resistance *Cell Death & Disease* **13** e2410

Wawrzyniak, E., Kotkowska, A., Blonski, J.Z., Siemieniuk-Rys, M., Ziolkowska, E., *et al* 2014 Clonal evolution in CLL patients as detected by FISH versus chromosome banding analysis, and its clinical significance *European Journal of Haematology* **92** 91-101

Wetterskog, D., Moshiri, A., Ozaki, T., Uramoto, H., Nakagawara, A *et al* 2009 Dysregulation of Platelet-Derived Growth Factor ß- receptor Expression by ΔNp73 in Neuroblastoma *Molecular Cancer Research* **7** 2031-2039

Wilding, J.L and Bodmer W.F 2014 Cancer cell lines for drug discovery and development *Cancer Research* **74** 2377-2384

Williams, R.D., Chagtai, T., Alcaide-German, M., Apps, J., Wegert, J *et al* 2015 Multiple mechanisms of MYCN dysregulation in Wilms tumour *Oncotarget* **6** 7232-7243

Woynarowski, J.M., Faivre, S., Herzig, M.C., Arnett, B., Chapman, W.G., *et al* 2000 Oxaliplatin-Induced Damage of Cellular DNA *Molecular Pharmacology* **58** 920-927

Wunschel, S., Jarman, K.H., Peterson, C.E., Valentine, N.B and Wahl, K.L *et al* 2005 Bacterial Analysis by MALDI-ToF Mass Spectrometry: An Inter-Laboratory Comparison *American Society for Mass Spectrometry* **16** 456-462

Xhao, W, Li, J and Mills, G.B 2017 Functional proteomic characterisation of cancer cell lines *Oncoscience* **4** 41-42

Yancovitz, M., Litterman, A., Yoon, J., Ng, E., Shapiro, R.L *et al* 2012 Intra- and inter-tumor heterogeneity of BRAF(V600E)) mutations in primary and metastatic melanoma *PLoS* **7** 29336

Yang, X., Cheng, Y., Luo, N and Changyang, G 2014 Nanomedicine to Overcome Cancer Multidrug Resistance *Current Drug Metabolism* **15** 632-649

Yao, Y and Dai, W 2014 Genomic instability and cancer *Journal of Carcinogenesis and Mutagenesis* **5** 2157-2158

Zahreddine, H.A., Culjkovic-Kraljacic, B., Assouline, S., Gendron, P., Romeo, A.A *et al*., 2014 The sonic hedgehog factor GLI1 imparts drug resistance through inducible glucuronidation *Nature* **511** 90-3

Zang, X., Ding, H., Zhao, X, Li, X., Du, Z., *et al* 2016 Anti-EphA10 antibody-conjugated pH-sensitive liposomes for specific intracellular delivery of siRNA *International Journal of Nanomedicine* **11** 3951-3967

Zardavas, D., Irrthum, A., Swanton, C and Piccart, M 2015 Clinical management of breast cancer heterogeneity *Nature Reviews Clinical Oncology* **12** 381-94

Zhang, X., Scalf, M., Berggren, T.W., Westphall, M.S. and Smith, L.M 2006 Identification of Mammalian Cell Lines using MALDI-ToF and LC-ESI-MS/MS Mass Spectrometry *Journal of The American Society for Mass Spectrometry* **17** 490- 499

Zhao, Y, Butler, E.B and Tan, M., 2013 targeting cellular metabolism to improve cancer therapeutics *Cell Death & Disease* **4** 532

Zhu, S., Lee, J.S., Gui, F., Shin, J., Perez-Atayde, A.R *et al*, 2012 Activated ALK collaborates with MYCN in Neuroblastoma pathogenesis *Cancer Cell* **21** 362-373